2019

Rapid disruption of cortical activity and loss of cerebral blood flow in a mouse model of mild traumatic brain injury

BOSTON UNIVERSITY

SCHOOL OF MEDICINE

Dissertation

RAPID DISRUPTION OF CORTICAL ACTIVITY AND LOSS OF CEREBRAL BLOOD FLOW IN A MOUSE MODEL OF MILD TRAUMATIC BRAIN INJURY

by

ELLEN WITKOWSKI

B.A., Kenyon College, 2010

Submitted in partial fulfillment of the

requirements for the degree of

Doctor of Philosophy

2019

Approved by

First Reader _____

Ian Davison, Ph.D.
Assistant Professor of Biology

Second Reader _____

Alberto Cruz-Martín, Ph.D.
Assistant Professor of Biology

ACKNOWLEDGMENTS

I am deeply grateful to the many people who have helped run experiments, offered guidance, and supported me in a myriad of ways throughout my research. First, thank you to Ian Davison for patiently teaching me to think like a scientist and always pushing for great instead of good. Much thanks also goes to:

My current and former labmates in the Lab of Neural Circuit Function, especially Yuan Gao, Dan Leman, Brett Dibenedictis, Esther Lee, and Alex Gavsyuk for their assistance with experiments, thoughtful questions, and comradery. Research failures and triumphs are best shared with friends (and over beer).

The Lab of Neural Circuit Formation for their insights, philosophical conversations, and making me feel like one of their own.

Bill Eldred and Gloria DeWalt for starting me on this journey of studying TBI.

Todd Blute for always making time to offer advice on imaging analysis or to pick me up when I was discouraged.

Alberto Cruz-Martín and William Yen for their aid in setting up and analyzing data from calcium imaging experiments.

The members of the Bio Optical & Acoustic Spectroscopy Lab, especially David Boas, Şefik Evren Erdener, Kivilcim Kiliç, Sreekanth Kura, Jianbo Tang, and Dmitry Postnov. The data collection and analysis on cerebral blood flow would not have been possible without them. Extra thanks to Evren for kindly and so promptly answering all of my questions even when he was in the airport leaving the country.

Shelley, Sandi, and all the members of the Graduate Program for Neuroscience for their continued guidance and ideas.

My triathlon girlfriends for long Sunday runs to recharge, and to former roommate Elysa for reminding me to see the big picture in life.

My family, especially my sister for her emails and songs to get me through the tough days, my mom for reminding me to have faith in myself, and my dad for his continuing curiosity and sage advice.

Finally, Matthew for always supporting me and my goals on this long journey. The wait was worth it.

RAPID DISRUPTION OF CORTICAL ACTIVITY

AND LOSS OF CEREBRAL BLOOD FLOW

IN A MOUSE MODEL OF MILD TRAUMATIC BRAIN INJURY

ELLEN WITKOWSKI

Boston University School of Medicine, 2019

Major Professor: Ian Davison, PhD, Assistant Professor of Biology

ABSTRACT

Every year 2.8 million Americans suffer a traumatic brain injury (TBI). Despite the prevalence and debilitating consequences of TBI, effective treatment options are scarce due to the limited understanding of the neurobiological effects of injury, especially in acute phases when the cellular processes leading to neuropathology are first initiated. To identify changes in neural function and cerebral blood flow (CBF) that might account for TBI-induced cognitive and sensory deficits, we took a multidisciplinary approach, examining synaptic function, cortical activity patterns, and microvascular hemodynamics. we used a weight drop model in mice to induce mild TBI, the most common form in humans, and focused on responses within the first hours of injury where existing data are particularly limited.

For synaptic function, we measured excitatory and inhibitory input onto pyramidal cells in the piriform cortex with whole-cell recordings in acute brain slices. Increased excitation appeared at one hour but excitatory-inhibitory balance was

reestablished by 48 hours, highlighting the importance of studying rapid-onset injury responses.

We also compared neural activity before and after TBI using *in vivo* two-photon calcium imaging of pyramidal cells in visual cortex. While neural activity substantially decreased in most cells one hour after injury, a minority of cells showed hyperactivation or prolonged increases in intracellular calcium, again indicating major physiological disturbances during immediate post-injury phases. Finally, we measured *in vivo* changes in CBF throughout the cortical microvasculature with laser speckle contrast imaging and optical coherence tomography, tracking injury effects up to three weeks after TBI. CBF and capillary flow were dramatically reduced within minutes and remained suppressed for over one hour. As neurons' high energetic needs require a constant supply of glucose and oxygen from local vasculature, decreased CBF likely contributes to altered neural activity and loss of ion homeostasis and thus potentially cognitive and sensory deficits after TBI.

Our results reveal that even mild injury creates rapid, pronounced, and heterogeneous alterations in neural activity and capillary flow. The transient nature of these effects suggests that the first two hours after injury may be a key window for delivering interventions, and that restoring CBF may reduce damage due to metabolic stress.

TABLE OF CONTENTS

LIST OF TABLES

LIST OF FIGURES

LIST OF ABBREVIATIONS

2P ..... two photon

BBB..... blood-brain barrier

Ca^{2+} .....calcium

CBF ..... cerebral blood flow

CCI..... controlled cortical impact

E-I ..... excitatory-inhibitory

EPSC..... excitatory postsynaptic current

FPI..... fluid percussion injury

IPSC ..... inhibitory postsynaptic current

KS test..... Kolmogorov-Smirnov test

NADH ..... nicotinamide adenine dinucleotide

OCT..... optical coherence tomography

OEF ..... oxygen extraction factor

ROI..... region of interest

TBI .....traumatic brain injury

CHAPTER ONE

Introduction to Traumatic Brain Injury

1.1 MOTIVATION

Traumatic brain injury (TBI) is defined as a disturbance in normal brain function from damage by an external force, such as an object striking the head, exposure to a strong air pressure blast, or rapid acceleration/deceleration (CDC, 2017). TBI is a major health concern with an estimated 69 million people throughout the world suffering a TBI every year (Dewan et al., 2018). Studies in the U.S. show that certain populations are more at risk for TBI than others. For example, men consistently have a higher incidence than women across all ages (Faul et al., 2010). Since the U.S.'s involvement in the wars in Iraq and Afghanistan, the number of military personnel with TBI has dramatically risen. Almost 50% of soldiers injured in combat suffered a TBI, making it one of the "signature injuries" of these wars (Arthur et al., 2007; Jackson et al., 2008). Seniors over the age of 65 and children under 4 are at the highest risk of TBI due to the susceptibility of these populations to fall (Faul et al., 2010). However, another one of the leading causes of TBI is motor vehicle accidents, which affects people of all ages (Faul et al., 2010). While some demographics are more likely to suffer a TBI than others, the high incidence and variety of causes of TBI make it a risk for everyone and warrant greater efforts to address this health concern.

TBI can lead to debilitating symptoms that can generally be divided into cognitive impairment, emotional instability, disturbed sensory processing, and physical disability (Gerberding and Binder, 2003; Levin et al., 1987; Lew et al., 2007) (**Table 1**). TBI can be

categorized as mild, moderate, or severe based on the Glasgow Coma Scale, but mild is by far the most common form, accounting for about 80% of head injury (Cassidy et al., 2004). Mild TBI symptoms are usually less extreme or last for shorter periods of time than severe injury, but mild TBI still results in impairments that can persist for months or years, especially memory deficits and headaches (Carroll et al., 2004; Rimel et al., 1981). Decades afterwards athletes who have previously suffered repeated head injuries (both concussive and subconcussive) may develop chronic traumatic encephalopathy, a neurodegenerative tauopathy characterized by memory loss, poor judgement, erratic behavior, and parkinsonism (McKee et al., 2009; Mez et al., 2017). Thus, although mild TBI is the least severe form of head trauma, it can still have debilitating long-term consequences.

Cognitive Impairment	Emotional Instability	Disturbed Sensory Processing	Physical Symptoms
Memory problems Attention deficits Slower processing speed Impaired judgement	Depression Severe mood swings Anxiety	Blurred vision Poor ocular tracking Difficulty suppressing background noise Reduced sense of smell	Headaches Fatigue Nausea Dizziness

Table 1 Common symptoms of TBI

Besides the reduced quality of life, lingering symptoms from mild TBI also create a large financial burden. Problems such as impaired memory and attention or headaches arising while reading prevent or limit the ability to work (Rimel et al., 1981). One group found that 34% of people who had previously been working were unemployed 3 months after suffering a mild TBI (Rimel et al., 1981). Additionally, symptoms may require

many physical or occupational therapy sessions leading to mounting health care bills. A study examining the direct and indirect cost of TBI estimated that mild TBI alone costs the country $17 billion every year (Max et al., 1991). Despite the high incidence, consequences, and economic burden of mild TBI, there is no clinically-proven treatment.

In this chapter we describe some of the hallmark pathologies of TBI, the most common animal models used to reproduce and study injury, the importance of timing, and our approach to answer remaining questions and better understand mild TBI.

1.2 HALLMARK PATHOLOGIES OF TBI

Much research has been done to determine what neurobiological changes are occurring after TBI to determine what causes the observed symptoms and to develop a treatment. The changes can be divided into primary and secondary injury. For primary injury the force inducing TBI (e.g., object striking the head) directly damages the brain such as by contusion, laceration, or stretching axons. The force also triggers harmful pathways that induce secondary injury over the hours to weeks after the initial hit. For example, if bleeding at the contusion site continues to occur, the accumulated blood will be toxic to cells and will elevate the intracranial pressure, putting increased pressure on neural tissue and blood vessels. Both primary and secondary injuries will be included in the pathologies briefly summarized below. Finally, it is important to note that TBI is a very heterogeneous injury in terms of the pathology and outcomes among the severities of injury (mild, moderate, or severe) and among different people with the same severity. This heterogeneity within severity type stems from the fact TBI can be result from a variety of causes (e.g., motor vehicle accident vs gunshot wound), but also from

differences in age and health among others (De Guise et al., 2009; Taylor et al., 2017). Thus, the pathologies mentioned may occur in some cases of TBI but not others. The most common pathologies seen after TBI, including mild TBI, are: diffuse axonal injury, ionic and glutamate imbalance, altered cellular & synaptic activity, inflammation, and changes in cerebral blood flow (CBF) and vasculature.

1.2.1 Diffuse axonal injury

One of the first pathologies detected by examining human tissue post-mortem and now serves as an effective biomarker detected with diffusion tensor imaging in living patients (Hulkower et al., 2013) is diffuse axonal injury, where axons swell and sometimes break apart. In very severe cases of TBI, axonal injury may occur at the time of injury from forces that rapidly deform or strain the brain (Smith and Meaney, 2000). More often though, axonal damage results from injury compromising the membrane around the axon, which blocks axonal transport. Vesicles, proteins and other products unable to move farther build up within the axon causing swelling and potentially complete severing of the axon (Maxwell et al., 1997). Focal axonal injury can be seen after more focal types of TBI that tend to occur in moderate and severe TBI, but mild trauma usually shows only diffuse or widespread axonal injury (Povlishock and Katz, 2005). Diffuse axonal injury is often considered to be the defining characteristic of human TBI pathology, especially since it is present in mild TBI when other pathologies are less prevalent (Blennow et al., 2012).

1.2.2 Ionic imbalance and glutamate release

Following TBI neurons release large amounts of glutamate and the ionic homeostasis so carefully maintained before injury is lost. Normally sodium and calcium influx and potassium efflux only occur as a part of neuronal firing, but TBI leads to unregulated movement of ions down their concentration gradients. The ion flux may result from opening of glutamatergic ion channels, but the mechanical force of TBI can also open mechanosensitive ion channels or create pores within the lipid membrane (Giza and Hovda, 2014). Loss of ionic homeostasis results in neuronal depolarization and the elevated levels of intracellular calcium in particular cause multiple disturbances. First, it can trigger the release of more glutamate and other excitatory neurotransmitters, creating a risk of excitotoxicity. The initial movement of ions combined with glutamate release can worsen the ionic imbalance by activating voltage- and ligand-gated ion channels that allow even more harmful influx and efflux. Across all ions, the net movement is influx, which drives water into the cell by osmosis and thus induces cell swelling (cytotoxic edema). Meanwhile, energy demand in the cell rapidly increases in attempt to reestablish ionic homeostasis (Blennow et al., 2012; Giza and Hovda, 2014). Second, calcium plays a role in *many* signal transduction pathways. When intracellular calcium rises, calpain proteases that degrade cell structural components and caspases involved in apoptosis are triggered. Both of these pathways can lead to neuronal death (Weber, 2012). Third, high intracellular calcium can overwhelm and damage mitochondria that normally buffer calcium ions. In conclusion, glutamate release combined with loss of ionic homeostasis, especially calcium, leads to a cascade of harmful mechanisms.

1.2.3 Altered neural and synaptic activity

Many studies have found altered neural and synaptic activity following TBI, including both increases and decreases in activity. In moderate to severe cases of injury, both humans and animals may have epileptic activity detected by electrophysiology or full-on convulsions (Annegers et al., 1998; Cantu et al., 2015; Nilsson et al., 1994). However, reductions in activity have also been detected for a range of injury severities with lower spontaneous firing in rodents and humans (Alves et al., 2005; Hansen et al., 2018) and decreased responses to stimulation in rodents (Johnstone et al., 2014; Johnstone et al., 2013). The mixed results may arise from differences in TBI severity, cause/model, brain region, time of measurement, or other factors. For examining synapses after injury, the majority of work (besides neurotransmitter concentrations) has been done in animals since techniques to answer cellular and molecular questions are normally invasive. In the cortex some groups have found more frequent excitatory input onto pyramidal cells in acute brain slices from rodents 1 week after injury (Cantu et al., 2015; Smith et al., 2015). At this same time point though excitatory input to the dentate gyrus of the hippocampus occurs less frequently (Witgen et al., 2005). Additionally, long-term potentiation in the hippocampus is inhibited for 2-4 weeks following injury in animals (Goldstein et al., 2012; Miyazaki et al., 1992; Reeves et al., 1995), indicating that other cellular processes affecting synaptic plasticity are also disturbed and may account for learning and memory deficits after TBI. Despite the lack of consensus on direction and timing of activity changes among studies, it is clear that cellular and synaptic activity are both disrupted by TBI.

1.2.4 Inflammation

Unsurprisingly, injury leads to inflammation. Starting in the acute phase (hours to days) after TBI, both microglia and astrocytes respond. Microglia develop an amoeboid morphology indicative of activation then migrate to damaged areas to release inflammatory cytokines and phagocytose cellular debris (Loane and Byrnes, 2010; Streit, 2000). Astrocytes also take on a swollen, hypertrophic morphology, release inflammatory signaling molecules, and also help take up excessive extracellular glutamate. Together with microglia, astrocytes form a glial scar which acts as a barrier between healthy and damaged tissue (Karve et al., 2016). While the mechanisms of glial activity after TBI have typically been studied in animals, evidence of microglial and astrocytic reactivity has been seen in humans as well, often in the form of residual glial scarring (Goldstein et al., 2012; Karve et al., 2016; Loane and Byrnes, 2010).

1.2.5 Changes in CBF and vasculature

The changes in CBF and vasculature after TBI are numerous, dynamic, and variable. While CBF may increase transiently at the time of blast injury (Chen and Huang, 2011) or days after trauma during the recovery process (Kelly et al., 1997; Martin et al., 1997), most forms of TBI result in significant decreases in CBF in both humans and animals (Golding, 2002; Jullienne et al., 2016; Kenney et al., 2016). The degree and duration can greatly depend on the severity and cause of injury. Since CBF is vital to providing glucose and oxygen to cells, large decreases in CBF can create a massive energy shortage, which is especially problematic when energy demand appears to spike in the first 30 minutes after TBI in animals (Yoshino et al., 1991) or longer in humans

(Bergsneider et al., 1997; Soustiel et al., 2005). Autoregulation, the physiological adjustments to maintain necessary CBF upon changes in pressure, is also perturbed after TBI indicating an inability for blood vessels to change their diameter or a problem with signaling these mechanisms (Bouma and Muizelaar, 1990; Jünger et al., 1997; Lewelt et al., 1980). The blood-brain barrier (BBB) can be compromised allowing fluid to accumulate in extracellular space resulting in vasogenic edema (Kenney et al., 2016). Moderate to severe TBI often results in hemorrhaging, especially in the subarachnoid region, which can later trigger vasospasm, the extreme constriction of blood vessels, which further reduces CBF (Jullienne et al., 2016). Although multiple causes of TBI can induce subarachnoid hemorrhage, vasospasm is particularly common after blast injury in humans (Armonda et al., 2006). Vasogenic edema, hemorrhaging, and cytotoxic edema related to energy shortage and loss of ionic homeostasis can all increase intracranial pressure, which greatly raises the risk of mortality (Balestreri et al., 2006). Even if there is no hemorrhaging, CBF to cells may still be prevented by thrombi, or blood clots, which have been detected within 30 minutes after TBI in animal models (Härtl et al., 1997; Schwarzmaier et al., 2010) and observed in humans post-mortem (Stein et al., 2004). Finally, there is evidence in both humans and animals of lasting structural damage to the vasculature after TBI. Vessel walls are sometimes thinned, collapsed, or torn, accounting for the observed hemorrhaging (Daneyemez, 1999; Hekmatpanah and Hekmatpanah, 1985; Rodríguez-Baeza et al., 2003). The drop in CBF, disruption of vascular processes, and altered vessel structure are thought to underlie much of the neural damage and deficits observed after TBI.

1.3 ANIMAL MODELS OF TBI

Over the years, different animal models of TBI have been developed to better understand injury and identify a therapeutic target. As mentioned above, TBI can induce a variety of pathologies, and different animal models reproduce certain aspects of injury better than others. The most common models include: fluid percussion injury (FPI), controlled cortical impact (CCI), blast injury, and weight drop impact acceleration.

1.3.1 Fluid percussion injury (FPI)

FPI involves a pendulum striking the piston of a syringe or reservoir of fluid to create a fluid pulse on the brain exposed with a craniotomy. FPI began in 1941 with use in cats to induce a compression-type of concussion as opposed to an acceleration model of injury (Denny-Brown and Russell, 1941). FPI went through several evolutions over the following decades until Dixon and McIntosh came out with the central and lateral FPI for rodents commonly used today (Dixon et al., 1987; McIntosh et al., 1989). Although the method for generating the fluid pulse is the same, the location of where the pulse is given influences the pathology that results. Central FPI given at the midline causes a focal type of injury, including contusion at the site of fluid pulse that progresses into a lesion, subarachnoid hemorrhage, and disruption of the blood-brain barrier (BBB). It also results in damage to the brainstem that increases the mortality rate (Morales et al., 2005; Xiong et al., 2013). In contrast, lateral FPI produces a combined focal and diffuse injury. There is cortical contusion at the pulse site but also diffuse subcortical neuronal damage, particularly in the hippocampus and thalamus, diffuse axonal injury, and large fluctuations in cerebral blood flow (Lyeth, 2016; Morales et al., 2005). Performance on

cognitive and motor tasks, such as working memory, declines with both types of FPI, showing some analogous symptoms to humans as listed in **Table 1** (Dixon et al., 1987; McIntosh et al., 1989). The severity of FPI can be adjusted by altering the starting height of the pendulum, but there can be significant differences in the results of a given pressure pulse between labs owing to the difficulty of measuring the pressure pulse at the brain rather than the FPI device (Lyeth, 2016). In general, the open-skull preparation, lesion at the site of the fluid pulse, and higher mortality rate suggest that this model is best suited for studying moderate to severe TBI.

1.3.2 Controlled cortical impact (CCI)

CCI has a similar set-up as FPI, but instead of a fluid pulse, a pneumatic or electromagnetic impactor hits and deforms the exposed brain tissue. Originally designed in ferrets (Lighthall, 1988), it was shortly modified for use in rodents by Dixon (Dixon et al., 1991). CCI creates a mostly focal injury with contusion at the impact site, neuronal loss in the cortex as well as hippocampus and thalamus, axonal injury in the brain stem and subcortical white matter, and subarachnoid hemorrhage (Dixon et al., 1991; Lighthall, 1988; Morales et al., 2005). Cognitive and motor deficits, like memory and learning impairment, are apparent after injury. Additionally, evidence of depression and anxiety has been found as well (Xiong et al., 2013) resembling the emotional dysfunction humans suffer after TBI. Multiple aspects of CCI (velocity, depth of impact, timing) can be modified for finely tuning the severity of injury, which also improves the reproducibility within and among different groups (Morales et al., 2005; Xiong et al.,

2013). However, like FPI, CCI requires exposing the brain and tends to create focal damage and lesions making it a better choice for moderate and severe forms of TBI.

1.3.3 Blast injury

Blast models of TBI have become more popular since veterans have been returning from the wars in Iraq and Afghanistan where they suffered exposure to improvised explosive devices (Hoge et al., 2008; Jackson et al., 2008). The blast injury can be generated in a variety of ways, including open field exposure to explosives and blast tubes coupled with explosives or compressed gas (Cernak et al., 2011; Goldstein et al., 2012; Kuehn et al., 2011; Long et al., 2009). With blast tubes the waveforms can be easily controlled and measured, but the blast waves traveling through tubes are usually simpler than those experienced by humans in an open field where the wave reflects off of objects (Gullotti et al., 2014). Differences in how the blast is generated and where the animal is positioned in reference to the blast or the blast tube make it extremely difficult to directly compare results between models, but some general findings have been consistent. Free movement of the animal's head seems to be key to inducing the acceleration/deceleration forces that lead to damage and neurological symptoms in the blast model (Goldstein et al., 2012; Gullotti et al., 2014; Tagge et al., 2018). The damage from blast TBI is more diffuse than that from either FPI or CCI with diffuse axonal injury and diffuse edema that can elevate intracranial pressure. The vascular system is especially perturbed after blast with breakdown of the blood-brain barrier and initially severe hyperemia followed later by vasospasm (Chen and Huang, 2011; Xiong et al., 2013). Blast TBI models usually show cognitive and motor impairment and increased

levels of stress as well (Cernak et al., 2011; Goldstein et al., 2012; Xiong et al., 2013). The strengths of blast models are the ability to create a more realistic mechanism of injury with a closed skull and to generate the diffuse axonal injury, one of the major hallmarks of TBI. Both of these strengths make the blast model a good candidate for studying mild TBI. However, the lack of a consistent type of blast model used in research, the simple waveforms generated by most blast tube set-ups, and the high variability of injury severity with some blast models (unpublished observation) argue for caution when considering this model.

1.3.4 Weight drop impact acceleration

Weight drop impact acceleration is another category of TBI model that has several variations. In all types a weight is dropped from a fixed height onto an animal's head. Two early versions of weight drop TBI involved either hitting the brain or the unprotected skull inducing a focal injury (Feeney et al., 1981; Shapira et al., 1988). In 1994 Marmarou introduced a weight drop model where the weight hits a metal disk (helmet) attached to the skull rather than the skull directly (Marmarou et al., 1994). The addition of the helmet allows the TBI to be closed-skull and limits the incidence of skull fracture while also inducing a diffuse injury. Throughout the brain, neurons and microvasculature are damaged, and the diffuse axonal injury that is a hallmark of human TBI is particularly common and widespread (Foda and Marmarou, 1994; Marmarou et al., 1994; Morales et al., 2005; Xiong et al., 2013). Like the other models of TBI, the Marmarou weight drop results in motor and cognitive deficits, specifically memory (Morales et al., 2005). Marmarou and previous models of weight drop have involved the

animal lying on foam padding, resulting in more of a compression-type of injury rather than acceleration. However, the acceleration force is thought to be the primary cause of concussion or mild TBI (Meaney and Smith, 2011), and as mentioned above previous studies in blast showed the importance of head movement for creating neural damage and deficits (Goldstein et al., 2012; Gullotti et al., 2014; Tagge et al., 2018), suggesting the Marmarou model could be improved. Keeping the animal stationary also increases the risk of an accidental secondary impact if the weight rebounds and falls on the animal again. To increase the accelerating head movement upon impact and prevent unwanted secondary injury, Kane proposed placing the animal on perforated foil that easily tears when the weight falls and propels the animal down onto foam padding in a rotational movement (Kane et al., 2012). This modified weight drop model is designed for a mild form of injury so it does not use helmets and results in minor motor deficits and immune responses on repeated impact. Overall, the weight drop models of TBI succeed in recreating the characteristic human pathology (diffuse axonal injury) and are more biologically relevant than open-skull models of injury. The modification by Kane and colleagues to incorporate greater acceleration forces significantly increases the similarity to mild TBI in humans.

1.4 A CASCADE OF PROCESSES

Although research has identified many of the pathologies occurring after TBI and developed multiple animal models to simulate human injury, there is still no clinically-proven treatment for TBI. All Phase III clinical trials for TBI have failed. A major obstacle to developing a treatment is the limited understanding of the *many* biochemical

processes that take part in the pathologies after injury and how these different processes interact. For example, consider two different pathways that both lead to loss of synapses: In pathway 1 TBI leads to damaged membranes surrounding axons resulting in impaired axonal transport and eventually complete severing of the axon and thus loss of downstream synapses (Povlishock and Katz, 2005). In pathway 2 TBI decreases CBF, depriving neurons of the oxygen and glucose necessary to maintain ionic gradients and neural communication. The imbalance of ion homeostasis, especially calcium, puts added stress onto the mitochondria that attempt to buffer ions, leading to anaerobic metabolism and release of reactive oxygen species that cause more oxidative stress (Weber, 2012). With enough stress and damage neurons will die, eliminating their synaptic contact. In these two pathways, the seemingly different processes of axonal damage and reduced cerebral blood flow can produce the same result of synapse loss, but it can be difficult to determine which pathway caused the effect and should be targeted for treatment. Furthermore, these two pathways also likely interact. The damage to axonal membranes that leads to impaired axonal transport has been shown to occur via influx of sodium and calcium ions (Maxwell et al., 1997) so ionic gradients are also disrupted in this pathway, which creates a larger energy demand to reestablish normal ionic concentrations, but energy supply may decreased by the drop in CBF or just by damaged mitochondria overwhelmed by the rise in calcium ions. With so many different processes that cascade to other processes or aggravate other ongoing processes, how do we identify the best target for treatment? The approach we have taken is to: 1) examine a variety of key and related functions: synaptic input, neural activity, and CBF, and 2) look for changes in

these functions early after mild TBI. If we can determine what some of the earliest changes after TBI are, we will have a better idea of what pathway to target in order to prevent the cascade of harmful processes downstream and mitigate the worsening of other processes currently under way.

1.5 OUR APPROACH: EARLY RESPONSES TO WEIGHT DROP INJURY

Firstly, we decided to focus on mild TBI since it is by far the most common type of head trauma (Cassidy et al., 2004), and offers the strongest possibility for effective treatment compared to more severe forms of TBI. To induce mild TBI we used a modified Marmarou weight drop model that included setting our animals on perforated foil to maximize acceleration forces. The FPI and CCI models involve directly impacting the exposed brain, limiting their biological relevancy and creating a focal injury. The blast model produces a diffuse injury, but not as much diffuse axonal injury as the weight drop models, and we encountered high levels of injury severity variability when previously using a blast model. Weight drop models use a realistic mechanism of injury that is closed skull and effectively reproduce diffuse axonal injury. The modification to add more acceleration forces only further increases the similarity to mild TBI in humans.

For our measurements we chose synaptic input, neural activity, and CBF since these are three vital parts of proper neural function and there are still large questions remaining as to what happens to them following TBI, especially within the first couple of hours after injury. The questions are described in more detail in the chapters that follow, but we will summarize them here briefly.

Because TBI leads to cognitive, sensory, and emotional deficits, researchers have tried to understand how activity in neurons responsible for these higher-level functions and synaptic input that drives neural activity is altered after injury. However, as discussed in the pathologies above, there has been a lack of consensus on the direction and time course of changes in activity after TBI. Studies measuring neural activity continuously or repeatedly at close time points show that levels of activity rapidly evolve after injury and can even switch directions from reduced to elevated activity so the conflicting findings among the field may be the result of differences in time of measurement (Ding et al., 2011; Hansen et al., 2018; Kharatishvili et al., 2006). Synaptic input, on the other hand, has rarely been examined in the first two hours of injury despite the prevalence of axonal injury and the findings that a decrease in synaptic activity is one of the first consequences of ischemia (Hofmeijer and Putten, 2012) when TBI also produces a significant drop in CBF (Jullienne et al., 2016). Detection of sudden shifts in activity, the frequency of axonal injury, and the fact that one injury-induced change can trigger a cascade of other harmful processes led us to examine both neural activity and synaptic input within the first hour of mild TBI to determine how neural function is initially disrupted.

For synaptic input, we measured both an early (1 hour) and intermediate (48 hours) time points to better elucidate the time course of synaptic changes. While many previous studies on TBI have focused on the hippocampus, we wanted to look at cortex because of its role in cognition and sensory processing that are affected by injury. Examining changes in sensory cortices in particular is advantageous since the cortical circuits and processing in these regions under normal conditions are well-known, and

sensory input is finely tunable allowing for detection of small differences in function that could be especially important for determining changes after mild TBI. Of the difference sensory cortices, we measured synaptic input in the piriform cortex because of the neuroinflammation we observed there within 24 hours of mild TBI. We found that there was greater excitatory input on pyramidal cells in the piriform cortex in acute slices made 1 hour after injury. Excitatory and inhibitory inputs were rebalanced at 48 hours after injury though, highlighting the importance of studying early time points.

To explore if changes in synaptic input and other processes alter neural activity in the acute phase of mild TBI, we performed *in vivo* calcium imaging of layer II/III pyramidal cells in the visual and barrel cortex. Since injury frequently reduces CBF, induces an immune response, and changes the extracellular space with elevated glutamate and potassium, we made our measurements of neural activity *in vivo*. With calcium imaging, we were able to examine neural activity over a larger population of cells and at a higher spatial resolution than electrophysiological techniques used in previous studies. We found a drastic suppression of neuronal firing in most cells, but a subset of cells became hyperactive about 1 hour after mild TBI. Other indicators of disturbed physiology were apparent, including prolonged elevation of intracellular calcium and spreading waves of increased calcium. *In vivo* imaging of neural activity confirmed rapid changes occur in multiple aspects of neural function and that these changes can be heterogeneous throughout the cell population so high spatial resolution techniques are valuable.

The early alterations in synaptic input, neural activity, and loss of calcium homeostasis may be due to a lack of energy from reduced CBF. Although a drop in CBF is well-established after TBI, there is a lack of information on blood flow through the microvasculature where oxygen and glucose delivery occur. However, previous work *post-mortem* shows structural and thus presumably functional changes in arterioles and capillaries (Daneyemez, 1999; Dietrich et al., 1994; Rodríguez-Baeza et al., 2003). We measured CBF *in vivo* at the resolution of individual capillaries in the visual cortex at multiple time points from 5 minutes to 3 weeks following TBI to determine the extent and time course of CBF disruption there. We found that CBF was substantially decreased within the first 10 minutes of mild TBI with significant vasoconstriction and dramatic increases in capillary stalling. CBF recovered by ~2 hours after injury, but the reduction in flow was almost certainly great enough to disrupt physiology and potentially account for the changes in synaptic input and neural activity that we observed.

With these three measurements of neural function and CBF, we have a better understanding of what alterations occur after mild TBI, especially in the acute phase of injury. Knowing more about what changes occur and the time course of these changes is key to developing a treatment for mild TBI. The following three chapters elaborate on the question, described the measurements, and explain our findings and their significance. In the final chapter we discuss the overall impact of our results and what they suggest about future directions to take for further elucidating the problem of mild TBI and potential therapeutic treatments.

CHAPTER TWO

Rapid Changes in Synaptic Strength after Mild Traumatic Brain Injury

2.1 INTRODUCTION

An estimated 2.8 million Americans suffer a traumatic brain injury (TBI) every year (Taylor et al., 2017), leading to debilitating symptoms such as seizures, cognitive impairment, emotional instability, and sensory deficits (Levin et al., 1987; Levin et al., 1990; Lew et al., 2007; McKee et al., 2009; Rimel et al., 1981). Mild injuries are most common, accounting for ~80% of cases (Cassidy et al., 2004). Although mild TBI causes little to no gross damage to neural tissue, its effects often persist for months or even years, significantly impacting employment and quality of life (Carroll et al., 2004; Rimel et al., 1981). Repeated injury significantly worsens both pathology as well as cognitive and motor impairments (DeFord et al., 2002; Laurer et al., 2001; Mouzon et al., 2012). Despite the high prevalence of mild TBI, treatment options remain limited due to our poor understanding of how injury affects neural function, especially in the acute phase after trauma.

Substantial evidence points to deficits in both structural and functional connectivity after mild TBI. Diffuse axonal injury is common, particularly in long-range projections, suggesting potential disruptions in network connectivity (Caeyenberghs et al., 2014; Pandit et al., 2013). TBI is also strongly linked to loss of excitatory-inhibitory (E-I) balance, acute seizures and post-traumatic epilepsy in both humans and animal models, and reduced thresholds for pharmacologically-induced seizures in rodents (Annegers et al., 1998; Chadwick, 2000; Golarai et al., 2001; Kharatishvili et al., 2006;

Lee and Lui, 1992; Nilsson et al., 1994; Zanier et al., 2003). While overt seizures are less common in mild injury, E-I imbalances have also been described. The hippocampus show increased excitability and spontaneous firing within 24 hours of mild TBI *in vitro*, and signs of reduced inhibition at 48 hours *in vivo* (Griesemer and Mautes, 2007; Reeves et al., 1997). However, other studies found opposing effects, with early increases in inhibition onto CA1 pyramidal cells and reduced excitatory efficacy one week later (Santhakumar et al., 2000; Witgen et al., 2005). While cortical effects are less well characterized, existing data also suggest disparate and time-varying effects on E-I balance. Activity in somatosensory cortex was suppressed within 24 hours after injury *in vivo* (Alves et al., 2005; Johnstone et al., 2013), but *in vitro* data showed increased excitatory input and action potential firing from 48 hours to one week post-TBI, and epileptiform activity 1-4 weeks later (Greer et al., 2012; Yang et al., 2010).

While some discrepancies may arise from differences in injury model or experimental system, the complex temporal dynamics of injury responses could also be a key factor. Ding and colleagues (2011) showed that cortical activity underwent a transition from initial suppression to dramatically elevated excitability at approximately two hours following injury, indicating that TBI responses can evolve rapidly during this early time window. While TBI effects begin to manifest immediately, few studies have addressed the acute periods spanning the first few hours after injury. Of these, only a handful have directly measured intracellular or synaptic function (Griesemer and Mautes, 2007), so that the neural mechanisms underlying dynamic changes in cortical responsiveness remain open.

Here we examined how mild TBI impacts both excitatory and inhibitory synaptic interactions in cortical circuits, including both a commonly used 48 hour time point, but also testing at 1 hour post-injury to probe acute injury stages. Using a modified weight drop model allowing free head movement typical of human injury, we consistently found localized neuroinflammatory responses in piriform cortex and neighboring entorhinal areas. To test for associated functional changes, we used whole-cell recordings in acute brain slices to examine synaptic input onto piriform pyramidal neurons at 1 hour and 48 hours after injury. Synaptic function was largely normal at 48 hours, but excitatory inputs were substantially increased at 1 hour post-TBI. Our data indicate that mild injury causes rapid disruptions in a cortical region that has received little attention, emphasizing the need to consider dynamic effects during immediate post-TBI periods that will be vital to identifying interventions matched to different phases of the injury response.

2.2 MATERIALS AND METHODS

2.2.1 Mice

All experiments were performed in adult male and female C57BL/6J mice 2-5 months of age. Animals were group housed in Boston University's animal care facility on a 12 hour light/dark cycle with *ad libitum* access to food and water. All procedures were performed in accordance with the Boston University Institutional Animal Care and Use Committee.

2.2.2 Injury model

Mild TBI was induced with a modified Marmarou model where a weight is dropped onto a metal helmet attached to the animal's skull (Marmarou et al., 1994) and the animal is unrestrained to allow free movement of the head and body to recapitulate the acceleration

and shear forces characteristic of human injury (Kane et al., 2012; Meaney and Smith, 2011). Prior to injury, animals were briefly anesthetized, the scalp over the midline was removed, and a stainless steel cylinder was cemented onto the midline at bregma (4 mm diameter; 4 mm tall; Zap Gel, Pacer; C&B Metabond, Parkell). After 3-7 days, mice received buprenorphine analgesia (0.125 mg/kg, subcutaneous), were briefly anesthetized with isoflurane, and placed on top of perforated foil in a custom-made TBI apparatus. A 150-200 g weight secured to fishing line (Stren high impact, Pure Fishing, Inc.) was dropped 150-240 cm through a guide tube onto the helmet implant, propelling the animal through the foil onto foam padding below (5 cm upholstery foam, Mybecca). The fishing line was set to a length that would prevent the possibility of double-hit injury. Animals were monitored in a cage on a heating pad until sternal.

2.2.3 Behavioral testing

We confirmed the efficacy of our injury model by investigating vestibulomotor deficits using a custom rotarod apparatus. Mice were placed on a rod that remained stationary for 10 seconds and then steadily accelerated from 4-40 rpm over 5 minutes. Performance was quantified as the latency to fall. Naïve mice were tested daily (3 trials, 5 minutes inter-trial interval) for 5 days before injury, at 1 hour following TBI on each injury day, and daily for 1 week afterwards.

2.2.4 Immunohistochemistry

In a separate cohort, we examined microglial activation with immunostaining for Iba1, a common neuroinflammatory marker for microglia and macrophages, at time points immediately after two injuries and 24 hours after three injuries. Mice were heavily

anesthetized with isoflurane and transcardially perfused with ice-cold artificial cerebral spinal fluid (ACSF) followed by 4% paraformaldehyde in 0.1 M phosphate buffer (PB). Brains were harvested and post-fixed overnight in 4% paraformaldehyde in 0.1 M PB at 4°C before undergoing a sucrose series and cryosectioning at 40 µm. Sections were blocked with 5% normal donkey serum in 0.1 M PB with 0.3% Triton X (PBTx) for 1 hour at 25°C then incubated overnight in anti-Iba1 rabbit polyclonal antibody 019-19741 (1:1000; Wako Chemicals, USA) diluted in PBTx at 4°C. The primary antibody was visualized by incubating with Alexa Fluor 488 donkey anti-rabbit secondary (1:500; Jackson ImmunoResearch Laboratories, West Grove, PA) diluted in PBTx for 2 hours at 25°C. Sections were imaged on a FluoView 300 confocal microscope (Olympus, Center Valley, PA) using a 20x 0.5NA objective and analyzed with ImageJ (NIH, Bethesda, MD).

2.2.5 Electrophysiology

Animals were heavily anesthetized with ketamine/xylazine and transcardially perfused with ice-cold slicing solution containing, in mM: 124 NaCl, 2.5 KCl, 1.25 NaH_2PO_4, 25 $NaHCO_3$, 75 sucrose, 10 glucose, 1.3 ascorbic acid, 0.5 $CaCl_2$ and 7 $MgCl_2$. Acute coronal slices (300 µm) of piriform cortex were cut with a vibratome using standard techniques (VT1200S, Leica, Buffalo Grove, IL). Slices were then transferred to ACSF containing, in mM: 124 NaCl, 3 KCl, 1.25 NaH_2PO_4, 26 $NaHCO_3$, 20 sucrose, 2 $CaCl_2$ and 1.5 $MgCl_2$, continuously oxygenated with 95/5% O_2/CO_2. Slices were visualized with a two-photon (2P) microscope (Ultima, Prairie Technologies, Middleton, WI) using a 40x 0.8NA objective and Dodt contrast imaging. Whole cell voltage clamp recordings were

made with electrodes (3-7 MΩ tip resistance) filled with internal solution containing, in mM: 10 HEPES buffer, 10 phosphocreatine disodium, 5 QX314-Cl, 3 MgATP, 0.5 NaGTP, and 0.5 EGTA. Recorded cells were visualized with Alexa 594 to confirm cell type. Membrane voltage was not corrected for liquid junction potential. Spontaneous and evoked excitatory and inhibitory postsynaptic currents (EPSCs and IPSCs) were recorded from superficial pyramidal cells with a Multiclamp 700B amplifier (Molecular Devices, Sunnyvale, CA) and digitized at 10 kHz (National Instruments PCI-6321) using custom Matlab routines (Mathworks, Natick, MA). Evoked synaptic responses were elicited by stimulating the lateral olfactory tract with glass microelectrodes (1-3 MΩ tip resistance) filled with ACSF using a stimulation isolator (World Precision Instruments, Sarasota, FL). Spontaneous synaptic currents were analyzed in Igor Pro (WaveMetrics, Lake Oswego, Oregon) using Taro Tools (https:sites.google.com/site/tarotoolsmember/).

2.2.6 Data Analysis

Animals were pseudo-randomly assigned to sham or TBI groups. All results are reported as distributions or single values are reported as mean ± SEM. Statistical significance was calculated using two-sample Kolmogorov-Smirnov tests for distributions, or paired or two-sample t-tests for means as noted in the results and figure legends. A p value of < 0.05 was considered statistically significant.

2.3 RESULTS

2.3.1 Mild injury induces behavioral deficits and neuroinflammation

We induced mild TBI using an unrestrained weight-drop model where free head movement recapitulates the acceleration and shear forces characteristic of human injury

(Kane et al., 2012; Meaney and Smith, 2011). We first confirmed that our model induced behavioral deficits and neuropathology consistent with mild TBI effects in previous studies. We delivered three repeated injuries at 24 hour intervals (150 g, 150 – 190 cm), and assessed vestibulomotor performance using a rotarod assay, starting 5 days before the injury series and continuing for 1 week afterwards (**Fig 2.1 A**-**B**). While pre-injury performance was similar in both groups, TBI significantly reduced latency to fall relative to sham mice over the three injury days (**Fig 2.1 C**: 92 ± 12 and 55 ± 13 seconds for sham and TBI groups; Two-sample t-test; $p = 0.002$). Within the TBI group, injury also significantly reduced latency to fall relative to initial baseline levels (85 ± 11 and 55 ± 13 seconds averaged over 3 baseline and injury days; Paired t-test; $p = 0.0002$). Performance in the sham group improved over the same time period, likely from a practice effect (75 ± 11 and 92 ± 12 seconds averaged over 3 baseline and injury days; paired t-test, $p = 0.007$). Deficits were also apparent after normalizing each animal's performance to pre-injury levels (**Fig 2.1 D**: 131 ± 10 and 70 ± 16 % averaged over 3 injury days for sham and TBI groups; Two-sample t-test; $p = 0.005$). The greatest deficits occurred on the first and third days of injury (**Fig 2.1 B**: KS test; $p = 0.019$ and $p = 0.034$ for the days 0 and 2). While performance of the TBI group recovered steadily to near-baseline levels over the following week, it was still reduced relative to sham animals at days 7-9 (**Fig 2.1 D**: 118 ± 14 % and 71 ± 9 % of pre-injury levels for sham and TBI groups; Two-sample t-test; $p = 0.012$). This partial recovery is consistent with other mild TBI studies (Koliatsos et al., 2011; Yang et al., 2013). Overall, we found a transient but reliable motor deficit consistent with mild injury.

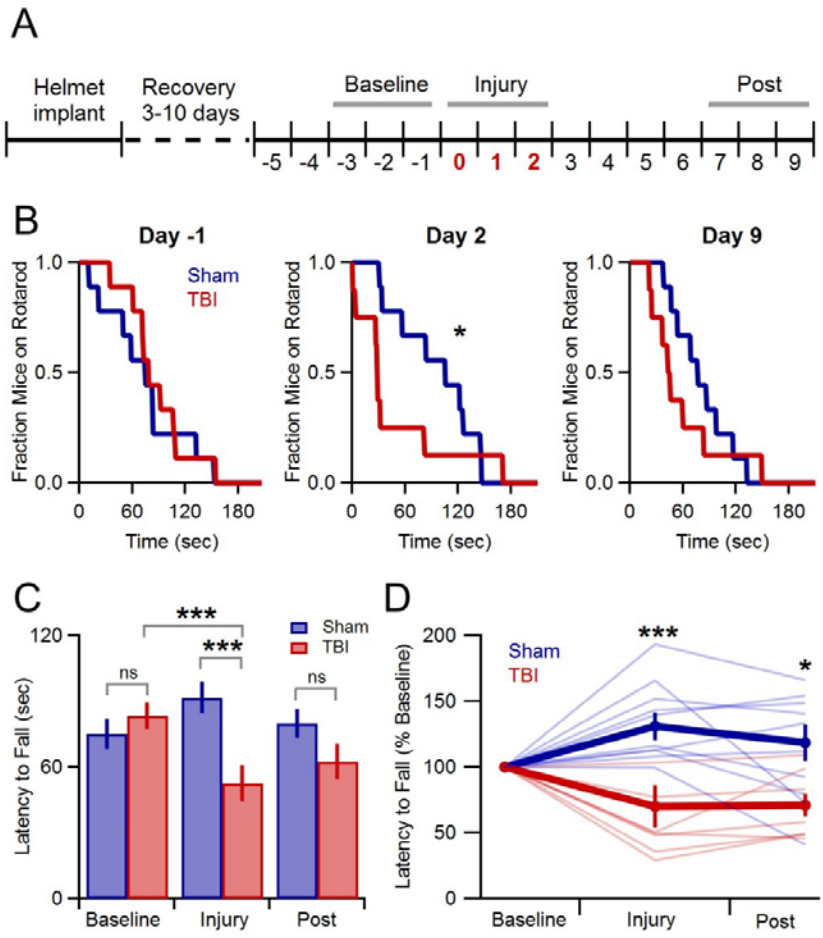

Figure 2.1 Transient Vestibulomotor Deficits after TBI
(**A**) Timeline of locomotor testing. Latency to fall was measured daily, and averaged over 3-day windows before, during, and after injury as shown. (**B**) Fraction of mice remaining on the rotarod over time shown for periods before, during, and after injury. Performance was similar for sham and TBI groups before injury (Day -1), but was reduced during the TBI period (Day 2) (KS test; $p = 0.034$; $k = 0.639$; $n_{(sham)} = 9$, $n_{(TBI)} = 8$ mice). (**C**) Mean latency to fall for each time period, showing decreased performance of TBI mice during the injury period (Paired t-test; $p = 0.0002$; $t(23) = 4.394$; $n = 8$ mice) and compared to sham mice during the injury period (Two-sample t-test; $p = 0.002$; $t(49) = -3.242$; $n_{(sham)} = 9$, $n_{(TBI)} = 8$ mice). (**D**) Pooled data showing shorter latency to fall for TBI relative to sham groups during the injury phase (Two-sample t-test; $p = 0.005$; $t(15) = 3.321$; $n_{(sham)} = 9$, $n_{(TBI)} = 8$ mice) and the recovery phase (Two-sample t-test; $p = 0.012$; $t(15) = 2.866$; $n_{(sham)} = 9$, $n_{(TBI)} = 8$ mice). * and *** indicate $p < 0.05$ and $p < 0.01$.

In addition to behavioral disruptions, TBI commonly leads to neuropathology including pro-inflammatory responses in astrocytes and microglia, which develop a swollen 'activated' morphology, migrate to the injury site, and release inflammatory cytokines (Kreutzberg, 1996; Loane and Byrnes, 2010; Nimmerjahn et al., 2005; Streit, 2000). Microglial activation is reliably seen across diverse TBI models (Davalos et al., 2005; Goldstein et al., 2012; Kaur et al., 1995; Shitaka et al., 2011; Tagge et al., 2018; Xu et al., 2016). To probe neuroinflammatory responses, we used Iba1 immunohistochemistry to label microglia and macrophages (Imai et al., 1996; Ito et al., 1998) and examined their morphology across a wide range of brain areas including neocortex, hippocampus, striatum, and piriform and entorhinal cortices (**Fig 2.2**). While microglia in sham animals appeared normal (**Fig 2.2 A, C, E, G**), TBI led to pronounced morphological changes including swollen somata and processes indicative of activation (**Fig 2.2 F, H**). Neuroinflammation was apparent at 24 hours following 3 injuries, and in one case immediately following the second injury. Microglial activation was reliably localized to the lateral inferior temporal lobes, particularly to piriform and entorhinal cortices (**Fig 2.2 F, H**) and olfactory tubercle (not shown), regions that have received little attention in TBI. Interestingly, we rarely found activation directly under the injury site or in the hippocampus (**Fig 2.2 B, D**), where is has commonly been seen after more severe injury (Reeves et al., 1997; Reeves et al., 1995; Santhakumar et al., 2000; Santhakumar et al., 2001; Witgen et al., 2005), perhaps due to differences in severity, impact site, or head movement in our model. Overall, however, these reliable and localized inflammatory responses are consistent with mild injury.

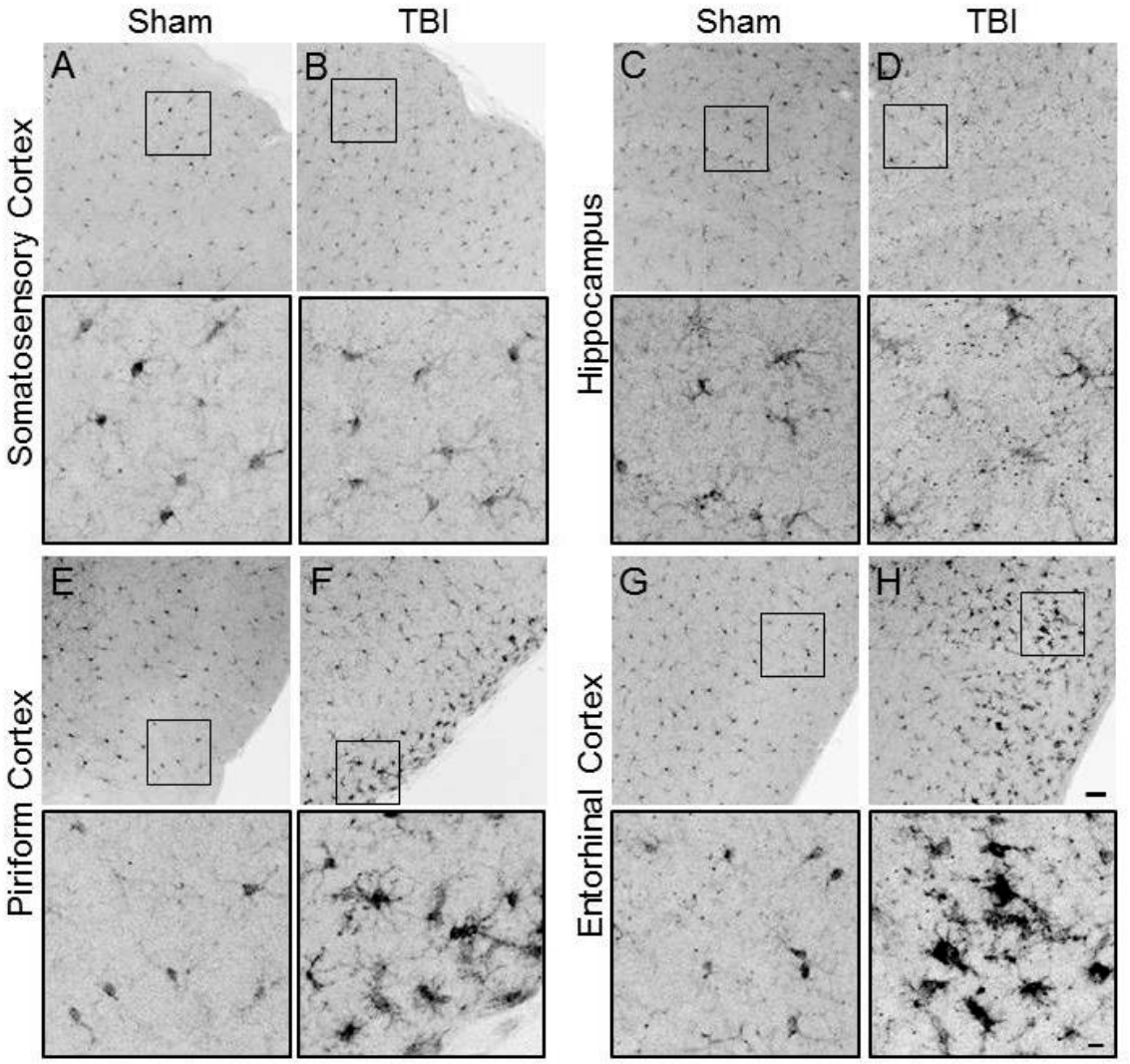

Figure 2.2 Mild injury leads to microglial activation in lateral inferior temporal lobes

(**A-H**) Iba1 immunostaining reveals microglial morphology in diverse brain regions at 24 hours following repeated mild injury. In most regions, microglia appeared largely similar between sham and TBI mice (**A-D**), but piriform (**E-F**) and entorhinal areas (**G-H**) consistently showed clusters with a swollen appearance characteristic of neuroinflammatory response in piriform and entorhinal areas. No activated microglia were seen in sham mice. Scale bars are 50 and 10 μm. $n_{(sham)} = 3$, $n_{(TBI)} = 4$ mice.

2.3.2 Synaptic input onto pyramidal neurons is unchanged 48 hours post-injury

TBI-induced deficits may arise at least in part from disrupted synaptic communication. While prior work has shown both increased cellular excitability (Griesemer and Mautes, 2007) and diffuse axonal injury leading to functional disconnection (Pandit et al., 2013), there are few direct measurements of how synaptic input is affected by mild TBI. The consistent presence of neuroinflammation in piriform led us to use this region to probe the functional effects of mild injury. We used whole-cell recordings in acute brain slices to test for TBI-induced changes in synaptic strength, examining both spontaneous and evoked synaptic input onto superficial pyramidal cells, the major excitatory cell type in this brain area (**Fig 2.3**).

Despite finding reliable microglial activation in piriform, we observed little change in spontaneous synaptic currents measured 48 hours after mild TBI. The mean amplitude of excitatory events was not statistically different between sham and TBI groups (**Fig 2.3 A, C**: 10.8 ± 1.0 and 10.1 ± 1.2 pA for sham and TBI; Two-sample t-test; $p = 0.652$). Frequency was similarly unchanged (**Fig 2.3 E**: 5.4 ± 1.2 and 7.2 ± 1.4 Hz for sham and TBI; Two-sample t-test; $p = 0.357$). While the more sensitive Kolmogorov-Smirnov (KS) test did detect a significant shift in the distributions of both amplitude and interevent interval, this effect was modest (**Fig 2.3 B, D**: KS tests; $p = 0.009$ and $p = 0.0003$ for amplitude and interevent interval). Overall, our data showed minimal effects on excitatory synaptic inputs.

TBI has also been linked to changes in inhibitory function (Reeves et al., 1997; Smith et al., 2015; Witgen et al., 2005), which plays a prominent role in balancing local

excitatory networks in piriform (Bolding and Franks, 2018; Franks et al., 2011; Large et al., 2016; Luna and Schoppa, 2008; Sheridan et al., 2014; Suzuki and Bekkers, 2011). Recording from the same pyramidal neurons, we examined inhibitory input by holding at excitatory reversal potential (+5 mV) (**Fig 2.3 F**). Similar to excitatory input, there was little to no change in either mean amplitude or frequency of sIPSCs after injury (**Fig 2.3 H, J**: Amplitude = 16.0 ± 1.2 and 15.6 ± 0.8 pA for sham and TBI; Two-sample t-test; p = 0.750; Frequency = 5.8 ± 0.7 and 5.1 ± 0.4 Hz for sham and TBI; Two-sample t-test; p = 0.354). Again, the higher-sensitivity KS test revealed a shift towards increased sIPSC intervals after injury (**Fig 2.3 I**: KS test; p = 0.026), but this effect was small in size. Altogether, both excitatory and inhibitory inputs were similar in sham and TBI animals, suggesting that injury either had minimal impact on synaptic transmission or that compensatory effects were already recruited at 48 hours after injury.

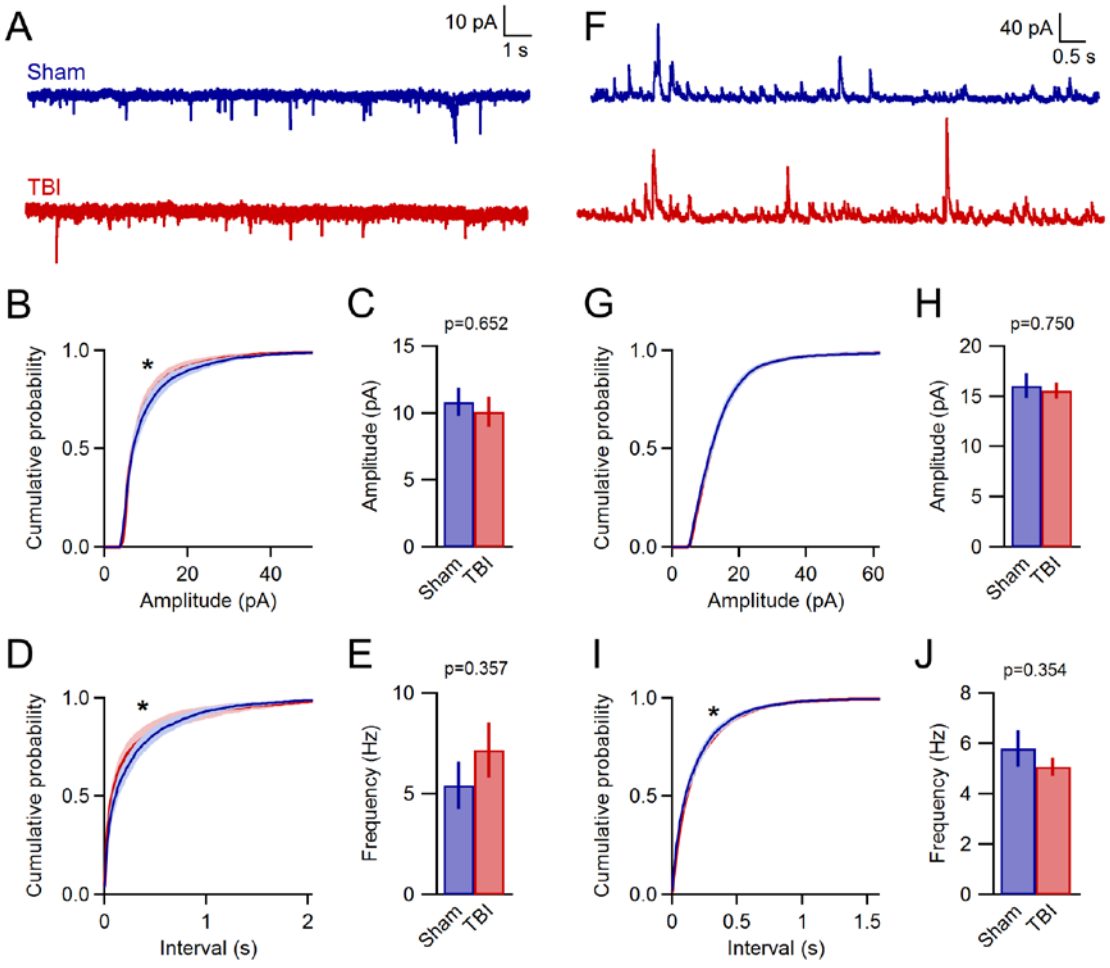

Figure 2.3 Spontaneous synaptic input is unchanged 48 hours post-injury
(**A**) Whole cell recordings of excitatory input onto superficial pyramidal cells in piriform cortex. (**B-C**) Amplitudes of excitatory events showed little to no change after TBI. Left, cumulative histograms (KS test; p = 0.009; k = 0.056; $n_{(sham)}$ = 1750, $n_{(TBI)}$ = 1377 events). Right, mean values (Two-sample t-test; p = 0.652; t(29) = -0.456; $n_{(sham)}$ = 9 mice, 14 cells; $n_{(TBI)}$ = 11 mice, 17 cells). (**D-E**) Interevent interval and mean frequency for excitatory events. The sEPSC interval distribution shifted slightly towards smaller values after TBI (KS test; p = 0.0003; k = 0.074; $n_{(sham)}$ = 1750, $n_{(TBI)}$ = 1377 events) but mean values were not significantly changed (Two-sample t-test; p = 0.357; t(29) = -0.937; $n_{(sham)}$ = 9 mice, 14 cells, $n_{(TBI)}$ = 11 mice, 17 cells). (**F**) Spontaneous inhibitory inputs onto the same superficial pyramidal cell recorded at excitatory reversal potential. (**G-H**) Cumulative histograms and mean values for sIPSC amplitude, which was unchanged by TBI (KS test; p = 0.300; k = 0.021; $n_{(sham)}$ = 2744, $n_{(TBI)}$ = 3213 events; Two-sample t-test; p = 0.750; t(29) = -0.322; $n_{(sham)}$ = 9 mice, 14 cells, $n_{(TBI)}$ = 11 mice, 17 cells). (**I-J**) Cumulative histogram of the interevent interval and mean bar graph of the frequency of inhibitory events. TBI led to a very slight decrease in frequency of

inhibitory inputs as seen by distributions but not by comparing means (KS test; p=0.026; k = 0.038; $n_{(sham)}$ = 2744, $n_{(TBI)}$ = 3213 events; Two-sample t-test; p=0.354; t(29) = 0.942; $n_{(sham)}$ = 9 mice, 14 cells, $n_{(TBI)}$ = 11 mice, 17 cells). * indicates $p < 0.05$ in KS tests.

Finally, to further probe how injury acts on piriform circuit function, we measured electrically evoked responses upon stimulating afferent axons of the lateral olfactory tract (LOT), which provides sensory input from olfactory bulb. LOT responses contain multiple components reflecting local interactions within piriform, including direct excitatory input from olfactory bulb, additional intracortical excitation from other local pyramidal neurons, and local inhibition from both feedforward and feedback inhibitory neurons (Franks et al., 2011; Large et al., 2016; Luna and Schoppa, 2008; Suzuki and Bekkers, 2007; Suzuki and Bekkers, 2011). Given the importance of E-I balance in cortical function in general (Xue et al., 2014), and in piriform in particular (Bolding and Franks, 2018), we tested how injury affects the relative contributions of excitation and inhibition in piriform pyramidal cells. Similar to spontaneous measurements, we first isolated excitatory inputs by holding at -70mV. LOT stimulation produced rapid onset, presumably monosynaptic EPSCs, as well as a secondary component due to local recurrent circuits. For consistency, we adjusted stimulus intensity to elicit similar levels of input in each cell (~200pA). We then measured corresponding GABAergic currents at the same stimulus intensity while holding at excitatory reversal (+5mV). Inhibitory currents scaled with excitatory responses but were typically larger, consistent with previous data in both piriform and neocortex and reflecting the higher conductance of $GABA_A$ receptors (Franks et al., 2011; Haider et al., 2012; Isaacson and Scanziani, 2011; Large et al., 2018; Large et al., 2016; Xue et al., 2014). We quantified an E/I ratio for

each cell based on the peak amplitudes of excitatory and inhibitory currents. Consistent with the minor effects on spontaneous input, E/I balance was not significantly altered at 48 hours after injury (**Fig 2.4**: 0.316 ± 0.033 and 0.386 ± 0.040 ratio for sham and TBI groups; Two-sample t-test; p = 0.185). These data further suggest that synaptic communication is either unaffected by mild injury, or has largely recovered at 48 hours.

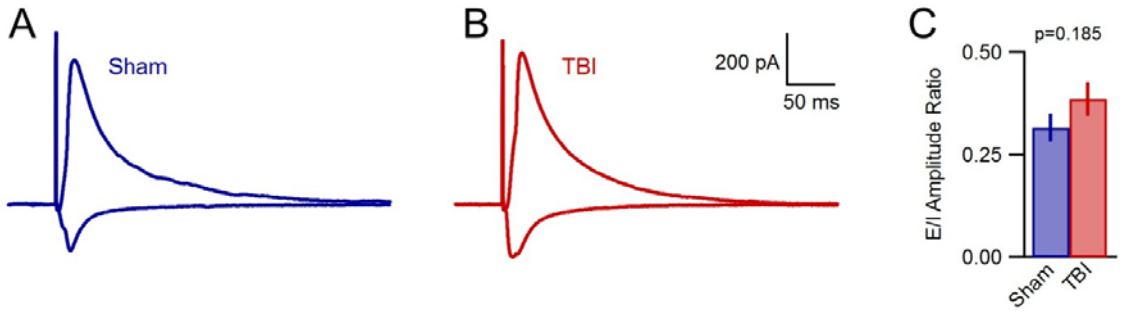

Figure 2.4 Excitatory-inhibitory balance remains stable at 48 hours post-injury (**A-B**) Excitatory and inhibitory inputs in the same piriform pyramidal cell upon electrical stimulation of the LOT. (**C**) There was little change in the ratio of excitatory to inhibitory amplitudes at 48 hours after TBI, suggesting that synaptic inputs were either unaffected by TBI or had already recovered at this time point (Two-sample t-test; p = 0.185; t(29) = -1.357; $n_{(sham)}$ = 9 mice, 16 cells, $n_{(TBI)}$ = 9 mice, 15 cells).

2.3.3 Mild TBI drives rapid loss of E-I balance at one hour post-injury

The lack of synaptic changes was unexpected given the behavioral and neuroinflammatory effects we observed. Compensatory effects may already contribute to recovery by 48 hours (Greer et al., 2012; Griesemer and Mautes, 2007), leading us to ask whether synaptic changes occur on faster timescales. A few *in vivo* studies have observed

rapidly evolving TBI responses during the hours after injury, including successive phases of reduced and heightened excitability (Ding et al., 2011; Hansen et al., 2018; Kharatishvili et al., 2006). Changes in excitability and E-I balance are a key neural consequence of TBI, and are strongly linked to seizure and post-traumatic epilepsy in human injury (Annegers et al., 1998). Although previous work has described loss of E-I balance, the direction and timing of these effects has been inconsistent across studies. Overall, there is limited data examining changes in intracellular physiology for mild closed-skull injuries, particularly within the first hours after trauma (Griesemer and Mautes, 2007; Reeves et al., 2000).We therefore tested for effects on synaptic activity in slices prepared one hour after a single injury.

In contrast to the 48-hour time point, TBI-induced changes in synaptic function were much more pronounced at one hour post-injury. TBI shifted the distributions for both sEPSC amplitude and interval towards larger and more frequent events (**Fig 2.5 A-B, D**: KS test; $p = 1e^{-08}$ for amplitude; $p = 1e^{-08}$ for interevent interval). Mean sEPSC amplitudes were also significantly increased (**Fig 2.5 C**: 8.8 ± 0.4 and 11.0 ± 0.5 pA for sham and TBI; Two-sample t-test; p = 0.002). Mean frequency showed a slight but non-significant upward trend as well (**Fig 2.5 E**: 2.8 ± 0.4 and 4.0 ± 0.4 Hz for sham and TBI; Two-sample t-test; p = 0.086). These data indicate that mild injury does in fact have clear effects on excitatory synaptic function, but that these are short-lived compared to more severe models.

Enhanced excitatory input was accompanied by a moderate shift towards shorter sIPSC intervals at one hour post-injury (**Fig 2.5 F, I**: KS test; $p = 1e^{-08}$), although mean

frequency was not significantly affected (**Fig 2.5 J**: 2.7 ± 0.3 and 3.8 ± 0.4 Hz for sham and TBI; Two-sample t-test; $p = 0.07$). Mean amplitude was also unchanged, although there was a slight shift in the sIPSC amplitude distribution (**Fig 2.5 G, H**: 12.8 ± 0.6 and 13.3 ± 0.5 pA for sham and TBI; Two-sample t-test; $p = 0.512$; KS test; $p = 0.0002$). Overall, while injury drove a moderate change in the frequency of inhibitory input onto pyramidal neurons, these changes were less substantial than the robust increase in excitatory input.

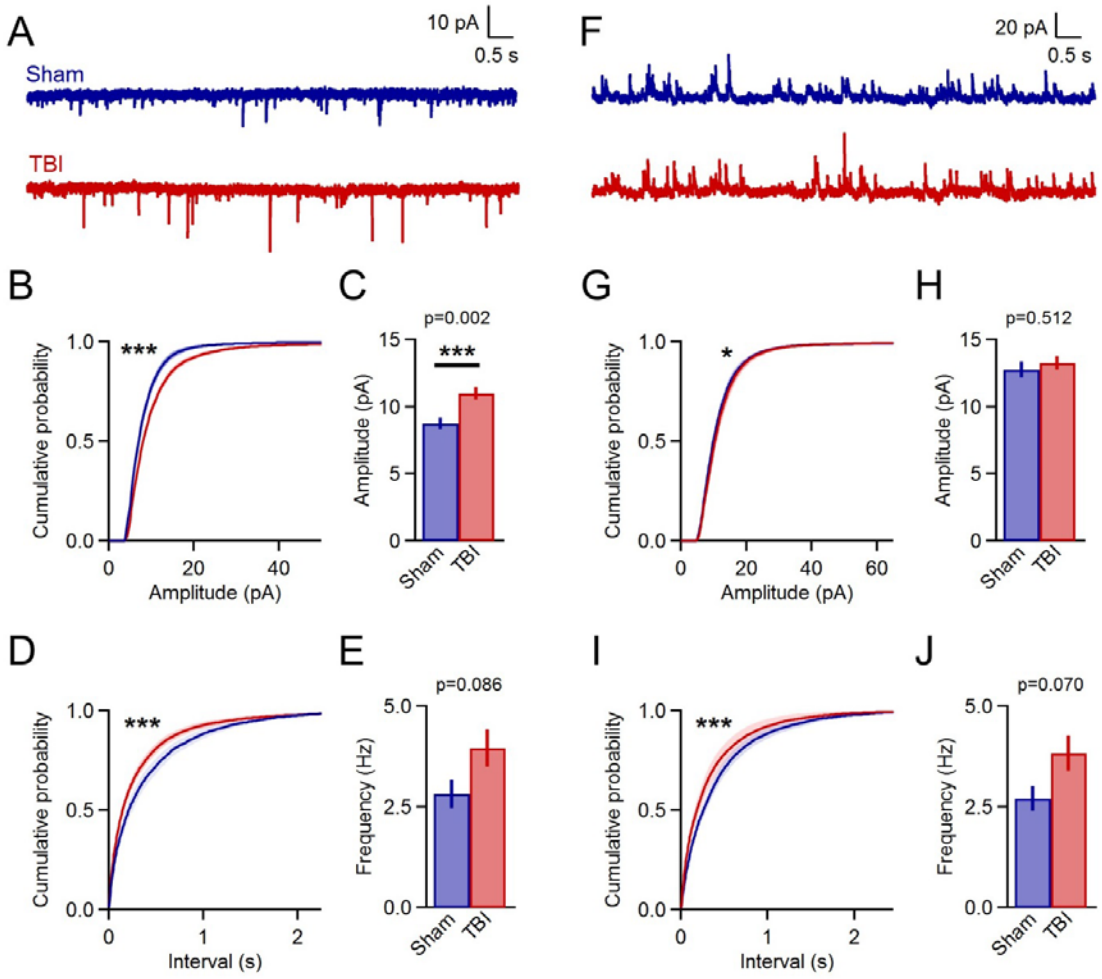

Figure 5. Rapid increases in excitatory input 1 hour after mild TBI
(**A**) Example traces showing spontaneous EPSCs onto pyramidal cells measured one hour after a single injury. (**B-C**) Cumulative histograms and mean values for sEPSC amplitudes. Excitatory events were significantly larger in the TBI group (KS test; $p = 1e^{-08}$; $k = 0.122$; $n_{(sham)} = 2016$, $n_{(TBI)} = 4050$ events; Two-sample t-test; $p = 0.002$; $t(46) = 3.201$; $n_{(sham)} = 8$ mice, 18 cells; $n_{(TBI)} = 12$ mice, 30 cells). (**D-E**) Cumulative histograms for sEPSC interval and mean frequency. Injury also increased the frequency of excitatory inputs were also more frequent after TBI as seen by examination of distributions but not for means (KS test; $p = 1e^{-08}$; $k = 0.101$; $n_{(sham)} = 2016$, $n_{(TBI)} = 4050$ events; Two-sample t-test; $p = 0.086$; $t(46) = 1.755$; $n_{(sham)} = 8$ mice, 18 cells; $n_{(TBI)} = 12$ mice, 30 cells). (**F**) Example traces showing spontaneous inhibitory inputs in superficial pyramidal cells one hour after injury. (**G-H**) TBI caused a slight increase in the amplitude distribution (KS test; $p = 0.0002$; $k = 0.049$; $n_{(sham)} = 2664$, $n_{(TBI)} = 6810$ events) but not in mean sIPSC size (Two-sample t-test; $p = 0.512$; $t(46) = 0.661$; $n_{(sham)} = 8$ mice, 18 cells; $n_{(TBI)} = 12$ mice, 30 cells). (**I-J**) TBI altered the interval distribution for inhibitory inputs (KS test; $p = 1e^{-08}$; $k = 0.102$; $n_{(sham)} = 2664$, $n_{(TBI)} = 6810$ events), but not the mean values (Two-

sample t-test; $p = 0.070$, $t(46) = 1.858$; $n_{(sham)} = 8$ mice, 18 cells; $n_{(TBI)} = 12$ mice, 30 cells). * and *** indicate $p < 0.05$ and $p < 0.01$ for t-tests, and $p < 0.05$ and $p < 0.0001$ for KS tests.

Elevated excitatory input without matching inhibitory changes could indicate a potential imbalance in these circuit elements during early injury phases. To test this idea, we again measured the excitatory and inhibitory components of evoked LOT responses at one hour after TBI. While we found a trend towards greater excitation, E-I ratios were highly variable, and this shift was non-significant (**Fig 2.6**: 0.700 ± 0.065 and 0.858 ± 0.060 ratio for sham and TBI; Two-sample t-test; $p = 0.082$). Thus, relative levels of excitation and inhibition were less affected in evoked than spontaneous inputs, perhaps due to differences in how these data emphasize afferent versus intracortical inputs. Overall, however, our major finding at one hour post-injury was a rapid increase in levels of excitatory input that were not paralleled by similar increases in inhibition, suggesting that loss of E-I balance is a common feature of both mild and severe injury.

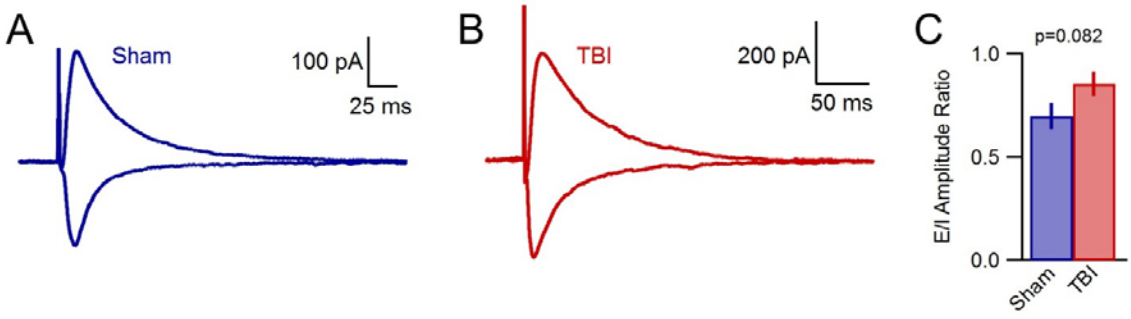

Figure 2.6 Injury has only small effects on evoked E-I balance 1 hour post-injury (**A-B**) Evoked excitatory and inhibitory inputs in piriform pyramidal cells upon LOT stimulation. (**C**) Excitatory-inhibitory ratio was slightly but non-significantly increased after TBI (Two-sample t-test; $p = 0.082$; $t(66) = -1.764$; $n_{(sham)} = 9$ mice, 28 cells**;** $n_{(TBI)} = 12$ mice, 40 cells).

2.4 DISCUSSION

While several studies have characterized changes in neural activity early after TBI, there is a lack of consensus on the direction of E-I shifts, and little work has directly addressed how synaptic interactions are affected acutely after trauma, particularly in mild forms of TBI. Here we characterized synaptic changes in piriform cortex, which showed consistent neuroinflammatory responses in our mild injury model and has been linked to generation and propagation of seizures in other paradigms. Excitatory synaptic function was only minimally affected at an intermediate 48-hr time point, in contrast to more severe models where changes last for days to weeks. At one hour after TBI, however, excitatory synaptic input was strongly enhanced and predominated over more limited changes in inhibitory input. Our data suggest that the synaptic consequences of mild TBI evolve rapidly over the hours following injury, highlighting a need to better understand the initial effects of trauma.

2.4.1 Early injury responses

The effects of TBI are often examined beginning 24 hours or later after injury, reflecting the need to understand chronic pathology. However, a few observations suggest that trauma drives complex changes on more rapid timescales. EEG recordings revealed hyperactivation and brief seizure activity in parietal cortex 1-2 minutes after cortical compression injury in rats, followed by a post-ictal depression lasting ≥2 hours (Nilsson et al., 1994). In contrast, *in vivo* Ca^{2+} imaging showed a decrease in hippocampal activity within seconds of blast injury in mice that recovered after ~60 minutes (Hansen et al., 2018). Similarly, EEG and multi-unit data in rat neocortex

revealed initial suppression 5-15 minutes after compression or percussion injury, followed by subsequent increases in excitability appearing approximately two hours after injury (Ding et al., 2011; Kharatishvili et al., 2006) and epileptic activity hours to weeks later (Kharatishvili et al., 2006). Thus, while responses to trauma may vary with brain region and injury model, they can also occur within minutes and evolve over time. Our data are consistent with dynamic injury effects, showing rapid changes in synaptic efficacy that appeared within an hour of injury but largely resolved over the ensuing 48 hours, even with repeated impacts. Given that synaptic function had largely recovered, we did not make additional measurements at later time points.

The mechanisms that drive initial synaptic changes and subsequent recovery are unclear. In addition to direct mechanical damage, TBI triggers numerous secondary cascades, including mitochondrial dysfunction and elevation of glutamate and intracellular calcium (Blennow et al., 2012; Giza and Hovda, 2014; Povlishock and Katz, 2005). Loss of homeostasis and depolarization can occur within minutes (Blennow et al., 2012; Giza and Hovda, 2014), and may contribute to the changes we observe. Axonal injury may also disrupt synaptic function but is typically thought to occur over hours to days except in cases of severe TBI (Povlishock and Katz, 2005). Recovery may occur through a variety of compensatory mechanisms that adjust excitability and synaptic strength to maintain balanced network activity. A wide range of cellular and synaptic adaptations occur over 24-48 hours after normal activity is perturbed (Ehlers, 2003; Keck et al., 2013; Turrigiano et al., 1998; Turrigiano and Nelson, 2004), and can appear as quickly 1-2 hours (Ibata et al., 2008). Structural adaptations such as axonal sprouting and

changes in dendritic spines also occur rapidly in response to disruptions such as stroke, injury, or loss of sensory input (Brown et al., 2008; Grutzendler et al., 2002; Keck et al., 2011; Majewska et al., 2006). While long-lasting synaptic changes are common in more severe injury (Alwis et al., 2012; Cantu et al., 2015; Kharatishvili et al., 2006; Santhakumar et al., 2000; Smith et al., 2015; Witgen et al., 2005; Yang et al., 2010), our data suggest that adaptive mechanisms may be engaged by 48 hours.

2.4.2 Injury and excitatory-inhibitory balance

While TBI affected both excitatory and inhibitory inputs, excitatory changes were much more pronounced. Loss of E-I balance underlies seizures and epilepsy, which are common outcomes of severe injuries in both humans and animal models (Annegers et al., 1998; Pitkanen et al., 2009). The role of the hippocampus in temporal lobe seizures and memory loss has made it a strong focus of TBI work (Chang and Lowenstein, 2003). Hippocampal function depends on its highly recurrent circuit organization, which is shared by piriform cortex, where pyramidal cells receive thousands of local intracortical connections spanning distances of ≥2 millimeters (Franks et al., 2011; Johnson et al., 2000). Piriform's highly interconnected excitatory network requires strong inhibition to prevent runaway activity (Bolding and Franks, 2018; Franks et al., 2011; Johnson et al., 2000), and is also strongly linked to seizures and epilepsy. Anterior piriform contains "area tempestas," a region highly sensitive to chemically-induced seizures (Gale, 1988; Piredda and Gale, 1985), which are propagated to other areas by posterior piriform and neighboring regions (Halonen et al., 1994; Tortorella et al., 1997). Seizure-induced hyperactivity and oxidative stress cause localized neuronal loss and atrophy in piriform

cortex in both humans and animal models of temporal lobe epilepsy (Candelario-Jalil et al., 2001; Chen and Buckmaster, 2005; Pereira et al., 2005). Despite its involvement in seizure activity in other contexts, piriform has not to our knowledge been examined after TBI.

Multiple mechanisms may underlie early enhancement of excitatory transmission. Increased sEPSC amplitudes could result from strengthening of individual postsynaptic sites via increased receptor content, as with classical activity-dependent plasticity mechanisms (Ehlers, 2003; Ibata et al., 2008; Keck et al., 2013; Turrigiano et al., 1998; Turrigiano and Nelson, 2004). Injury can also increase membrane excitability, however, and changes in levels of resting activity in the piriform network may also play a role. We did not block action potentials in order to measure spontaneous and evoked responses in the same cell, so we cannot clearly distinguish between synaptic input from spontaneous vesicle fusion and release driven by firing in other piriform neurons. Since local connections are typically composed of multiple synaptic contacts (Franks and Isaacson, 2006), elevated spontaneous activity would also generate more larger events. Similarly, changes in inhibitory frequency may reflect changes in either presynaptic release probability, spontaneous firing, or both.

Given selective enhancement of spontaneous excitatory input, the lack of significant changes in evoked E-I balance was unexpected. We note that we did find a strong trend towards increased excitation at one hour after TBI ($p = 0.082$), as well as high variability consistent with heterogeneous injury effects in both animal models and humans (Carroll et al., 2004; Lingsma et al., 2010; Xiong et al., 2013). Another possibility is that TBI acts

preferentially on intracortical associational synapses rather than ascending afferent inputs. Intracortical inputs will be emphasized in spontaneous measurements as their more proximal dendritic location will be less affected by electrotonic filtering (Bathellier et al., 2009). LOT stimulation primarily drives afferent inputs onto distal dendrites, followed by a smaller secondary input from intracortical circuits. Determining the cause of the E-I imbalance is an important question for future studies. Pharmacological methods may help test for selective changes in ascending pathways versus local intracortical circuits (Franks and Isaacson, 2005; Tang and Hasselmo, 1994).

2.4.3 Involvement of piriform in injury

We consistently found neuroinflammation in piriform and surrounding areas, which have previously received little attention in TBI research. While trauma-induced damage has been described in diverse brain areas, including somatosensory and prefrontal cortex, the majority of work has focused on hippocampus (Golarai et al., 2001; Griesemer and Mautes, 2007; Hansen et al., 2018; Reeves et al., 1997; Reeves et al., 1995; Santhakumar et al., 2000; Santhakumar et al., 2001; Witgen et al., 2005; Zanier et al., 2003). While we found mild hippocampal neuropathology in one case, it was inconsistent across animals. The reasons for selective damage in piriform and entorhinal areas are unclear but may be due to the free head movement allowed by our model. Activated microglia were most prominent in ventrolateral areas opposite the dorsal impact site, consistent with a coup-contrecoup effect causing damage on the opposite side of the brain (Courville, 1942). Piriform's extensive axonal pathways may also make it particularly sensitive to diffuse axonal injury, which tends to affect long-range

projections (Caeyenberghs et al., 2014; Pandit et al., 2013). Afferent inputs to piriform can course ≥5 mm along the base of the brain, and both intracortical fibers and piriform projections extend over longer distances than those in neocortex (Franks et al., 2011; Johnson et al., 2000). Disruptions in piriform are consistent with a broad range of sensory deficits seen in both human injury and animal models, including visual and auditory systems as well as olfaction. Further work will be needed to test whether synaptic disruptions are confined to piriform or extend more widely across other brain areas.

2.4.4 Outlook

The fast onset and subsequent recovery of synaptic changes is a key finding of our study, highlighting the need to address the complex interactions between initial damage and compensatory responses during early phases of TBI. Long-term pathology and/or neurodegeneration are initiated by processes occurring at the time of injury (Goldstein et al., 2012; McKee et al., 2009), and a deeper understanding of early time windows will be critical for targeting appropriate interventions to different injury phases. While our *in vitro* approach allowed detailed synaptic characterization, it may also relieve some factors contributing to injury in the intact brain, potentially accounting for why vestibulomotor deficits persisted at 48 hours even though synaptic changes had largely recovered. Slicing removes a large portion of network interactions and substantially reduces background activity (Hájos et al., 2009; Lipton and Whittingham, 1984; Moyer and Brown, 2002), potentially countering the effects of hyperexcitability. TBI also substantially reduces cerebral blood flow (DeWitt and Prough, 2003; Golding, 2002; Kenney et al., 2016), compounding trauma with metabolic stress. Slices are perfused with

oxygenated recording solutions that could alleviate these energetic factors. Interestingly, the increases in excitatory input we see here have parallels with synaptic responses in hypoxia, stroke, and epilepsy (Bolay et al., 2002; Fleidervish et al., 2001; Hofmeijer and Putten, 2012; Naylor et al., 2013). It will be important for future work to examine how mild injury acts *in vivo* to better capture the interactions between synaptic disruptions, altered excitability, and oxidative stress.

CHAPTER THREE

Disruptions in Neural Activity and Calcium Homeostasis after Mild Traumatic Brain Injury

3.1 INTRODUCTION

Every year an estimated 69 million people suffer a traumatic brain injury (TBI) (Dewan et al., 2018), resulting in cognitive deficits, emotional instability, and in extreme cases seizures and even death. The majority of TBIs are mild and associated with less severe or lasting symptoms (Cassidy et al., 2004), but even the mild form of injury disrupts employment and daily living. In fact by some estimates mild TBI alone costs the country almost $17 billion every year (Gerberding and Binder, 2003), providing more motivation for studying and developing a treatment for mild TBI.

Much of the previous research examining changes in neural function after TBI has centered around the hippocampus since this region plays a pivotal role in memory and temporal lobe seizures, which are both affected by injury (Annegers et al., 1998; Levin et al., 1990; Nilsson et al., 1994; Rimel et al., 1981). By comparison the neocortex has received considerably less attention, but cognitive functions dependent on the neocortex, such as sensory processing and executive function are also greatly impaired after TBI (Mattson and Levin, 1990; Proskynitopoulos et al., 2016; Stablum et al., 1996; Thiagarajan et al., 2011). Furthermore, sensory cortex specifically presents an

advantageous region for examining neural activity following injury since information processing and circuits in sensory cortex are well understood, and sensory input is finely adjustable and highly reproducible for before and after injury comparison.

The relatively few studies that have looked at activity in the sensory cortex after mild TBI have found evidence of increased excitability (Greer et al., 2012; Nilsson et al., 1994) or a combination of shifts towards excitation and inhibition depending on time of measurement after injury (Ding et al., 2011) or depth within the cortex (Johnstone et al., 2014). The lack of consensus on how neural activity is altered following mild TBI shows that further experiments are necessary to clarify how neural activity changes and highlights how results are influenced by how measurements are made. The problem of timing can be solved by repeated measurements or multiple time points, but making measurements *in vivo* versus *in vitro* or an altered state presents another issue, especially for TBI. Admittedly, answering some questions about neural function, such as synaptic inputs, typically requires *in vitro* preparations or *ex vivo* slices. However, previous work looking at pathology after TBI consistently points to changes in multiple biological systems, including the vascular and immune systems, arguing for keeping the brain and its components intact as much as possible. For example, cerebral blood flow has reliably been shown to decrease in both humans after injury and in animal models of TBI (Golding, 2002; Jullienne et al., 2016; Kenney et al., 2016). Additionally, microglia, the brain's resident immune cells, swarm to the site of damage, releasing inflammatory cytokines and ingesting debris from damaged tissue (Kreutzberg, 1996; Loane and Byrnes, 2010; Nimmerjahn et al., 2005; Streit, 2000). The nervous, vascular, and immune

systems all work together to ensure proper brain function normally, but they all affect one another after injury too, which is why making *in vivo* measurements in the brain after TBI is so critical. Some of the previous work has employed *in vivo* electrophysiological techniques, such as electroencephalography and microelectrode implants (Ding et al., 2011; Johnstone et al., 2014; Nilsson et al., 1994), but these approaches are limited in spatial resolution or range. In contrast, advances in multiphoton imaging and calcium (Ca^{2+}) indicators allow for measuring neural activity in a large population of cells at a single-cell resolution.

In this study to understand how neural function is altered after mild TBI, we compared neural activity before and after a weight drop injury using *in vivo* Ca^{2+} imaging in visual and somatosensory cortices. We found a split in activity where the majority of cells were suppressed after injury but a minority became hyperactive, showing Ca^{2+} transients for extended durations. Additionally, we also observed a loss of intracellular Ca^{2+} regulation in individual cells and occasionally throughout the cortical tissue in waves resembling cortical spreading depolarization. Overall, the altered neural activity and loss of Ca^{2+} homeostasis indicate that even mild TBI severely disrupts normal physiology in the early acute phase of injury. The heterogeneity of activity changes emphasize the value of looking at populations of cells at a high resolution in this study and in our planned future experiments.

3.2 METHODS

3.2.1 Animals and cranial window implants

All experiments were performed in transgenic mouse lines expressing the Ca^{2+} indicator GCaMP in pyramidal cells in cortical layers II/III and V (Thy1-GCaMP3 or Thy1-GCaMP6f, Jax # 017893 and 025395). Mice were 2 - 3 months in age. Animals were group housed in Boston University's animal care facility and kept on a 12 hour light/dark cycle with *ad libitum* access to food and water. All procedures were done in accordance with the Boston University Institutional Animal Care and Use Committee. Animals were implanted with acute cranial windows following established procedures. Briefly, animals were given an injection of dexamethasone (2 mg/kg, I.M.) and anesthetized with isoflurane. A cranial window (3 mm in diameter) was drilled over primary visual or barrel cortex taking care to leave the dura intact. The exposed brain was covered with 1-1.5% agarose and a glass coverslip, and sealed with adhesive (Vetbond, 3M) and dental cement (C&B Metabond, Parkell). A stainless steel cylinder (4 mm diameter; 4 mm tall) for inducing mild TBI was glued onto bregma (Zap Gel, Pacer), and a custom-made stainless steel headpost was attached to the skull with dental cement (C&B Metabond, Parkell). Animals were transferred directly from the surgery table to the 2-photon microscope for imaging after window implantation without interrupting anesthesia.

3.2.2 Injury model

Mild TBI was induced using a modified Marmarou model where a weight is dropped onto the metal cylinder attached to the animal's skull (Marmarou et al., 1994), and the animal is unrestrained to allow free movement of the head and body to recapitulate the

acceleration and shear forces characteristic of human injury (Kane et al., 2012; Meaney and Smith, 2011). After baseline imaging and about 1 minute before injury, the animal received buprenorphine analgesia (0.125 mg/kg, subcutaneous) and was placed in a custom-made TBI apparatus. A 150 g weight was dropped 110-120 cm through a guide tube onto the metal cylinder implant, propelling the animal through a perforated foil layer onto foam padding below (5 cm upholstery foam, Mybecca). The weight was secured to fishing line (Stren high impact, Pure Fishing Inc.) set to a length that prevents double-hit injury. Animals were then quickly returned to the imaging set-up with isoflurane anesthesia. The injury procedure was short enough that animals did not wake up from anesthesia.

3.2.3 2-photon (2P) in vivo Ca^{2+} imaging

Calcium signals were visualized in pyramidal cells in layer II/III of sensory cortex (visual or barrel) through the cranial window using video rate imaging with a 2P microscope (Movable Objective Microscope Sutter Instruments, Novato, CA) incorporating a Ti:Sapphire laser (920 nm, Mai Tai, SpectraPhysics, Santa Clara, CA), a 16x objective (Nikon, Melville, NY), and a resonant scanner (Hamamatsu, Bridgewater, NJ). We acquired time series for 10-15 minutes at 31 Hz and 2x magnification. Z-stacks were acquired using a 5 μm z-step at 1-2x magnification, with a 30-frame average at each depth. Data was collected using MScan software and viewed and converted to tiff stacks for analysis using MView software (Sutter Instruments).

3.2.4 Data analysis

Regions of interest (ROIs) were manually identified and raw Ca^{2+} transients were analyzed using custom Matlab routines (MathWorks Inc., Natick, MA). Briefly, signals from each ROI were converted to normalized fluorescence over baseline ($\Delta F/F_0$). Ca^{2+} events were identified for further analysis using a threshold of 3 standard deviations over resting activity, lasting for 7 frames or longer. Persistently fluorescent cells were manually identified in Z-stacks and had fluorescence signals ~2X-10X as bright as nearby background fluorescence. The 3D position of the cells relative to the z-stack was determined. For analyzing clustering of constantly fluorescent cells, the 3D positions of all neurons were identified in a separate z-stack and used as a reference to determine the average pairwise distance among different-sized groups of cells. The average pairwise distances were calculated by bootstrapping (10,000 times) from the reference of 3D positions of all cells. All results are reported as mean ± SEM, except for fluorescence waves where only 2 waves were seen. Statistical significance was calculated using paired t-tests as noted in the results and figure legends. A threshold of $p < 0.05$ was considered statistically significant.

3.3 RESULTS

To characterize cortical pathophysiology during early time periods after mild TBI, we compared resting activity patterns the same group of pyramidal cells in the visual and barrel cortices before and after injury *in vivo*. Using video-rate 2P microscopy in transgenic mice expressing GCaMP3 or GCaMP6f in excitatory neurons, we characterized several features of injury, including chronic increases in intracellular Ca^{2+},

concerted moving waves of neuronal activation, and dysfunctional forms of population activity including both suppression and hyperactivation.

3.3.1 Injury causes persistent elevation of intracellular Ca^{2+}

Intracellular Ca^{2+} is a key regulator of numerous intracellular processes, and is tightly regulated in neurons (Brini et al., 2014). Elevation of Ca^{2+} has been associated with cellular pathology in TBI and numerous other disease states (Brini et al., 2014; Camandola and Mattson, 2011). Prior to measuring activity dynamics, we first examined how mild TBI acts on resting Ca^{2+} levels in pyramidal cells in layer II/III of the visual or barrel cortex. We surveyed multiple regions in the exposed cortical area both before and after injury by performing Z-stacks throughout the imaging window, spanning from the cortical surface down through layer II/III (**Fig 3.1**). Prior to injury, resting fluorescence was dim, reflecting normal low intracellular Ca^{2+} levels as well as the low resting signals of GCaMP. Injury reduced overall signal intensity throughout the tissue (**Fig 3.1 C**). It is unclear whether this reflects a bona fide reduction of intracellular Ca^{2+}, or other changes affecting image acquisition such as altered tissue scattering. Surprisingly, after injury we observed a subset of highly fluorescent cells in about 30% of the z-scans (8/26 regions in 5/7 animals). Some cells showed mainly somatic fluorescence (**Fig 3.1 A**), but others showed elevated fluorescence throughout their dendrites as well (**Fig 3.1 B**). To probe whether fluorescence increases were due to chronically elevated Ca^{2+} rather than neuronal spiking activity that coincided with image acquisition, we also acquired time series scans of these neurons at 30 Hz for several minutes (**Fig 3.1 C-D**). These data confirmed that once elevated, fluorescence remained uniformly high over extended

periods, and showed no evidence of firing-related transients, suggesting that intracellular Ca^{2+} concentration was not being properly regulated. While a small number of persistently fluorescing cells were present before mild TBI (3/26 regions in 2/7 animals), perhaps as a result of the window implant procedure, the number of cells was dramatically increased after injury.

Interestingly, cells with chronically elevated Ca^{2+} were not immediately apparently in initial post-injury imaging data, but instead emerged after a delay (**Fig 3.1 C**). While we resumed imaging ~10 minutes after injury, persistently fluorescing cells were first observed at 67 ± 19 minutes on average (range: 18-174 min). In one case, we repeatedly scanned the same cortical region throughout the post-injury period, which confirmed that the loss of Ca^{2+} regulation resulted from a slower process emerging over the first few hours after trauma.

Persistently fluorescent cells sometimes appeared spatially clustered, suggesting that pathophysiology was driven by a local factor common to these neurons. To quantitatively test for a nonrandom spatial distribution, we used to bootstrap analysis to ask whether the set of fluorescent cells were closer to one another than predicted by a randomly selected group of neurons. We measured the 3D positions of all neurons in one of our imaging volumes, and used this as a reference to compare the pairwise distances between persistently fluorescent cells with pairwise distances between a randomly selected group of cells of the same size (averaged over 10,000 repeats for a bootstrap analysis; group sizes: 2-5, 9, 11, and 13 cells) (**Fig 3.1 E-F**). Fluorescent neurons were significantly more clustered together than predicted by chance in 5 of 12 Z-stacks, (**Fig**

3.1 F: $p < 0.05$), and were also more closely clustered than the average of the random distribution in 5 of the 7 remaining stacks. Overall, we found that cells with chronically elevated fluorescence were often colocalized, suggesting the presence of a spatial component that disrupts their ability to maintain physiological Ca^{2+} levels.

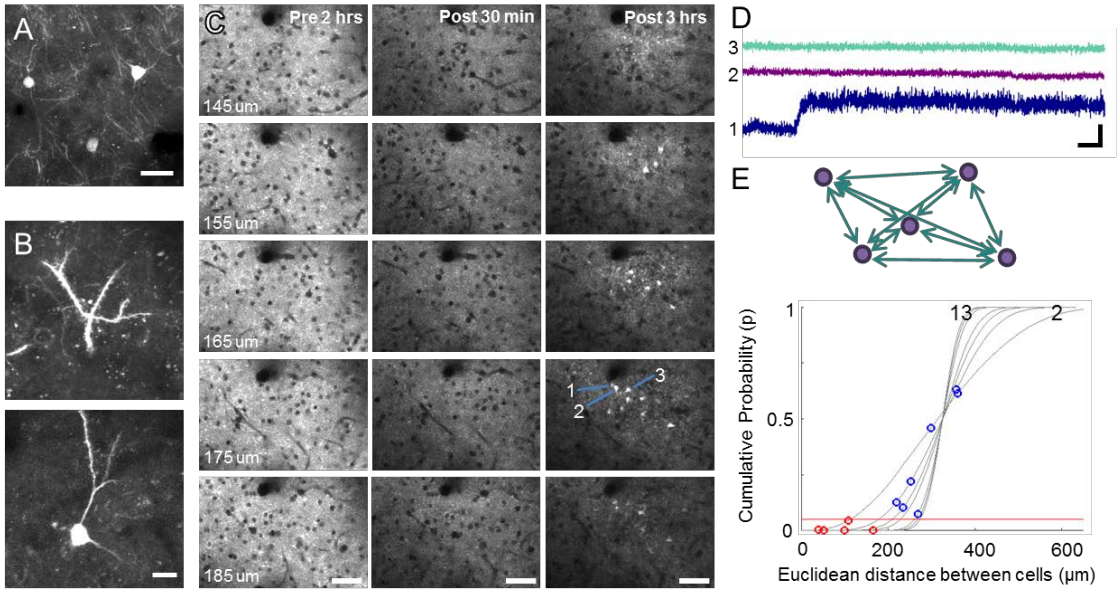

Figure 3.1 Constantly fluorescent cells after mild TBI
(**A-B**) Mild TBI led to the increased appearance of cells with high, constant levels of fluorescence, which was sometimes confined to the soma, but in other cases also extended to the dendrites. Scale bars = 10 μm. (**C**) Chronically fluorescent neurons were not visible in immediately post-injury scans, but appeared after a delay of ≥18 minutes following mild TBI. Scale bars = 50 μm. (**D**) Once elevated, fluorescence levels remained constantly high, and lacked transients typically generated by spiking activity. Scale bar = 100% $\Delta F/F_0$ and 10 sec. (**E**) To test for spatial clustering of neurons with chronically elevated Ca^{2+}, we measured their average pairwise distances. In a separate reference z-stack, we determined the 3D position of all neurons and performed a bootstrap analysis (10,000 repeats) to determine the distribution of pairwise distances between cells in a group of equal size to each of the groups of cells with elevated Ca^{2+} (group sizes: 2-5, 9, 11, and 13 cells). (**F**) The cumulative distributions of the pairwise distances of cells of different sized groups determined by bootstrap analysis of a reference z-stack are shown as gray lines. Distributions for groups of 2 and 13 cells are labeled at the top, and a probability of 0.05 is shown as a red line. The average pairwise distances between elevated Ca^{2+} cells are represented as red or blue circles along the distributions from groups of corresponding sizes. 5 of the 12 groups of elevated Ca^{2+} cells were significantly clustered (red circles; $p < 0.05$) while the remaining 7 groups (blue circles) were not. 5 of the remaining 7 groups were still more clustered than average as they were $p < 0.5$.

3.3.2 Transient, concerted waves of pathophysiological activity

In two of nine injured animals we also observed a massive wave of fluorescence that slowly advanced across the imaging area, representing a surge of intracellular Ca^{2+} throughout the soma and processes of neurons (**Fig 3.2**). These waves traveled at a rate of ~6 mm/min, and the cortical tissue remained fluorescent for ~3 min, matching the kinetics of prolonged spreading depolarization (Hartings et al., 2017). Spreading depolarization is a wave of a breakdown of ion gradients, including large Ca^{2+} influx, that is frequently seen following TBI (Fabricius et al., 2006; Lauritzen et al., 2011; Nilsson et al., 1993; Rogatsky et al., 2003; Sato et al., 2014; von Baumgarten et al., 2008; Zhang et al., 2002) or ischemia (Dreier, 2011) when cells no longer have enough energy to maintain their ionic gradients and are at risk for cytoxic edema and infarct formation (Hartings et al., 2017; von Bornstädt et al., 2015). Interestingly, these fluorescent waves appeared between 1-2 hours (65 min and 103 min) after mild TBI, similar to the time that we began to observe prolonged Ca^{2+} elevation in individual cells. An initial wave of spreading depolarization often occurs at the time of injury in open-skull TBI models (Nilsson et al., 1993; von Baumgarten et al., 2008; Zhang et al., 2002), which would not be measured in our experimental design. However, secondary waves can also occur hours to days after TBI (Rogatsky et al., 2003; von Baumgarten et al., 2008) and are linked to infarct expansion in ischemia (Hartings et al., 2017; Nakamura et al., 2010), suggesting that they negatively impact long-term cellular health. As we were not imaging continuously, it is unclear whether waves were absent in the other 7/9 animals or were simply not captured during our recording periods. While we cannot be certain that

fluorescence waves reflected spreading depolarization or a similar phenomenon, they point to another form of marked pathophysiology arising after injury.

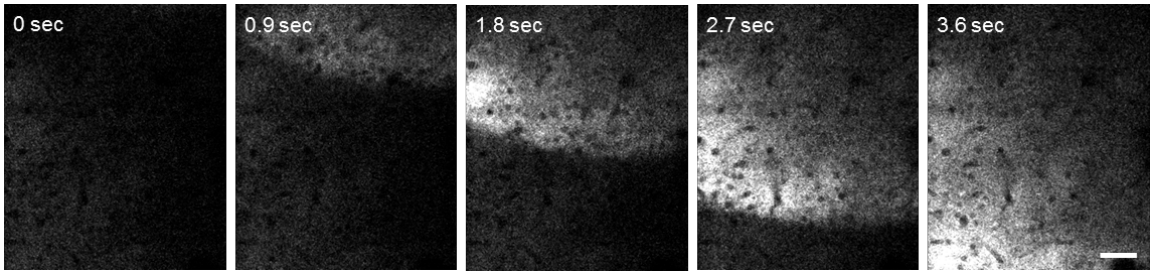

Figure 3.2 Coordinated waves of elevated Ca2+ appear after injury
Large fluorescence waves traveling at ~6 mm/min were seen in two of nine animals 1-2 hours after mild TBI. The sudden increase in intracellular Ca^{2+} levels throughout the entire tissue and the kinetics of the waves strongly suggests spreading depolarization. Scale bar = 50 μm.

3.3.3 Injury has diverging effects on neural activity

To examine changes in the dynamics of cortical activity patterns after mild TBI, we used video-rate imaging to track Ca^{2+} dynamics in populations of layer II/III pyramidal cells, comparing the periods ~2 hours before injury with phases up to 3 hours after injury. We acquired data from a series of single planes encompassing ~150 neurons (**Fig 3.3 A**), each over a period of approximately 10 minutes, and quantified spontaneously occurring transients exceeding 3 standard deviations of baseline fluorescence.

Before mild TBI resting activity was relatively sparse, consistent with prior observations in anesthetized mice in the absence of sensory stimulation. While most

neurons showed detectable Ca^{2+} transients during the imaging period, they were relatively infrequent, occurring on average less than once per minute. We were able to reliably track some neurons before and after injury and found that mild TBI had strongly diverging effects on activity levels in different neurons, measured approximately 1 hour after injury (61 ± 5 min). After trauma, activity of some neurons was starkly suppressed (**Fig 3.3 B**) while others showed much more activity with long durations of fluorescence that lasted over a minute (**Fig 3.3 C**). In contrast to the persistently fluorescent cells, however, signals from these neurons eventually returned to baseline levels. Closer examination of the fluorescence traces confirmed that the prolonged events were typically composed of multiple individual transients, indicating that they likely reflected repeated high-frequency bursting in these neurons (**Fig 3.3 D**). Thus, mild TBI led to a dichotomy in neural activity with some cells being suppressed while others became hyperactive.

Comparison of the whole population of cells before and after injury showed that the overall effect was a decrease in neural activity (**Fig 3.4**). The scattered activity detected in most neurons throughout the field of view before mild TBI was strongly suppressed about an hour after injury except for a minority of hyperactive cells (**Fig 3.4 A**). While 78% of cells showing at least one calcium transient over the ~10-minute imaging period, only 48% of cells were active following trauma (**Fig 3.4 B**: Paired t-test; $p = 0.020$). Furthermore, in the cells that remained active, the frequency of transients was reduced from 0.43 events/min/ROI to 0.15 events/min/ROI (**Fig 3.4 C**: Paired t-test, $p = 0.020$). Since the hyperactive cells made up a small portion of the population, they did

not greatly influence the percentage of active cells or frequency. However, the extended bursting in these cells was long enough to drive a trend towards increased event duration after mild TBI, but this difference was non-significant (**Fig 3.4 D**: Paired t-test; $p = 0.120$). In contrast to TBI, sham injury had no discernible effect on either the percentage of active cells, frequency of events, or event duration (**Fig 3.4 B-D**), indicating that changes in activity were due to trauma rather than acute surgical procedures or extended anesthesia.

Altogether, injury had diverse and inconsistent effects on activity. While mild TBI caused strong suppression of most cortical neurons, a minority of cells showed dramatic hyperactivity that elevated intracellular Ca^{2+} for long periods. Prolonged Ca^{2+} increases are likely to either reflect injury-induced cellular stress on these neurons, to induce additional cellular damage, or both.

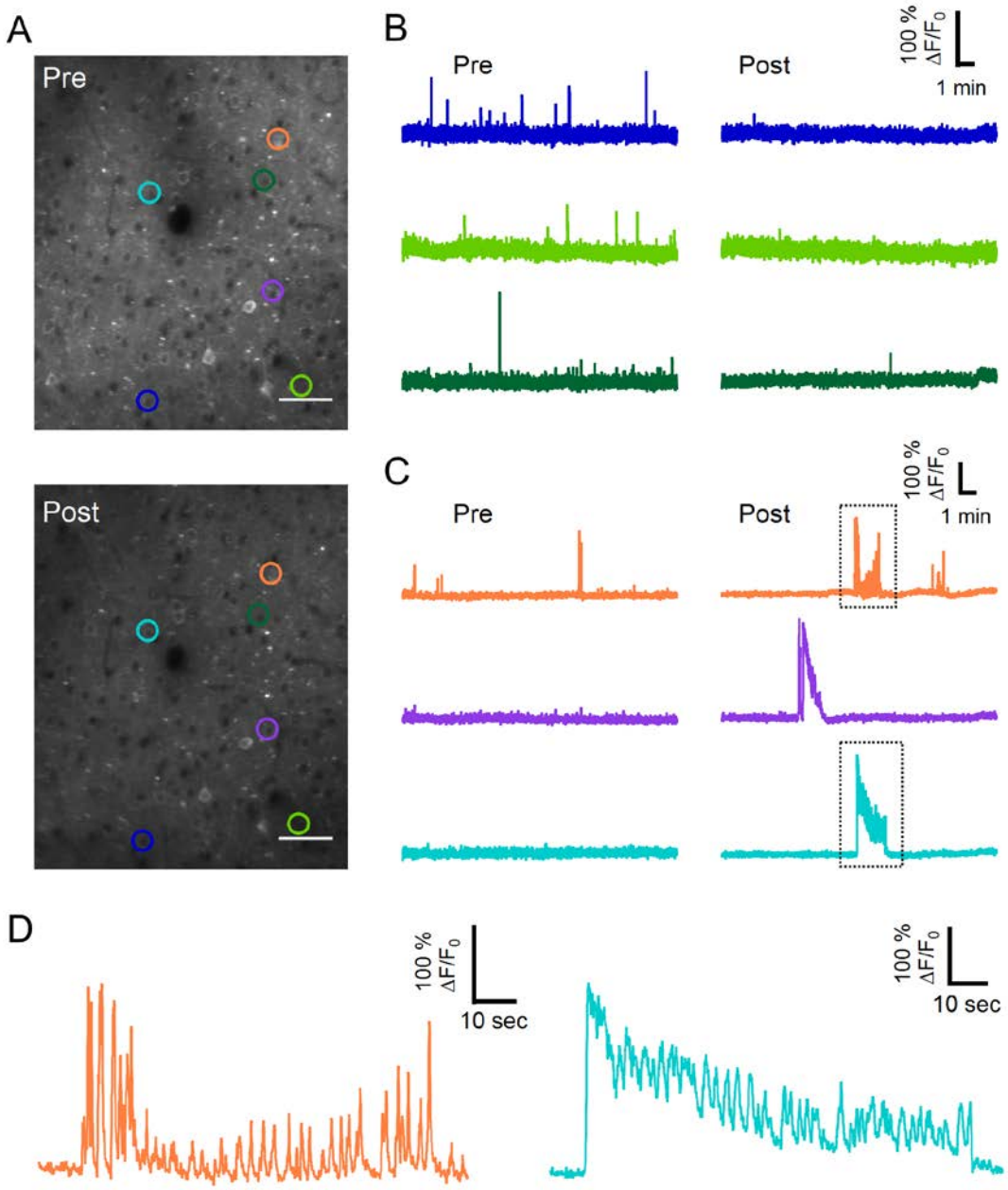

Figure 3.3 Mild TBI has divergent effects on activity of individual cortical neurons (**A**) Imaging the same population of GCaMP-expressing layer II/III pyramidal cells before (top) and after injury (bottom). Scale bars = 50 µm. (**B-C**) Comparison of the same ROIs pre- and post-injury revealed a combination of suppression (B) and hyperactivity, including bursting events lasting >1 minute (C). (**D**) Closer examination of hyperactivity confirms that the fluorescent transients have a shape typical of GCaMP kinetics.

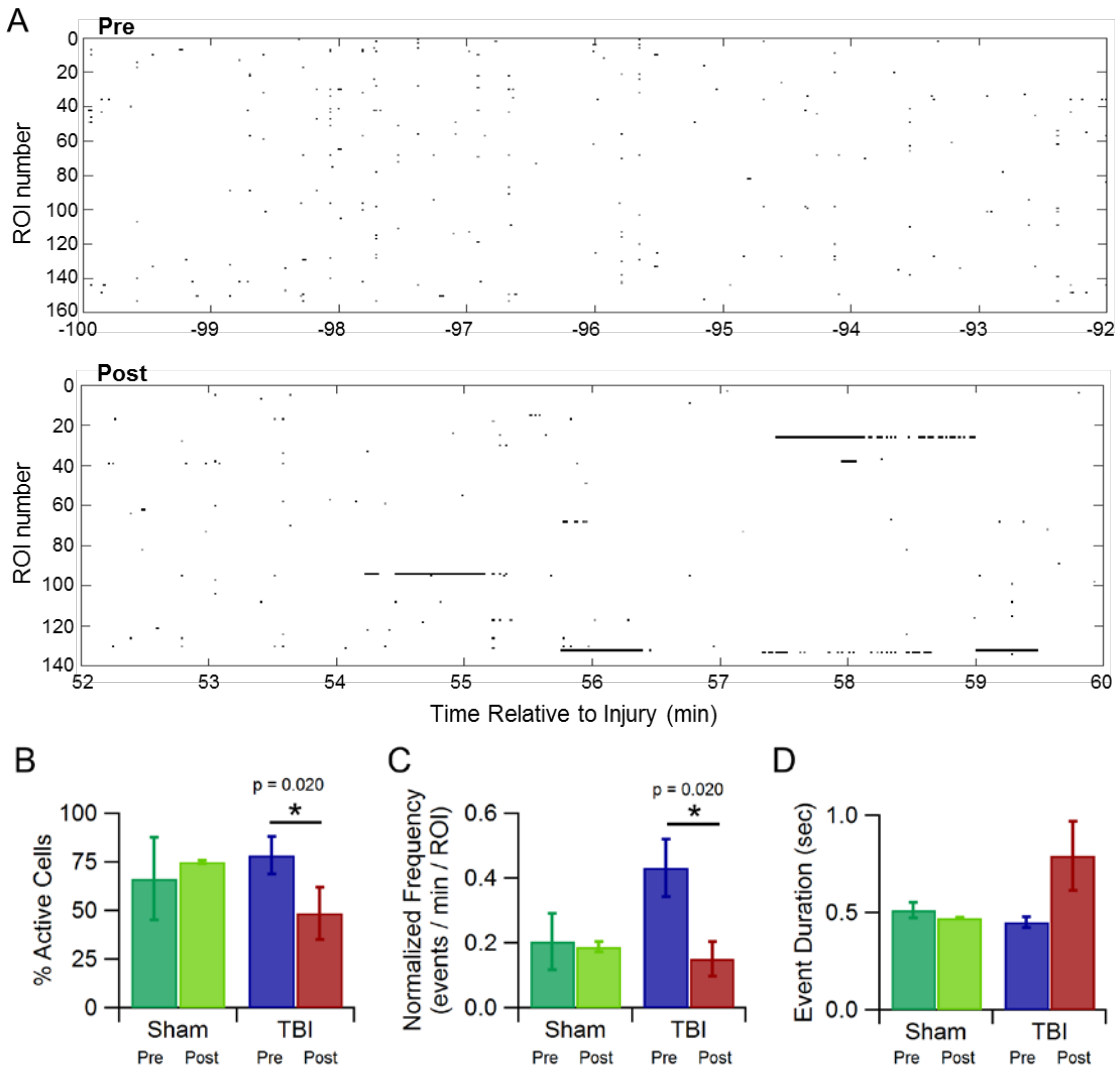

Figure 3.4 Mild TBI causes overall reductions in activity in the neuronal population (**A**) Raster plots of Ca^{2+} transients from all ROIs show sparse scattered activity before injury that was greatly reduced after injury except in a few hyperactive ROIs. (**B-D**) Quantification of activity changes confirm significantly lower percentage of active neurons (**B**: Paired t-test; p = 0.020; t(4) = 3.777; n = 5 mice) and a decreased normalized frequency of each neuron after mild TBI (**C**: Paired t-test, p = 0.020; t(4) = 3.717; n = 5 mice). Event durations trended towards a longer duration but not significantly (**D**: Paired t-test; p = 0.120; t(4) = -1.974; n = 5 mice).

3.4 DISCUSSION

There is little cellular-level *in vivo* data addressing how mild TBI affects neural function in sensory cortices in the early periods following injury. We used 2P Ca^{2+} imaging to examine changes in neural activity patterns in primary visual and somatosensory cortex *in vivo* before and after mild TBI, finding multiple indicators of abnormal physiology lasting for hours after trauma. This included cells that showed consistently elevated intracellular Ca^{2+} lasting several minutes or longer, as well as massive waves of increased fluorescence that may reflect spreading depolarization. Cortical population activity had a dichotomous shift where activity in the majority of cells was suppressed, but a minority of cells showed pronounced hyperactivation. Our results show that even mild TBI can greatly alter neural function and that these alterations are both rapid and heterogeneous.

3.4.1 Loss of calcium homeostasis

Our cellular-resolution measurements of cortical injury responses revealed several signs of disrupted physiology. Both the persistently fluorescent cells and the slow traveling waves of fluorescence indicate extremely high, prolonged levels of intracellular Ca^{2+}. While Ca^{2+} influx is typically used as a proxy for neuronal firing, previous TBI research has shown that the normally tight regulation of Ca^{2+} concentration is frequently lost after injury (Deshpande et al., 2008; Hansen et al., 2018; Nilsson et al., 1993; Sun et al., 2008; Weber et al., 2001). Thus, the fluorescence increases we see after injury is likely to represent increased resting levels of intracellular Ca^{2+} independent of ongoing firing, rather than spiking-dependent increases. With those findings in mind, we analyzed

fluorescence fluctuations closely to ensure that their kinetics matched those of normal GCaMP animals and thus represented neural activity. We quickly recognized constantly fluorescent cells and the waves of fluorescence as separate phenomena. Since they did not show fluorescence fluctuations, we assume that their fluorescence is just from elevated baseline levels of intracellular Ca^{2+}.

The waves of fluorescence we saw closely resembled spreading depolarization, a breakdown of transmembrane ion gradients including a large influx of Ca^{2+} (Hartings et al., 2017). Spreading depolarization, and ensuing spreading depression where a wave of suppressed activity follows spreading depolarization, are commonly seen in both TBI and ischemia (Fabricius et al., 2006; Hartings et al., 2017; Lauritzen et al., 2011). Previous work has shown that spreading depolarization is a consequence of a mismatch in energy supply and demand (von Bornstädt et al., 2015), typically the result of the reduced cerebral blood flow (CBF) that is a well-established effect of TBI (Golding, 2002; Jullienne et al., 2016; Kenney et al., 2016). Maintenance of ionic gradients and neural activity requires a consistent supply of oxygen and glucose to local neural tissue (Erecińska and Silver, 1994) so decreases in CBF can quickly lead to ionic imbalance. Additionally, disruption of CBF could explain the spatial clustering of persistently fluorescent cells, which could be due to local reductions in CBF in a subset of vessels causing nearby cells to be more deprived of oxygen and glucose. Heterogeneity in cerebral microvascular flow has previously been seen in rodents under conditions of high intracranial pressure mimicking TBI (Bragin et al., 2013). Alternatively, breakdown of the blood-brain barrier could cause local release of factors harmful to neurons. Previous

studies occluding a single vessel demonstrated rapid and localized disruptions in neuronal function, spreading depression, and ultimately cell death with prolonged occlusion (Blinder et al., 2010; Shih et al., 2013). The fact that numbers of persistently fluorescent cells were relatively small, rather than all neurons in a volume, and the cells were not always clustered suggests another factor may be responsible for inducing such high intracellular levels of calcium in these cells. The persistently fluorescent cells may have some intrinsic property that makes them more vulnerable to ionic imbalance after TBI. The transgenic animals we used express GCaMP broadly in excitatory pyramidal cells, including layer II/III, and so provide little information about cell-type specificity of injury effects. Future experiments that identify genetically defined classes of cortical neurons should allow further characterization of how injury acts on diverse cell types, including inhibitory interneurons. Imaging approaches should also allow longitudinal measurements to test how initial injury responses in cells relate to their eventual fate.

Whether elevated intracellular calcium is a consequence of altered CBF or another process, the loss of ion homeostasis is an indicator of extremely unhealthy tissue. While all ion concentrations are tightly controlled, Ca^{2+} is particularly highly regulated due to its involvement in a wide range of signal transduction pathways, ranging from neural firing to synapse strength to gene expression (Brini et al., 2014; Weber, 2012). Intracellular Ca^{2+} rises after TBI are likely due to either influx of extracellular Ca^{2+} (Lusardi et al., 2004; Wolf et al., 2001) or release of intracellular stores (Staal et al., 2010), both of which are likely to trigger unwanted pathways such caspases that signal apoptosis or proteases that degrade the cytoskeleton (Weber, 2012). Additionally, ionic

imbalances can cause a host of other problems, including cytotoxic edema from water influx, mitochondrial damage due to overwhelmed buffering of Ca^{2+} ions, and membrane depolarization that activates voltage-gated channels and worsens ion imbalance (Weber, 2012). Although increased intracellular Ca^{2+} does not guarantee neuronal death, it is one of the key processes in infarct formation (Hartings et al., 2017) and has been linked to impaired memory after TBI (Deshpande et al., 2008).

3.4.2 Heterogeneous shifts in neural activity

TBI suppressed activity in the majority of cells but also greatly increased activity in a minority. The net decrease in activity is in agreement with several *in vivo* measurements of cortical neural activity taken within 5 minutes - 2 of hours after TBI (ranging from mild to severe) (Alves et al., 2005; Ding et al., 2011; Kharatishvili et al., 2006). The level of decrease that we observed, about 30% by percentage of active cells and 60% by frequency, indicates a substantial disruption of normal activity even after mild TBI. The hyperactivation in a subset of cells neighboring the suppressed cells also points to disturbed physiology, such as excitotoxicity, but makes further interpretation more challenging. Previous work examining neural function after TBI has seen differences in activity depending on the layer of cortex (Johnstone et al., 2014). A recent imaging study in hippocampus also observed a dichotomy among cells in the same region (Hansen et al., 2018), where a small fraction of cells had sustained elevation of intracellular Ca^{2+} but recovered after several minutes. The ability to resolve distinct effects in different subsets of cells highlights the strength of Ca^{2+} imaging, but does not reveal what is driving the dichotomy in activity.

Similar to the loss of Ca^{2+} homeostasis above, a decrease in CBF may also help account for the reduction in neural activity, implying that cells lacked the energy to fire after mild TBI. Suppression of activity is frequently seen after ischemia (Dreier, 2011; Hartings et al., 2017). As mentioned above, the drop in CBF would have to be heterogeneous among the vessels though to be the only factor accounting for differences in cell response. There is very likely capillary flow heterogeneity after TBI (Bragin et al., 2013; Ostergaard et al., 2014), but we would expect to see groups of cells surrounding vessels become hyperactive if this was the case. Instead, whether cells show reduced or increased activity after mild TBI may depend on factors such as circuit connectivity or intrinsic cellular properties. Alternatively, some intrinsic property of the cells could explain their unusual behavior, such as greater expression of glutamatergic receptors that are stimulated by excessive levels of extracellular glutamate seen after TBI (Blennow et al., 2012). Transgenic animals with additional fluorescent markers expressed under cell-type specific promoters or labeling connectivity between cells with transynaptic viruses could be used to explore these options. Finally, hyperactive cells may be part of a homeostatic response to increase baseline network activity back to pre-injury levels. Again, some intrinsic factor could account for the faster response in some cells than others to become more active again. *In vivo* Ca^{2+} imaging in this study revealed numerous, heterogeneous effects of mild TBI on neural function, but future experiments will be necessary to further characterize these changes and determine what causes them.

3.4.3 Imaging approaches for characterizing TBI

In conclusion, we used 2P Ca^{2+} imaging to compare *in vivo* neural activity before and after mild TBI. We found robust decreases in overall neural activity and evidence of elevated intracellular calcium, indicating large disruptions in normal physiology even though injury was mild. The heterogeneity of cells' responses highlights the importance of using Ca^{2+} imaging and other techniques that allow for high spatial resolution. The rapidity with which these changes occurred emphasizes the importance of studying TBI in the acute phase after injury to identify the initial changes and thus determine the most effective targets for treatment.

The difficulty of measuring the effects of TBI in the intact brain has posed as a major hurdle in understanding the physiological consequences of injury. Electrophysiological approaches such as electroencephalography, electrocorticography, or microelectrodes provide powerful and temporally precise readouts of activity but are limited in their spatial resolution and/or the range over which they can measure. Imaging methods have provided important insight into other pathological states such as stroke and neurodegeneration (Grienberger et al., 2012; Winship and Murphy, 2008), are only beginning to be applied to injury (Hansen et al., 2018). Advancements in multiphoton imaging and genetically-encoded calcium indicators now allow for simultaneously measuring neural activity from large populations of neurons at single-cell resolution. This approach provides a unique perspective on the effects of injury, for instance allowing one to see the heterogeneity of TBI responses even between neighboring cells. Imaging tools also have the potential for longitudinal measurements examining how the long-term

function of individual neurons and/or identified cell types depends on their initial responses at the time of injury. Additionally, measuring activity on a single-cell resolution in the sensory cortex can provide unique insight into neural function by allowing detection of the response to sensory stimuli and calculation of tuning for individual cells. For example, in future experiments in the visual cortex we aim to look at the direction and orientation selectivity of cells before and after mild TBI to see how processing of sensory information is potentially altered when other aspects of physiology are changed.

CHAPTER FOUR

Dramatic Reductions in Cerebral Blood Flow in Microvasculature following Mild Traumatic Brain Injury

4.1 INTRODUCTION

At least 2.8 million Americans suffer a traumatic brain injury (TBI) every year (Taylor et al., 2017), leading to emotional and cognitive deficits that can affect quality of life, employment, and create a huge financial burden (Levin et al., 1987; Max et al., 1991; Rimel et al., 1981). Mild TBI is the most common form, accounting for ~80% of head injury (Cassidy et al., 2004), but even mild TBI can lead to symptoms that persist for months to years (Carroll et al., 2004). Despite the prevalence and debilitating consequences of TBI, it is unclear what neurobiological changes lead to the emotional and cognitive deficits. One key change after injury that has been identified as a potential source of neurological dysfunction is a decrease in cerebral blood flow (CBF).

Reduced CBF has been consistently observed after TBI in a variety of injury models, including fluid percussion injury (DeWitt et al., 1997; Hayward et al., 2011; Muir et al., 1992; Pasco et al., 2007; Yamakami and McIntosh, 1991; Yuan et al., 1988), controlled cortical impact (Bryan et al., 1995; Thomale et al., 2002), blast (Bir et al., 2012; Rodriguez et al., 2018), and weight drop injury (Buckley et al., 2015; Nilsson et al., 1996). Human studies have also shown decreased CBF following mild to severe TBI (Bartnik-Olson et al., 2014; Bouma et al., 1992; DeWitt and Prough, 2003; Jullienne et al., 2016).

While the imaging techniques used in previous studies (radiolabeled microspheres, arterial spin labeling MRI, and diffuse correlation spectroscopy) provide insight on global and regional blood flow, they do not measure CBF at the arteriole and capillary level. Since this part of the microvasculature is where oxygen and glucose exchange occurs (Sakadžić et al., 2014), a disruption of CBF here would directly perturb neural function. Post-mortem examination of the microvasculature has confirmed that structural changes occur in microvessels even if they have not previously been able to be observed *in vivo*. Thinning of vessel walls (Daneyemez, 1999; Dietrich et al., 1994; Hekmatpanah and Hekmatpanah, 1985; Rodríguez-Baeza et al., 2003), capillary hemorrhages (Daneyemez, 1999; Dietrich et al., 1994; Hekmatpanah and Hekmatpanah, 1985; Oppenheimer, 1968) and microthrombosis in vessels 100 μm or smaller (Hekmatpanah and Hekmatpanah, 1985; Stein et al., 2004) were detected in animal models of TBI or human patients who died shortly after head injury. Furthermore, the amount of neuronal necrosis was highly correlated to the density of microthrombi (Stein et al., 2004), emphasizing the harmful consequences of limiting CBF in the microvasculature.

In addition to limitations of spatial resolution for *in vivo* CBF measurements, many studies only examine CBF at a few time points often due to the invasiveness of the CBF measurement or need to inject exogenous tracers. Doppler optical coherence tomography does not require any tracers, can penetrate down to the microvasculature when coupled with a cranial window, and has extremely high spatiotemporal resolution

down the level of individual capillaries (Huang et al., 1991; Schmitt, 1999; Srinivasan et al., 2010).

Here we used chronically implanted cranial windows to obtain detailed views of how injury affects CBF at high spatial and temporal resolution. We employed laser speckle contrast imaging and Doppler optical coherence tomography to measure CBF *in vivo* at a capillary-level resolution both acutely (within minutes) and chronically (up to 3 weeks) after TBI to directly measure the disruption of CBF in the microvasculature and the time course of this disruption. After a mild weight drop injury, we observed a dramatic reduction in CBF (60%) within 5-10 minutes that endured for at least hour. CBF was substantially blocked in the microvasculature as evidenced by stalling in about 50% of capillaries within 10 minutes of TBI. The extremely rapid drop in CBF, particularly in the microvasculature, highlights the need to examine CBF at immediate post-injury time points and develop a treatment to target recovery of blood flow in small vessels.

4.2 METHODS

4.2.1 Animals & chronic cranial windows

All experiments were performed in 2-5 month old male and female C57BL6/J mice in accordance with guidelines of the Boston University Institutional Animal Care and Use Committee. Animals were group housed on a 12 hour light/dark cycle with *ad libitum* access to food and water. Chronic cranial windows were implanted using standard procedures (Holtmaat et al., 2009). Briefly, animals were anesthetized with isoflurane, a craniotomy (3 mm in diameter) was performed over left primary visual cortex leaving the dura intact, and covered with a glass plug made up of 3-4 circular coverslips glued

together with optical adhesive. The window was sealed with agarose and adhesive (Vetbond, 3M). A stainless steel cylinder (4 mm diameter; 4 mm tall) for inducing mild TBI was glued onto bregma (Zap Gel, Pacer). A custom-made stainless steel headpost was attached to the right side of the skull (Loctite 404, Henkel Corp.). The implant was covered with dental cement (C&B Metabond, Parkell). Animals recovered for ≥2 weeks before confirming normal capillary flow, and experimental measurements began at ≥3 weeks post-surgery.

4.2.2 Injury model

Mild TBI was induced using a modified Marmarou model where a weight is dropped onto a metal cylinder attached to the animal's skull (Marmarou et al., 1994) and the animal is unrestrained to allow free movement of the head and body to recapitulate the acceleration and shear forces characteristic of human injury (Kane et al., 2012; Meaney and Smith, 2011). Animals were imaged for ~20 minutes prior to injury, and received buprenorphine analgesia at ~3 minutes prior to TBI (0.125 mg/kg, subcutaneous). Mice were quickly transferred to a custom TBI apparatus and a 150 g weight was dropped 110-120 cm through a guide tube onto the metal cylinder implant, propelling the animal through the foil onto foam padding below (5 cm upholstery foam, Mybecca). The weight was secured to fishing line (Stren high impact, Pure Fishing, Inc.) set to a length that prevents potential double-hit injury. Animals were quickly returned to imaging, within 3-5 minutes. About half of our animals (5/9) received both sham and mild TBI treatments, allowing within-animal comparison.

4.2.3 Laser speckle contrast imaging

Injury-induced changes in CBF were measured at high time resolution with laser speckle contrast imaging (Boas and Dunn, 2010). The brain surface was illuminated with a speckle pattern using a 785 nm laser diode (Thor Labs, LP785), collimator, and aspheric lens for beam expansion. Images were collected every ~1.5 seconds with a polarizer and camera lens (Edmund Optics, VZM 600i) and CMOS camera (Basler, acA2040-90μmNIR). Changes in speckle contrast due to local flow-induced scattering were calculated as the ratio of standard deviation of intensity over the mean over a moving 7x7 pixel window using pylon software (Basler, Exton, PA). Speckle contrast images were converted into an index of local flow by taking the inverse of the squared speckle contrast, using a plug-in for ImageJ (NIH, Bethesda, MD). CBF in each animal was quantified for three different regions of interest (ROIs) in the parenchyma spaced throughout the cranial window, where each ROI's blood flow index frame-by-frame values were normalized to the mean of the last 30 frames before injury, and the 3 ROIs were averaged to give a single index of relative CBF for each animal over the acquisition period.

4.2.4 Optical coherence tomography (OCT)

Volumetric imaging of microvascular flow was examined with a spectral-domain OCT system with a 1310 nm center wavelength and 170 nm bandwidth, and a linear CCD (Thorlabs Telesto II) operating at 76,000 A-scans/second. With a 10x objective (Mitutoyo Plan Apochromat Objective, 0.28 NA), the axial and transverse resolution was 3.3 μm. Angiograms were generated with a decorrelation-based method comparing the

intensity and phase of two repeated B-scans to identify dynamic tissue. Tomographic data was collected with custom LabView routines (National Instruments, Austin, TX). For calculating vessel diameter, angiograms were made from a 1000 μm^2 ROI and scanned at 1000 $pixel^2$ resolution. For examining capillary stalls, angiograms were made from a 600 μm^2 ROI scanned at 400 $pixel^2$ resolution. Vessel diameter was quantified using ARIA algorithms in Matlab (Bankhead et al., 2012) applied to angiograms thresholded in ImageJ. A subset of vessels ranging from ~8-60 μm in diameter were measured for all time points and normalized to their diameter at baseline before TBI. Since the largest changes in diameter were observed at 5 minutes and 1 hour after injury, single values of normalized vessel diameter following TBI without a time point (Figure 2, panels D-E, G-H) are the mean change in normalized vessel diameter at 5 minutes and 1 hour.

The number and duration of capillary stalls were manually identified from angiogram images using custom Matlab routines. ImageJ was used to visualize angiogram images to manually count the total number of capillary segments. Temporarily stalled segments were defined as those alternating between visible and not visible in angiogram time series. Continuously stalled segments were defined as those that were not visible during the entire time series but reappeared at a later time point. Stall incidence, point prevalence, and cumulative duration were calculated based on temporarily stalled segments.

4.2.5 Two-Photon (2P) In Vivo Ca^{2+} Imaging

Structural stability of the vascular tree was examined using retroorbital injections of FITC-dextran (50 μl, 5% W/V in PBS, Sigma Aldrich) and imaging on a 2P microscope

(Ultima Investigator, Bruker, Middleton, WI) incorporating a Ti:Sapphire laser (920 nm, Mai Tai DeepSee, SpectraPhysics, Santa Clara, CA) and a 20x objective (Mitutoyo Plan Apochromat Objective, 0.42 NA). Z-stacks of the vasculature were acquired before and after both sham and TBI treatments (~330 μm depth, 3 μm steps). Z-stacks were visualized in ImageJ for manually comparing vascular structure between time points. Subsets of z-stacks containing capillary beds were registered using custom Matlab routines and overlapped images were made in ImageJ.

4.2.6 Statistical Analysis

All results are reported as mean ± SEM. Statistical significance was calculated using Two-sample t-tests, One-way ANOVA, or repeated measures ANOVA as noted in the results and figure legends. Following ANOVAs a Tukey test was used for multiple comparisons. For determining the relationship between the baseline vessel diameter and diameter change, Igor Pro's curve fitting tool (Wavemetrics, Lake Oswego, OR) was used to compare the chi-square values of different built-in fits. A p value of < 0.05 was considered statistically significant.

4.3 RESULTS

Generalized decreases in CBF after TBI are well-documented, suggesting that oxidative stress may be a major component of injury. Many questions remain about which elements of the vascular system are affected, however, and few studies have examined CBF at the time of injury when the processes ultimately leading to long-term pathology are first triggered. Effects on the microvasculature, a critical site of oxygen and glucose exchange (Sakadžić et al., 2014), are particularly poorly understood. To address

these issues, we made longitudinal measurements of CBF *in vivo* starting within minutes after mild TBI and continuing up to 3 weeks.

4.3.1 Mild injury causes rapid, pronounced, and long-lasting loss of CBF

We monitored the time course of TBI-induced loss of CBF over a large region of cortex with laser speckle contrast, which provides a spatially averaged readout of blood flow across cortical layers based on local scattering effects (Boas and Dunn, 2010). We acquired images encompassing the majority of our ~7 mm^2 cranial window every ~1.5 seconds, beginning 20 minutes prior to injury and continuing for approximately 3.5 hours after trauma.

Mild injury caused a striking decrease in relative CBF that was apparent as soon as imaging could be resumed at ~3 minutes, and extended throughout the entire imaging field (**Fig 4.1**). We first used the spatial resolution of speckle imaging to test whether loss of CBF showed any variability across the cortical surface. Mild TBI is usually thought to cause diffuse, widespread trauma, but it is not clear whether the resulting physiological effects are uniform or instead vary according to local tissue feature. To test for variation across our imaging window, we quantified blood flow index values for three widely distributed ROIs (**Fig 4.1 A**, top). The extent and time course of CBF decreases were similar across all ROIs within each animal (**Fig 4.1 B**), indicating that injury had uniform effects across a relatively large cortical area.

We next addressed the magnitude and time course of CBF reduction, averaging all ROIs to obtain a single index of blood flow in each animal. Across animals, CBF dropped to approximately 40% of pre-injury levels within 15 minutes after injury, levels

that are associated with loss of consciousness (Verweij et al., 2007) and neural death if reduction is prolonged (Shibata et al., 2004). CBF remained depressed by ≥50% for over an hour before gradually recovering at approximately 1.5 - 2 hours. We quantified CBF at discrete time points relative to injury (-15, 5, 10, 15, 30, 60, 90, 120, 150, and 180 minutes), and found that CBF was significantly lower than pre-injury levels from 5 minutes to 1 hour after mild TBI (**Fig 4.1 C**: Repeated measures ANOVA; $p < 0.0001$). On the other hand, CBF in sham animals remained stable for the entire imaging period in sham animals, apart from fluctuations likely reflecting drift in illumination source. (**Fig 4.1 C**: 1.037 ± 0.020 relative CBF; Repeated measures ANOVA; $p = 0.063$).

Together, continuous monitoring of CBF with speckle imaging revealed a dramatic and widespread drop after mild injury, indicating that neurons were likely subject to substantial metabolic stress for extended periods.

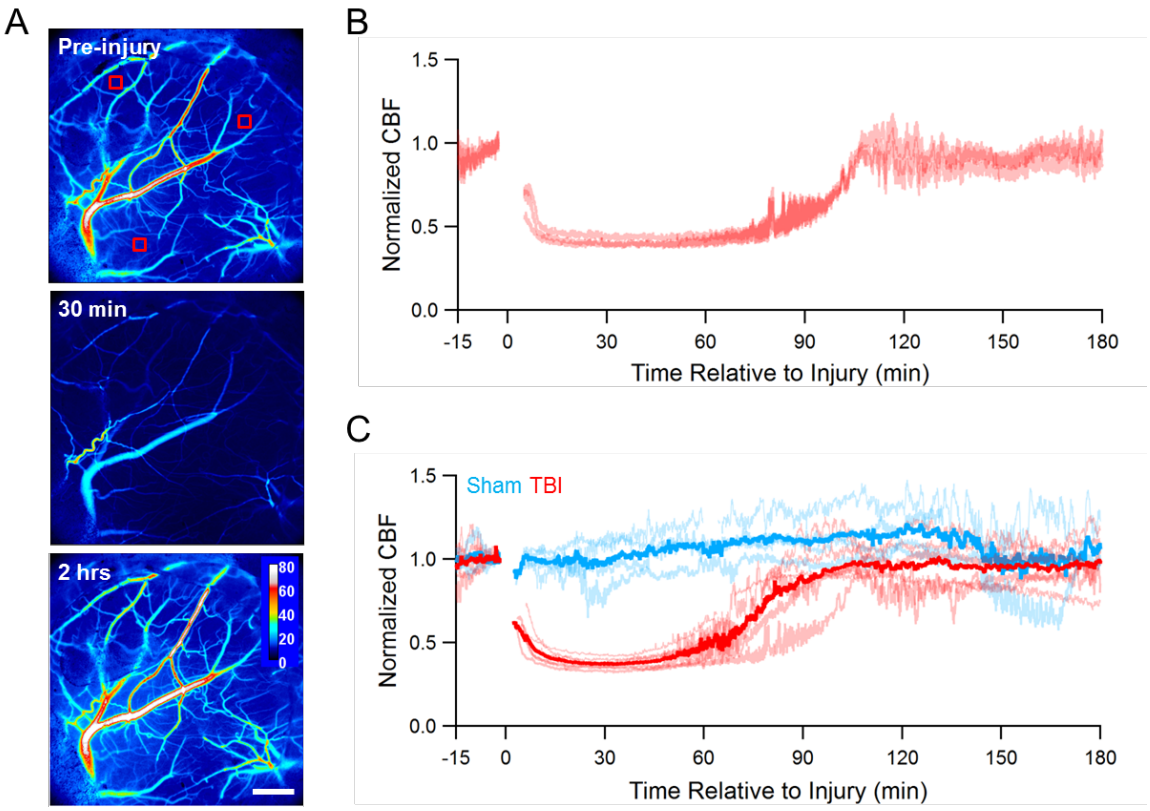

Figure 4.1 Mild injury causes widespread decreases in CBF within minutes
(**A**) Speckle contrast images of the cortical surface before and after TBI. Boxes indicate ROIs used to compare CBF at different spatial locations (top). Scale bar = 500 µm. (**B**) CBF changes were almost identical among the 3 ROIs, indicating uniform reductions across the imaging area. (**C**) Mean CBF changes averaged across all animals in sham and injury groups (blue and red, respectively). Light colors show data from individual animals, and dark colors indicate the mean. CBF remained stable in sham animals, but dropped dramatically within minutes after mild TBI and remained suppressed for 1.5-2 hours after injury (Repeated measures ANOVA; $p < 0.001$; $F(9) = 42.816$; $n_{(sham)} = 4$ mice, $n_{(TBI)} = 6$ mice.

4.3.2 *Mild TBI alters vascular tone*

While the causes of CBF loss revealed by speckle imaging are unclear, one possibility is that injury disrupts normal vascular tone. CBF is actively regulated by neural activity, which alters vessel diameter through contraction of arteriolar smooth muscle (Devor et al., 2007; Fernández-Klett et al., 2010; Hill et al., 2015) and possibly by capillary pericytes (Peppiatt et al., 2006). Normal autoregulation can be disturbed by TBI, resulting in either increases or decreases in vessel diameter (DeWitt et al., 1986; Ekelund et al., 1974; Härtl et al., 1997; Schwarzmaier et al., 2010). Vasospasm, the pathological constriction of vessels associated with subarachnoid hemorrhage, can also occur several days after more severe TBI (Martin et al., 1995; Martin et al., 1992; Werner and Engelhard, 2007). Few studies have been able to examine vessel diameter immediately after TBI, and no studies have looked at smaller penetrating vessels that change diameter directly in response to neural activity (Hill et al., 2015) . To test for changes in vascular tone after mild TBI, we made functional angiograms of the cerebral vasculature with optical coherence tomography (OCT), and compared the diameter of identified vessels over multiple time points before and after injury (**Fig 4.2 A-C**).

Interestingly, TBI had non-uniform effects on vessel diameter, indicating that injury had complex and diverse effects. While on average vessel size was stable in sham animals (**Fig 4.2 B**), TBI led to a mix of both constriction and dilation, with constriction predominating (**Fig 4.2 C**). Across all TBI animals, the majority of vessels showed constriction within the first hour of injury (**Fig 4.2 D**), consistent with the reduction seen with laser speckle imaging. While the combination of constriction and dilation partially

canceled each other, reducing the mean change after injury, the magnitude of TBI-induced changes was even more dramatic (**Fig 4.2 E**: 8.89% ± 0.52 and 25.81% ± 0.93 absolute change in normalized diameter averaged over 5 min and 1 hour for sham and TBI; Two-sample t-test; $p = 1.408e^{-48}$). On average, vessel diameter was significantly decreased at both 5 minutes and 1 hour after mild TBI compared to sham-injured animals (**Figure 4.2 F**: 5 min: 0.989 ± 0.020 and 0.869 ± 0.038 for sham and TBI; Two sample t-test, p = 0.022; 1 hour: 0.984 ± 0.036 and 0.831 ± 0.049 for sham and TBI; Two sample t-test; p = 0.026). The variations in the sham group likely arose from normal physiological variability or differences in isoflurane anesthesia, a known vasodilator.

Changes in diameter were mostly transient, similar to the time course of reductions seen with laser speckle imaging. On average, vessel diameter returned to baseline levels by two hours and remained largely stable up to three weeks after injury. Overall, TBI-induced changes in vessel diameter were largely confined to the acute period within one hour after trauma.

The combination of constriction and dilation could reflect either variability in injury itself, or differences in how it affects different elements of the vascular tree. Arteries contain smooth muscle layers that contract or relax to actively change their diameter (Harper et al., 1984) while veins typically respond more passively to alterations in blood pressure (Kılıç and Akakın, 2008). To test for differential injury responses, we identified a subset of vessels as arteries or veins based on flow direction from matching dynamic light scattering OCT angiograms (Lee et al., 2012). Both arteries and veins constricted similarly after TBI, although effects were slightly greater in arteries,

consistent with their more robust contractile machinery (**Fig 4.2 G**: 0.74 ± 0.05, 0.81 ± 0.02, and 1.05 ± 0.017 for arteries, veins, and unidentified vessels, respectively; One-way ANOVA; $p = 2.219e^{-07}$). Dilation occurred largely in vessels that were not readily categorized which showed a combination of dilation and constriction.

Another possibility is that injury responses vary with vessel size, reflecting functional subtypes such as arteries, arterioles, and capillaries that rely on different contractile processes. Capillaries contain pericytes in place of the smooth muscle found in arteries and arterioles (Golding, 2002). We sampled from vessels 8 – 60 μm in diameter, which will include arterioles, venules, and potentially capillaries, and examined the relationship between pre-injury diameter and TBI-induced changes. Vessels ≥ 30 μm usually constricted while vessels between 8 - 30 μm could either dilate or constrict (**Fig 4.2 H**). The relationship between initial size and injury-induced changes was best fit by an exponential function ($y = 0.686 + 0.589*\exp(-(x-5.76)/10.149)$; $\chi^2 = 12.887$). The unclassified vessels where dilation occurred were smaller on average than the combined arteries and veins (not shown, 17.18 ± 1.3 and 21.05 ± 1.2 μm for unknown and arteries/veins; Two sample t = test; p=0.027). Vessels smaller than 8 μm were difficult to accurately quantify and were excluded from analysis.

Overall, mild TBI led to significant changes in vessel diameter beginning within 5 minutes of injury and lasting over an hour. While both constriction and dilation could occur, the net effect was a decrease in diameter, especially in vessels ≥ 30 μm wide. These data are consistent with results from speckle imaging, and further indicate that injury causes sustained vasoconstriction likely to contribute to the reduction in CBF.

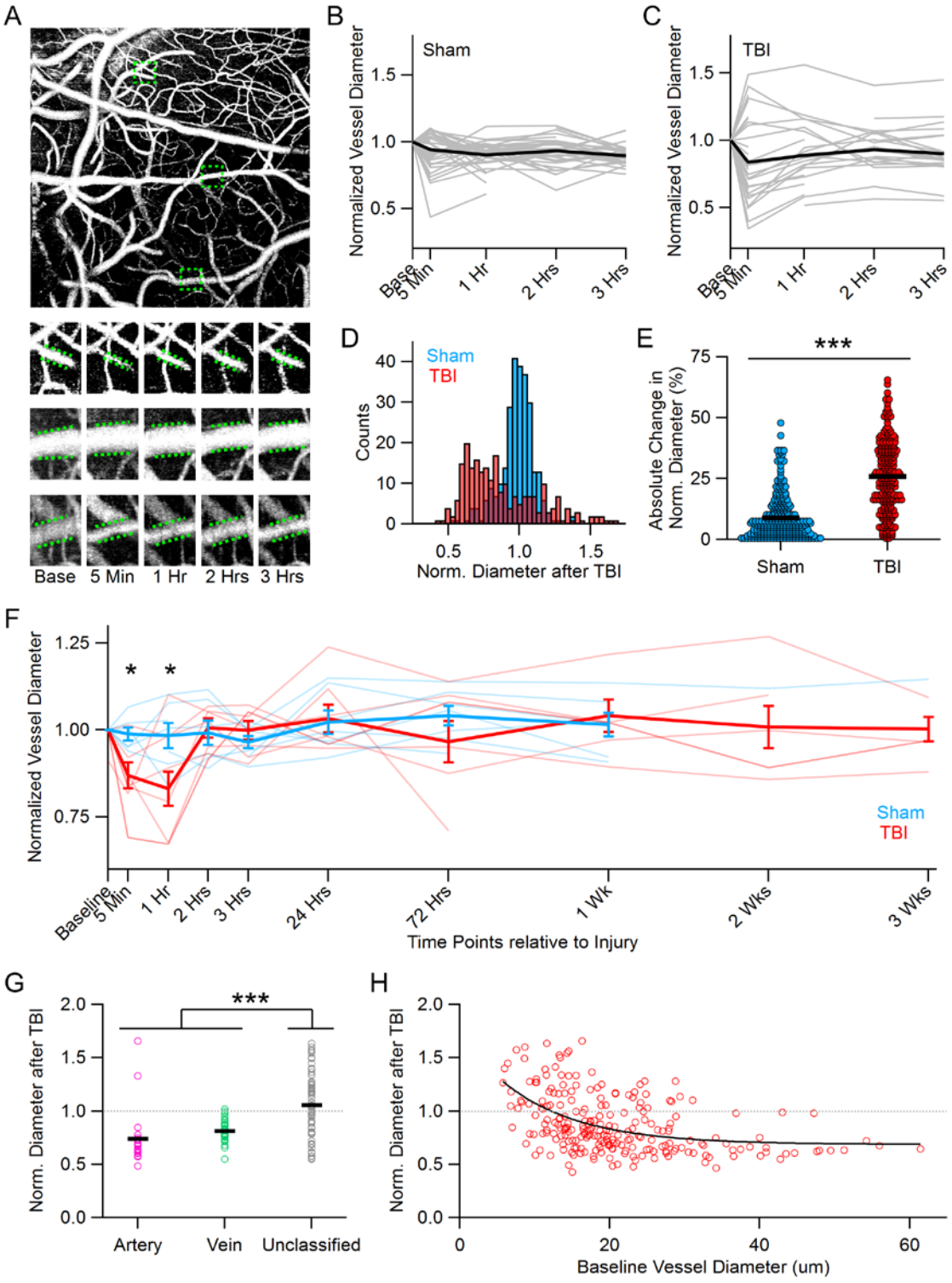
A
Base
5 Min
1 Hr
2 Hrs
3 Hrs
B
Sham
Normalized Vessel Diameter
1.5
1.0
0.5
Base
5 Min
1 Hr
2 Hrs
3 Hrs
C
TBI
Normalized Vessel Diameter
1.5
1.0
0.5
Base
5 Min
1 Hr
2 Hrs
3 Hrs
D
Sham
TBI
Counts
40
30
20
10
0
0.5
1.0
1.5
Norm. Diameter after TBI
E
***
Absolute Change in Norm. Diameter (%)
75
50
25
0
Sham
TBI
F
Normalized Vessel Diameter
1.25
1.00
0.75
* *
Sham
TBI
Baseline
5 Min
1 Hr
2 Hrs
3 Hrs
24 Hrs
72 Hrs
1 Wk
2 Wks
3 Wks
Time Points relative to Injury
G
***
Norm. Diameter after TBI
2.0
1.5
1.0
0.5
0.0
Artery
Vein
Unclassified
H
Norm. Diameter after TBI
2.0
1.5
1.0
0.5
0.0
0
20
40
60
Baseline Vessel Diameter (um)

Figure 4.2 Fluctuations in vascular tone after mild TBI
(**A**) Top, functional OCT angiogram used for measuring vessel diameter. Bottom, examples of individual vessels quantified at each time point. (**B**) Normalized diameter for 52 vessels after sham treatment. (**C**) Subsequent mild TBI in the same animal drives diverse effects on vessel diameter including both increases and decreases. (**D**) Distribution of normalized diameters for 5 minutes and 1 hour time points. Data from sham animals remains stably clustered around 1, while values in TBI animals show increased spread and are consistently shifted to smaller diameters. (**E**) TBI animals showed a much greater magnitude of change independent of direction (Two-sample t-test, $p = 1.408e^{-48}$; $t(506) = -16.355$, $n_{(sham)} = 7$ mice; $n_{(TBI)} = 7$ mice). (**F**) Mean change in vessel diameter across all time points, for both individual animals (light colors) and pooled data (dark colors). TBI caused significant constriction at early time points (5 minutes: Two sample t-test; $p = 0.022$; $t(11) = -2.666$; $n_{(sham)} = 7$ mice; $n_{(TBI)} = 7$ mice; 1 hour = Two sample t-test; $p = 0.026$; $t(12) = -25.344$; $n_{(sham)} = 7$ mice; $n_{(TBI)} = 7$ mice). (**G**) Change in diameter for different vessel types averaged over 5 minutes and 1 hour time points. Arteries and veins were significantly more constricted than unclassified vessels (One-way ANOVA; $p = 2.219e^{-07}$; $F(113) = 17.6$; $n_{(arteries)} = 12$; $n_{(veins)} = 34$; $n_{(unclassified)} = 60$). (**H**) Constriction and dilation depend of initial vessel size before injury. The relationship is best fit by an exponential function ($y = 0.686 + 0.589*\exp(-(x-5.76)/10.149)$; $\chi^2 = 12.887$).

4.3.3 Mild TBI causes long-lasting interruptions in capillary flow

Vasoconstriction will reduce flow to the capillary bed, a critical site for maintaining neuronal energy supply which delivers approximately half of total O_2 under resting conditions and becomes the primary source during high metabolic demand or reduced CBF (Sakadžić et al., 2014). To examine the microvascular effects of injury, we used the high spatial and temporal resolution of OCT to simultaneously monitor flow in approximately 200 capillary segments. We acquired a time series of OCT images every ~7.5 seconds and characterized flow changes within each segment over a period of ~8.5 minutes (**Fig 4.3 A**).

Previous work showed that while flow is normally robust throughout the capillary network, a small fraction of segments show brief flow 'stalls' lasting a few seconds (Erdener et al., 2017; Reeson et al., 2018). Prior to injury, we found stalls were similarly brief and infrequent. Mild TBI dramatically increased both the number and duration of stalls. Within 10 minutes of injury, over half of capillary segments showed some degree of stalling during the acquisition period, and many segments were continuously occluded for the entire approximately 8.5-minute imaging period (**Fig 4.3 B**). The number of temporarily and continuously stalled segments decreased over time as microvascular flow gradually recovered over the hours following injury.

To characterize the extent of reduced capillary flow, we quantified the number and duration of temporary stalls for all time points. First, the percentage of segments stalling at least once during the imaging period, or stall incidence, increased from 10% at baseline to 54% and 34% at 10 minutes and 1 hour after mild TBI, respectively (**Fig 4.4**

A: Repeated measures ANOVA; $p < 0.0001$). The increase in stall incidence denotes a disruption of CBF in the majority of capillaries, and thus oxygen and glucose delivery to neighboring neurons.

To further characterize the length of CBF disruptions, we also quantified the total time any individual capillary was stalled during the imaging period. Cumulative stall duration more than tripled from 10% to 37% of the total 8.5-minute imaging period at 10 minutes post-injury (**Fig 4.4 B**: Repeated measures ANOVA; $p < 0.0001$). Stalls were thus greatly increased in length as well as affecting a larger fraction of vessels. The combination of long temporary stalls and the approximately 25% of capillaries continuously stalled in some animals indicates a long-lasting interruption of metabolic supply to local neuronal populations. Thus, TBI leads to extensive, long-lasting, and complete interruption of blood flow to localized regions of cortical tissue.

We combined stall incidence and duration to obtain a measure of the average fraction of segments stalled at any point in time, or point prevalence. 10 minutes after injury, 22% of capillary segments were stalled on average (**Fig 4.4 C**: Repeated measures ANOVA; $p < 0.0001$), exposing a massive disturbance of CBF and thus oxygen and glucose delivery to the region. Capillary flow in the sham group remained stable, with no changes in incidence, cumulative duration, or point prevalence.

The dramatic increase in stalling persisted for over an hour after TBI, and cumulative duration continued to fluctuate throughout the three-hour imaging session before stabilizing at 24 hours. Even with a near complete recovery of CBF by two hours (at least by our measurements), the disruption of CBF acutely after mild TBI was

extensive and certainly large enough to disturb neuronal function (Cruz Hernandez et al., 2017).

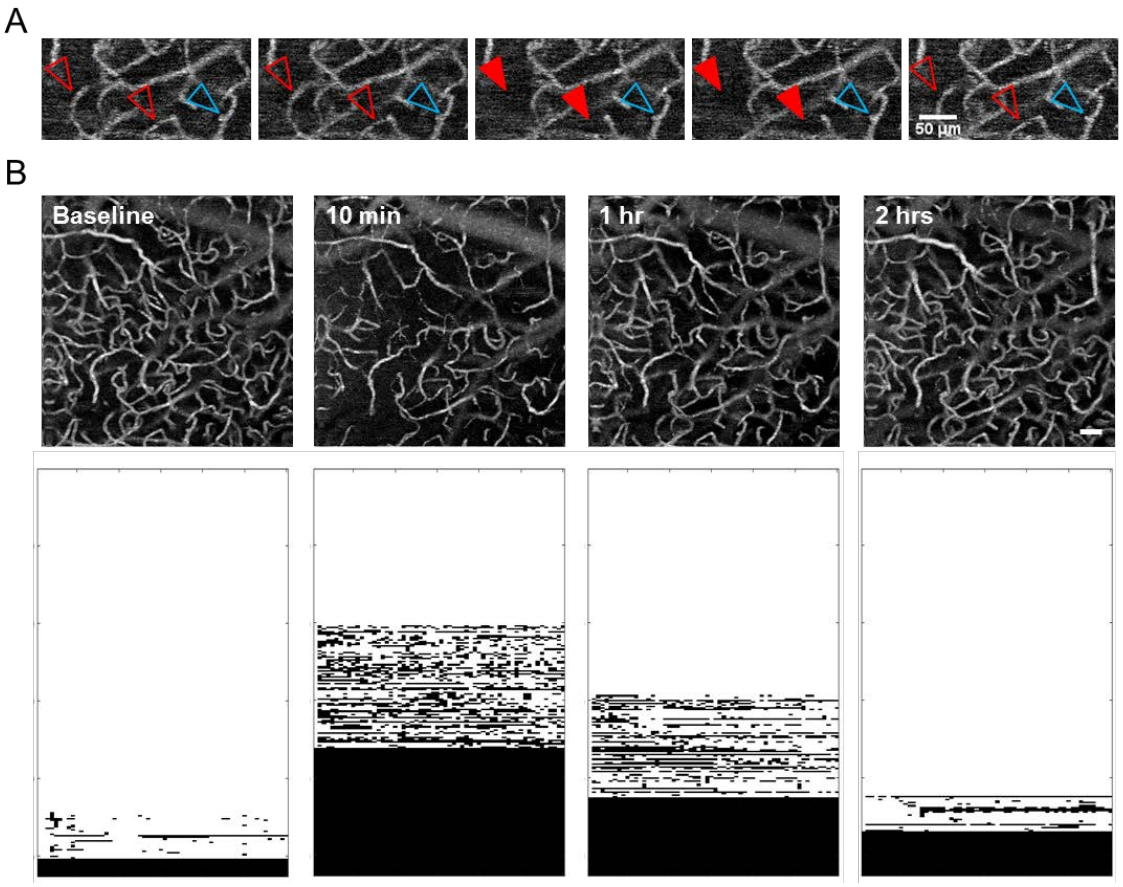

Figure 4.3 Dramatic increase in temporary and continuous capillary stalls after mild TBI

(**A**) Capillary stall angiogram sequence showing segments with temporary stalls (red arrows) and segments with continuous flow (blue arrows). Red arrows are filled on frames where segments are stalled. (**B**) Top, maximum time and volume projections of capillary stall angiograms on the day of injury. Segments that are not visible were continuously stalled during the 8.5 minute imaging period. Scale bar = 50 µm. Bottom, associated stallograms for each time point showing stalls as black ticks similar to a raster plot. Thus, continuous stalls are represented with solid black lines, temporary stalls with alternating black and white, and segments with continuous flow as white.

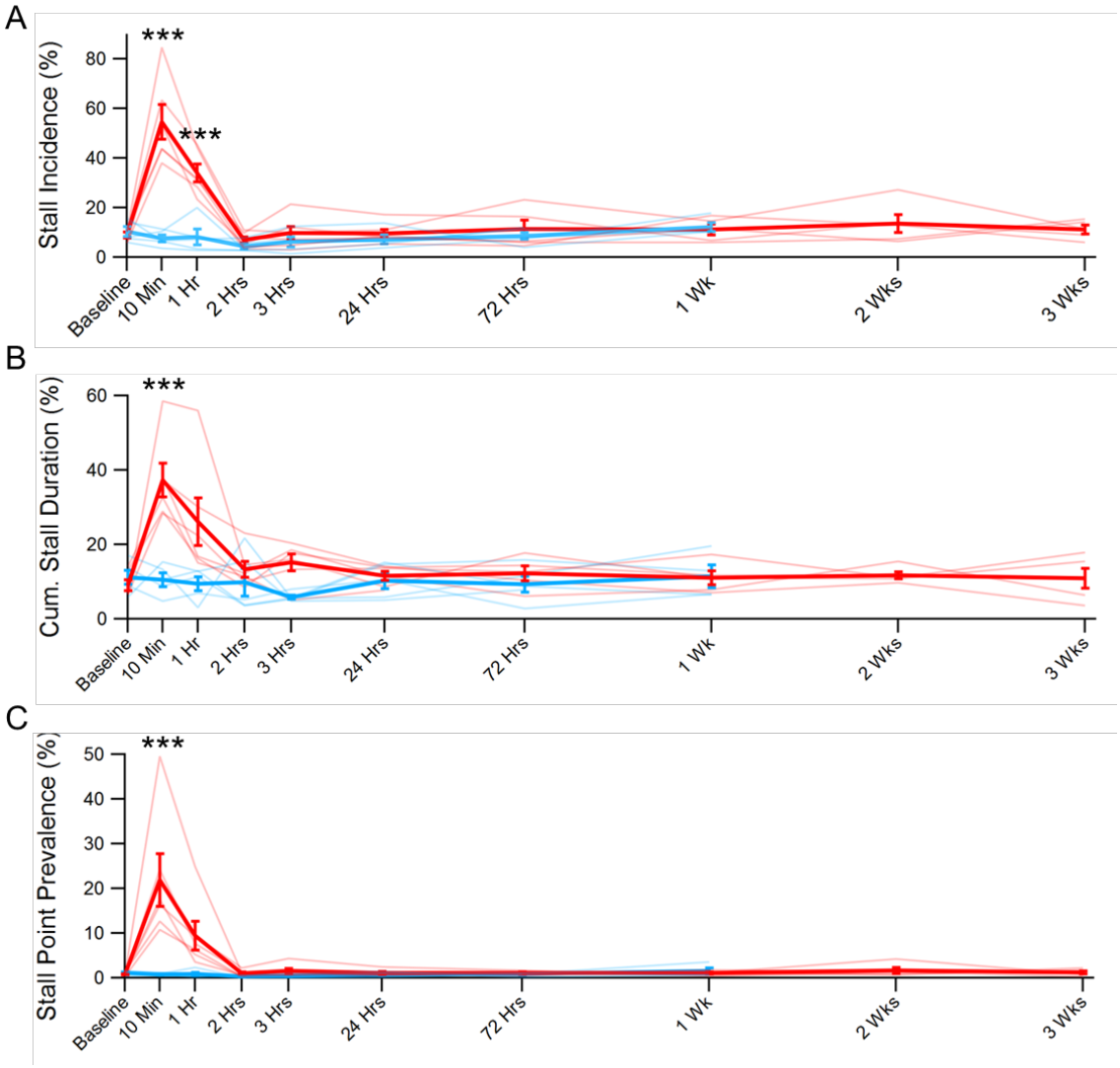

Figure 4.4 Elevated number and duration of temporary capillary stalls in acute phase of mild TBI

(**A**) Percentage of segments that stalled at least once during the imaging period (stall incidence) significantly increased at 10 minutes and 1 hour after mild TBI compared to before injury (54% and 34%; Repeated measures ANOVA; $p < 0.0001$; $F(9) = 26.083$; $n_{(sham)} = 5$ mice, 8 time points; $n_{(TBI)} = 6$ mice, 10 time points). (**B**) Similarly, the percent of total time over the imaging period in which stalls occurred (cumulative stall duration) also rose at 10 minutes post-injury (37%; Repeated measures ANOVA; $p < 0.0001$; $F(9) = 9.444$; $n_{(sham)} = 5$ mice, 8 time points; $n_{(TBI)} = 6$ mice, 10 time points). (**C**) Taking both incidence and duration into account, the percentage of segments stalled at any point during the imaging period was also elevated at 10 minutes following mild TBI (22%; Repeated measures ANOVA; $p < 0.0001$; $F(9) = 10.120$; $n_{(sham)} = 5$ mice, 8 time points; $n_{(TBI)} = 6$ mice, 10 time points).

4.3.4 Structural integrity of the vascular tree is intact

Prolonged capillary stalls of > 20 minutes can occur even in healthy tissue, and appear to cause subsequent pruning (Reeson et al., 2018). Similarly, injury-induced stalls could cause long-term structural changes in the cortical microvasculature. To test this possibility, we imaged microvascular anatomy before and after injury using 2P imaging of FITC-dextran injected into the vasculature. We found no anatomical differences at time points up to two weeks after mild TBI (**Fig 4.5**). Together with the finding of functional flow recovery on the day of injury, these data imply that mild TBI does not lead to chronic deficits in CBF, pointing towards immediate post-injury periods as a key target for interventions.

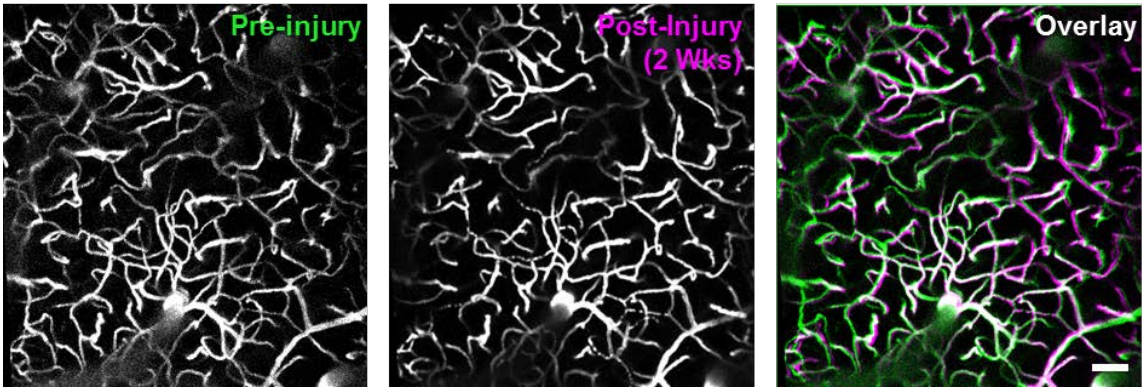

Figure 4.5 Injury has little or no effect on long-term microvascular structure
Comparison of the microvasculature before (left) and after (middle) injury shows that capillary stalling did not lead to structural changes (right, pseudocolored overlay). Scale bar = 100 μm.

4.4 DISCUSSION

Taking advantage of the high spatial and temporal resolution offered by cranial imaging windows, we performed a detailed characterization of cerebral blood flow throughout the 3 hour period after mild TBI, and continuing up to 3 weeks after injury. We measured blood flow through the microvasculature down to the level of capillaries from 10 minutes to 3 weeks after injury. Examining flow in capillaries allowed us to detect CBF disruptions at a critical site of oxygen and glucose exchange. We found dramatic decreases in both relative CBF and blood flow through capillaries within 10 minutes and lasting at least 1 hour after injury before recovering. The diameter of arteries and veins also substantially changed at these early time points with larger vessels frequently constricting while smaller vessels both constricted and dilated. Despite the dramatic functional changes in CBF, we did not find structural changes in the vasculature when looking up to 2 weeks after mild TBI. Examining CBF *in vivo* within minutes (and up to 3 weeks) following injury enabled us to detect the first disturbances in CBF that likely initiate the cascade of harmful pathways that occur after mild TBI.

4.4.1 Time course of disrupted CBF

Vascular disruption figures prominently in both human TBI and animal models (Jullienne et al., 2016; Kenney et al., 2016; Salehi et al., 2017). Neuronal tissue is highly energetically demanding, necessitating dense vascularization and strong neurovascular coupling to dynamically adjust CBF to ongoing metabolic requirements (Blinder et al., 2010; Blinder et al., 2013; Hirsch et al., 2012; Iadecola, 2004; Pittman, 2011). Accordingly, neuronal function declines rapidly when metabolic supply is disrupted.

Pathophysiology emerges within minutes of stroke (Hofmeijer and Putten, 2012), and the severity of damage depends critically on the duration of reduced flow (Jones et al., 1981). Energetic stress due to TBI is likely to show a similar relationship, making it critical to accurately characterize the time course of vascular dysfunction.

Loss of CBF was already apparent when we resumed imaging at ~2-4 minutes, and continued to drop until ~20 minutes. Pronounced vasoconstriction and capillary stalls were also present by 5-10 minutes after TBI. CBF remained strongly reduced for ≥1 hour after mild injury, and depressed for 1.5-2 hours. Local flow disruptions can generate pathological depolarization and dendritic blebbing within 2-3 minutes (Hofmeijer and Putten, 2012; Murphy et al., 2008), and long-term neuropathology and cell death can take place within an hour (Jones et al., 1981). Several studies have linked extended duration of CBF reductions to worse outcome after injury in humans (Bartnik-Olson et al., 2014; Kelly et al., 1997; Langfitt et al., 1977; Struchen et al., 2001). Similarly, the degree of reduction we found had strong potential for causing pathophysiology. In humans, abnormal EEG activity appears when flow drops to ~50%, with further decreases causing severe effects including loss of consciousness, disrupted ionic homeostasis, reactive oxygen species generated by anaerobic metabolism, and permanent neuronal damage (Verweij et al., 2007). The probability of cell death and infarction are significantly increased by longer reductions (Jones et al., 1981). While our model is not associated with permanent neuronal loss, a 50-60% decrease in CBF lasting over an hour will cause substantial oxidative stress.

The relatively transient nature of vascular disruption emphasizes the importance of understanding injury responses in immediate post-injury periods. In humans, CBF measurements are typically only available several hours after injury. In animal models, many studies have described CBF effects between 2 hours to 3 days after TBI (Bir et al., 2012; Bryan et al., 1995; Buckley et al., 2015; DeWitt et al., 1997; Hayward et al., 2011; Kallakuri et al., 2015; Nilsson et al., 1996; Rodriguez et al., 2018; Thomale et al., 2002; Yamakami and McIntosh, 1991), but far fewer have looked within the first 2 hours of injury. Those studies that have examined general CBF changes early lack the resolution to visualize the smaller penetrating vessels or the capillary bed, where oxygen and glucose delivery occurs (DeWitt et al., 1997; Muir et al., 1992; Nilsson et al., 1996; Rodriguez et al., 2018; Yuan et al., 1988).

Furthermore, most existing data are based on more severe open-skull injuries that directly disturb the vasculature and lead to larger, longer-lasting effects (Bir et al., 2012; Ekelund et al., 1974; Thomale et al., 2002). Data are particularly lacking for our mild closed-skull injury model, which mimics the mild TBI most common in humans (Cassidy et al., 2004). A weight drop model in rodents found decreased CBF at 4 hours that recovered by 24 hours (Buckley et al., 2015; Shen et al., 2007) or no significant change in CBF until 1 week (Kallakuri et al., 2015). We did not see reduced CBF beyond 2 hours, perhaps due to use of a milder injury model or to the relatively long distance between imaging and injury sites. While our weight drop model induces diffuse injury (Kane et al., 2012; Marmarou et al., 1994), injury effects may be even stronger closer to the site of impact (Bryan et al., 1995). Overall, our results are broadly consistent with existing data,

but suggest that the key window for vascular effects is within the first 1-2 hours of injury, a time range that has received little attention in prior work

4.4.2 Localized microvascular disruption

The dense capillary network is critical for maintaining uniform and consistent oxygenation of neural tissue. Vasoconstriction in larger vessels will reduce supply to the microvasculature, which would require increased capillary exchange to compensate (Sakadžić et al., 2014). Instead, we found a pronounced loss of microvascular flow after injury, with over half of capillaries showing some stalling and on average 22% non-functional at any point during the first hour. Modeling suggests that capillaries have a nonlinear effect on net CBF, with 20% capillary loss corresponding to a ~50% reduction in overall flow (Cruz Hernandez et al., 2017), consistent with our speckle imaging results.

Besides impacting net flow levels, extensive capillary stalls could have even more severe effects on local scales. Oxygenation falls off rapidly with increasing distance from arterioles (Devor et al., 2011; Moeini et al., 2018), dropping by ~30-50% at 100 μm from the vessel center depending on activity levels (Devor et al., 2011; Moeini et al., 2018). This rapid falloff is normally countered by the dense branching of the microvascular network, which places most neurons within 15 μm of a local vessel (Tsai et al., 2009). This distance will be substantially increased by widespread capillary stalling, which may lead to localized pockets of metabolic starvation. Consistent with this idea, occlusion of even a single penetrating arteriole leads to rapid and highly localized loss of neuronal function, spreading depression, and eventual cell death (Blinder et al., 2010; Shih et al.,

2013). While microvascular flow is normally able to redistribute to accommodate focal disruptions (Blinder et al., 2010; Schaffer et al., 2006), this appeared to be prevented by the extensive stalling caused by injury. Together, our findings suggest that it will be important to consider local heterogeneity as well as net changes in CBF when evaluating injury severity.

4.4.3 Oxidative stress and neuronal pathology

A key goal is to understand how long-term deficits emerge from the biological responses initiated at the time of injury. Even mild TBI can lead to substantial neuropathology and degeneration, especially for repetitive injury as seen with chronic traumatic encephalopathy (Goldstein et al., 2012; McKee et al., 2009) Energetic stress due to loss of cortical perfusion may trigger diverse harmful biochemical cascades that continue to cause cellular damage even after flow is restored (Blennow et al., 2012; Giza and Hovda, 2014; Povlishock and Katz, 2005). Trauma and/or reduced CBF lead to loss of ionic homeostasis, which is linked to cortical spreading depolarization (Fabricius et al., 2006; Hartings et al., 2017; Lauritzen et al., 2011) and mitochondrial dysfunction (Kislin et al., 2017). Spreading depolarization causes a surge in intracellular calcium, further stressing mitochondria and limiting their ability to generate ATP, buffer intracellular calcium, and negate reactive oxygen species (Kislin et al., 2017), forming a negative feedback loop that worsens oxidative stress. Mitochondria can take up to a week to recover after TBI (Kislin et al., 2017), allowing reactive oxygen species time to cause more oxidative stress and tau hyperphosphorylation (Melov et al., 2007; Sultana and Butterfield, 2010). Decreased CBF is unlikely to fully account for all deficits, as TBI

causes a complex suite of effects, such as diffuse axonal injury that will disrupt neural connectivity in addition to cellular health (Povlishock and Katz, 2005). However, the prominence of vascular dysfunction in mild injury suggests that strategies for restoring CBF will offer a promising avenue for reducing the contribution of metabolic stress to long-term deficits.

4.4.4 Possible mechanisms & future directions

The primary mechanisms that drive loss of CBF are unclear. One possibility is that it is due to reduced flow in pial and penetrating vessels that supply the capillary network which are normally regulated by activity and were substantially constricted after injury. Pathological bursting and/or excitotoxicity at the time of trauma may disrupt normal neurovascular coupling, driving pathological vasoconstriction. Constriction could also arise as overcompensation for increased arterial pressure, which rises shortly after fluid percussion injury in rats (DeWitt et al., 1997; Prins et al., 1996). However, the direction of pressure changes are inconsistent in human TBI (Stocchetti et al., 1996). Alternatively, TBI may act directly on the vascular system itself, and is known to disrupt autoregulation (Enevoldsen and Jensen, 1978; Jünger et al., 1997; Lewelt et al., 1980; Overgaard and Tweed, 1974), and lead to vasospasm several days after more severe TBI. Finally, constriction could result from direct compression of vessels by increased intracranial pressure, linked to fast-acting anoxic edema (Risher et al., 2009).

Another, non-exclusive possibility is that CBF effects arise at the level of capillaries, where red blood cell movement is more easily disrupted. Capillary stalls occur even under normal conditions (Erdener et al., 2017; Reeson et al., 2018), and may

be highly sensitive to reductions in supply from upstream vessels. Capillary flow may also be blocked by pathological constriction of the pericytes surrounding these vessels, as seen in stroke and hypoxia (Fernandez-Klett and Priller, 2015; Hall et al., 2014; Yemisci et al., 2009). Finally, injury may affect the 'stickiness' of capillary walls. TBI can cause leukocyte and platelet adhesion to arteriole and venule walls, forming microthrombi that block blood flow (Clark et al., 1994; Hekmatpanah and Hekmatpanah, 1985; Schwarzmaier et al., 2010; Stein et al., 2004). In a mouse model of Alzheimer's, capillary stalls were increased by neutrophil adhesion to the capillary lumen, contributing to reduced CBF and cognitive dysfunction (Cruz Hernandez et al., 2017). It is unclear whether adhesion effects are rapid enough to account for the onset of stalling at 10 minutes after TBI though. Lastly, capillary disruptions could also lead to a secondary reduction in larger vessel diameter, where arterioles constrict to balance elevated intraluminal pressure from stalling or to slow blood flow in order to increase oxygen extraction from blood (Ostergaard et al., 2014).

Future work could help determine the primary causes of CBF effects. Visualizing pericytes and smooth muscle *in vivo* (Iliff et al., 2014) would help uncover the role of constriction of capillaries vs. penetrating vessels during acute injury periods. Combining vascular imaging with measurements of local neural activity or tissue oxygenation (Sakadžić et al., 2010) would provide further insight into the local metabolic consequences of long-lasting capillary stalls. Finally, our data suggest that vascular interventions offer a potential avenue for alleviating the effects of injury. Countering vasoconstriction with vasodilators may help restore flow (Kassell et al., 1992; Sobey et

al., 1996). Antibodies that inhibit leukocyte adhesion also reduced capillary stalling in a mouse model of Alzheimer's disease (Cruz Hernandez et al., 2017), and may offer similar benefits after TBI. Overall, our data identify the first 1-2 hours after injury as an important time window for countering loss of cortical perfusion and metabolic stress.

CHAPTER FIVE

Discussion of Changes in Neural Function and Cerebral Blood Flow after Mild Traumatic Brain Injury

5.1 SUMMARY

In this thesis we examined how neural function and CBF change in cortex early after mild TBI. We used a modified weight drop model of TBI that creates strong impact acceleration forces while keeping the skull closed and intact similar mild TBI in humans. We looked at early time points starting measurements 5 minutes to 1 hour after injury to catch some of the first disruptions in neural function and CBF that may trigger other harmful cascades. For synaptic input and CBF, we repeated measurements later in order to shed more light on the time course of these changes to know when the therapeutic window occurs.

In chapter 2 to see how synaptic activity is altered after mild TBI, we recorded synaptic input onto pyramidal cells in the piriform cortex in acute slices made 1 hour after a single injury or 48 hours after 3 repeated injuries. At 1 hour we found that there was an increase in the amplitude of excitatory inputs onto cells but no substantial change in inhibitory inputs, indicating a shift towards greater excitation in the acute phase of mild TBI (Effect 1 in **Fig 5.1)**. The excitatory-inhibitory balance recovered by 48 hours, emphasizing the need to study TBI-induced changes early after injury. Additionally, we identified piriform cortex as a novel and important region to study in TBI since it is prone

to excitability after trauma, which may parallel the piriform's hyperexcitability in epilepsy.

For chapter 3 we asked whether injury affects cortical activity which underlies cognitive and sensory function that are commonly disrupted by TBI. We compared activity in layer II/III pyramidal cells in the visual cortex before and after mild TBI by 2P *in vivo* imaging of transgenic mice expressing GCaMP. We saw a split in neural activity with the majority of cells showing significantly less activity but a subset becoming hyperactive 1 hour following injury. We also observed groups of cells with persistently elevated intracellular Ca^{2+} (Effect 2 in **Fig 5.**1) and a massive fluorescence wave resembling spreading depolarization. The suppression of activity and loss of ion homeostasis both point to major physiological disruption in neurons probably from a lack of energy to perform or maintain these two functions. Detecting these changes at 1 hour or earlier further highlights how rapidly pathology begins after TBI and the value of examining neural function early.

Finally, in chapter 4 we tested the idea that mild TBI disturbs CBF through microvasculature, which would lead to metabolic stress and potentially long-term pathology. We made *in vivo* measurements of general CBF almost continuously with laser speckle contrast imaging and of hemodynamics through the microvasculature at regular intervals with optical coherence tomography (OCT). Both measurements were done before and within 5-10 minutes after mild TBI in the visual cortex. Blood flow through the microvasculature was followed chronically out to 3 weeks following injury. We found that general CBF and flow through the microvasculature dramatically dropped

within minutes after injury at our first time point. Arterioles and venules constricted and dilated though the overall change was vasoconstriction, which likely reduced CBF (Effect 3 in **Fig 5.1**). 10 minutes after mild TBI, almost a quarter of capillaries were stalled at any point during acquisition, indicating an extreme disturbance in CBF early after injury (Effect 4 in **Fig 5.1**). All CBF measurements recovered by ~2 hours after TBI and remained fairly stable for 3 weeks. Despite the recovery, the large decrease in CBF for over an hour was almost certainly great enough to impair neural function. While previous studies have seen general CBF reductions *in vivo* and structural evidence of altered capillaries, OCT allowed for the first *in vivo* measurements of blood flow through the microvasculature at the capillary level after mild TBI.

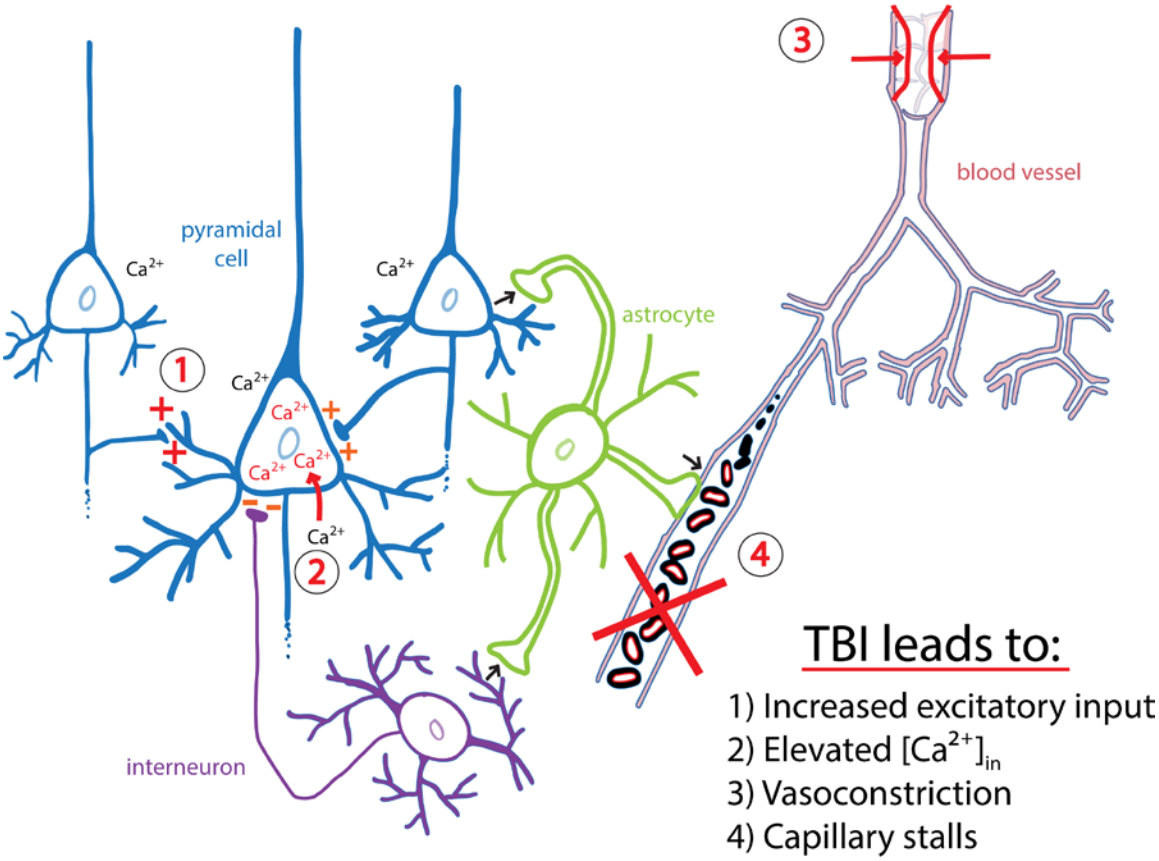

Figure 5.1 Summary of rapid TBI-induced changes in neural function and loss of CBF

Within the first two hours of injury, mild TBI induces increased excitatory input onto pyramidal cells (effect 1), elevated intracellular Ca^{2+} (effect 2), and suppressed neural activity (not shown). The changes in neural function may be a result of metabolic stress from reduced CBF caused by vasoconstriction of penetrating vessels (effect 3) and capillary stalling (effect 4) occurring during this time.

5.2 INTEGRATING RESULTS

We used three distinct but complementary methods (synaptic input, neural activity, and CBF) to understand both neural and vascular pathophysiology after mild TBI. While these methods may seem fairly independent from one another at first glance, they are actually closely tied together and thus provide a window on highly interrelated processes. The combination of excitatory and inhibitory input along with intrinsic membrane properties of a neuron determines whether the neuron is excited enough to fire an action potential. Neural activity is also closely tied to the vascular system, where the firing of neurons signals an increase in CBF to meet the metabolic demands associated with activity, particularly ion flux. When CBF is disturbed, neurons do not have enough energy to be active. If CBF is extremely low or high, however, and the neuron does not have enough energy to maintain ionic gradients or re-establish them after an initial burst of activity. As a result, normal ion flux associated with action potentials will not occur, and the neuron will not be active. Thus, the three measurements of synaptic input, neural activity, and CBF are related and can be integrated to provide a larger view of what is occurring in the brain following mild TBI.

5.2.1 Synaptic input and neural activity

When we measured excitatory and inhibitory input onto pyramidal cells in the piriform cortex, we found an increase in the amplitude of excitatory inputs in acute slices made 1 hour after injury, indicating a shift towards greater excitation early after mild TBI. Examination of neural activity about one hour following injury, however, showed elevated activity in a minority of cells, but the majority was strongly suppressed. The

results of synaptic input and neural activity might seem at odds with one another, but a closer look at the details of how the two measurements were made and other results we found can reconcile these differences.

Data on synaptic input and neural activity were collected from separate regions of the brain: piriform cortex vs visual cortex (barrel cortex was used for measurements other than direct neural activity). Both of these regions are part of primary sensory cortex, but their organization and connectivity is very different. Piriform cortex is a form of paleocortex, consisting of three layers with extensive recurrent connectivity that results in runaway hyperexcitation without substantial inhibitory input to keep it in check (Bolding and Franks, 2018; Franks et al., 2011; Johnson et al., 2000). Piriform cortex also does not have topographic organization like other primary sensory areas. In contrast, visual cortex belongs to neocortex with six layers and does have topographical maps. It has local inhibitory inputs, but not the recurrent excitatory connections of regions of paleocortex and archicortex (e.g., hippocampus). Differences in the intrinsic properties of the regions could help explain why one region showed a shift towards excitation but the other did not.

While there was a difference in brain area between measurements of synaptic input and neural activity, an even greater difference was in the acute *ex vivo* versus *in vivo* set-up. Investigating synaptic activity at this level requires recording from acute brain slices where CBF and much of the extracellular space have been replaced by artificial cerebral spinal fluid and many neural connections have been cut. Much effort is put into keeping neurons healthy for recording by providing a consistent supply of the

necessary salts, sugars, and oxygen in the artificial cerebral spinal fluid. However, researchers know from previous studies that the CBF and extracellular fluid are drastically altered after TBI. CBF is typically significantly reduced for hours to days depending on the severity of injury (Salehi et al., 2017), limiting the delivery of oxygen and glucose that cells need in order to be active or even just maintain ionic gradients. The lack of an energy source can inhibit activity and collapse ion gradients so there is a massive efflux of potassium and influx of Ca^{2+} into neurons (Giza and Hovda, 2014). Additionally, inflammatory cytokines released by glia are also present in the extracellular fluid. In support of the previous findings of altered CBF and extracellular space, our experiments showed a large reduction in CBF and elevated intracellular Ca^{2+} levels in neurons as detailed in chapters 4 and 3, respectively. Thus, the acute *ex vivo* preparation for recording synaptic input that uses artificial cerebral spinal fluid significantly alleviates the energy crisis and harmful concentrations of ions and cytokines in the extracellular fluid that can now dissipate away in the acute slice bath. This does not mean that we should discard *in vitro* and *ex vivo* experiments, but it does emphasize the biological relevancy and value of *in vivo* measurements and argues against directly comparing our acute *ex vivo* and *in vivo* experiments.

Finally, it is important to remember that even if CBF and the extracellular fluid are normal, synaptic input is not the only factor in determining whether or not a neuron will be active. As stated above, intrinsic properties of the cell, such as resting membrane potential and input resistance, also influence whether a neuron will fire. Future

experiments measuring the intrinsic properties of cells could provide a more complete picture of neuronal function after TBI as described below.

5.2.2 Neural activity and CBF

The results from the neural activity and CBF measurements that we made *in vivo* complement each other. As previously mentioned, while a subset of cells was hyperactive about one hour after mild TBI, the majority of neurons showed a large decrease in activity. We also observed a sharp drop in general CBF and occlusion of blood flow through the microvasculature for at least one hour. Given the strong coupling between CBF and neural activity that exists under normal circumstances, the similar direction and timing of the results makes sense. The coupling is a bi-directional relationship though so a major reduction in CBF could quickly prevent neuronal firing from lack of energy required for activity (although there may be a momentary burst of activity), or the decrease in activity means a lower metabolic demand, resulting in lower CBF (Girouard and Iadecola, 2006). Furthermore, neurovascular coupling is frequently disrupted following TBI (Ginsberg et al., 1997; Richards et al., 2001) so the decrease in one may not directly change the other. So how do we interpret these two changes in relation to one another?

Even if neural activity and vascular adjustments are no longer coupled after mild TBI, the two systems would still affect one another since neurons always require oxygen and glucose to be healthy. It is estimated that about half of the energy in the brain is used for synaptic activity, but the other half goes towards re-establishing ionic gradients after ion flux and biosynthetic processes, such as maintaining the phospholipid membrane

(Verweij et al., 2007). Recall that CBF was reduced down to 40-50% of baseline levels as estimated from laser speckle contrast imaging and modeling calculations of the percentage of stalled capillaries. Given that the drop in CBF (both general and through the microvasculature) was so large, the CBF decrease was very likely responsible for some of the neuronal suppression.

The fact that we observed neurons with elevated intracellular Ca^{2+} indicates that normal ionic homeostasis was lost in at least some cells after TBI, providing further evidence that there was not enough energy to keep neurons healthy.

Additionally, we have very preliminary data from imaging both neural activity and CBF in an animal following injury (**Fig 5.2**). Although we did not perform a typical linescan of individual blood vessels, we were able to minimize our field of view enough to scan a region of tissue at a high enough rate to detect the passage of red blood cells in capillaries running in parallel to the imaging plane. We observed a stall in flow of red blood cells in one of the capillaries, and about one minute into the stall we also saw an extremely prolonged large amplitude fluorescent transient in a neighboring cell, indicating high levels of intracellular Ca^{2+} and likely hyperactivity. The spatial proximity and temporal sequence of the capillary stalling and intracellular Ca^{2+} increase strongly suggests that neural activity can be affected by highly localized changes in microvascular flow. Thus, the extensive capillary stalling that we observed after mild TBI in chapter 4 could influence function in a large population of neurons.

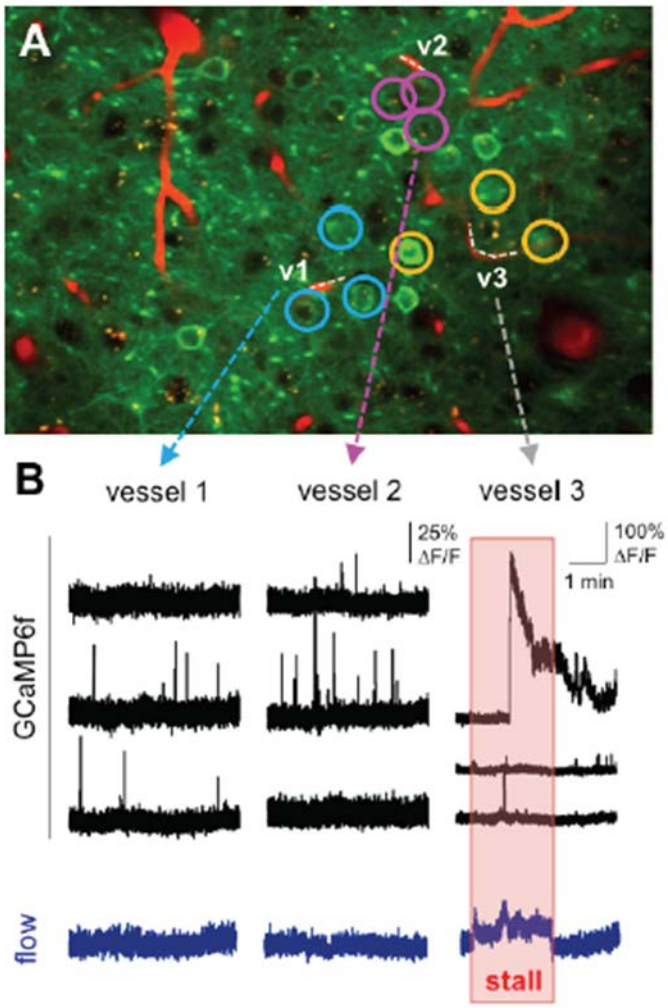

Figure 5.2 Abnormal Neural Activity during a Capillary Stall
(**A**) Simultaneous 2P imaging of neural activity and CBF in a Thy1-GCaMP6f animal injected with FITC-dextran. (**B**) Representative fluorescent calcium traces and blood flow through adjacent capillaries reveals hyperactivity in one cell after stalling in a nearby capillary.

5.3 FUTURE DIRECTIONS: FURTHER ELUCIDATING THE PROBLEM

With our current findings on synaptic input, neural activity and CBF, and recognizing the limitations of each technique, it is important to think about future directions to better understand the changes occurring in the cortex after mild TBI and what some potential therapeutic targets are.

5.3.1 Electrophysiological measurements

As stated above, it would be useful to examine the intrinsic properties of cells, especially the resting membrane potential and the rheobase since these measurements would tell us more about a cell's excitability. We could easily measure the intrinsic properties in acute slices to complement our study of synaptic input. Given how much CBF and the extracellular environment is altered after TBI though, we would strongly consider making these measurements *in vivo* with whole-cell patch clamp recordings or sharp intracellular recordings. There has been success with *in vivo* whole-cell patch clamp recordings allowing for detection of subthreshold inputs in addition to picking up action potentials and determining resting membrane potential (Lee et al., 2006; Margrie et al., 2002). Some of the earlier *in vivo* patch experiments had to be done in very superficial layers of tissue (≤150 um), but more recent studies and advancements in automating patching show that recordings can be made from cortical cells 800-1000 μm below the surface (Kodandaramaiah et al., 2012; Marlin et al., 2015). Alternatively, sharp intracellular recordings have been used for very accurately measuring resting membrane potential and cell firing in for years (McIlwain and Creutzfeldt, 1967; Schneider et al., 2014; Svoboda et al., 1999). The *in vivo* measurement of intrinsic properties could not be

directly compared to our synaptic inputs measured in acute slices, but the added benefit of *in vivo* recordings may outweigh being able to make a direct comparison.

5.3.2 Evoked neural activity

We examined spontaneous neural activity *in vivo* in the visual cortex, which is one of the most studied regions of the brain so the circuitry and levels of spontaneous activity are well-known. However, we have not yet taken advantage of the fact that we can measure sensory function at a cellular level with sensory-evoked neural activity. By presenting our animals with visual stimuli of moving sine wave gratings while Ca^{2+} imaging before and after mild TBI, we can calculate the orientation and direction selectivity of cells. Spontaneous activity is a simple readout of neural function, but if we want to understand more about what changes in the brain lead to cognitive and sensory deficits, we should also look at the neural response when neurons are processing natural patterns of sensory information and engaging in computations that rely on intrinsic properties and intracortical connectivity. For the primary visual cortex, this sensory information is visual stimuli, such sine wave gratings. Visual stimuli are highly reproducible, allowing for consistency before and after injury and among animals. Previous studies using sine wave gratings have established a standard method for calculating orientation and direction selectivity indexes and also serve as a reference for baseline pre-injury measurements.

5.3.3 Chronic imaging of neural activity

With our spontaneous neural activity measurements, we have looked at an acute time point within 3 hours after mild TBI. Focusing on this early phase is important for

discovering some of the first changes that occur following injury so that we can prevent or mitigate harmful cascades from occurring. However, it would also be valuable to chronically measure neural activity, both spontaneous and evoked, in order to determine the time course of changes in activity. Knowing the time informs us of when the therapeutic window for treating altered activity or other process that occur. For example, in ischemic stroke there is a defined time window in which medication for breaking down blood clots is effective. After the window of 4.5 hours though, the medication may be more harmful than beneficial (Lees et al., 2010). Determining how long neural activity is disturbed will tell us during what time frame we can potentially address it. Additionally, we could track neurons over time and see if their change in the acute phase predicts their fate, such as if hyperactive cells evolve to become suppressed or constantly fluorescent cells that have lost their ionic balance.

5.3.4 Combined neural activity & CBF

To confirm a more direct link between the reduction in CBF and altered neural activity and intracellular Ca^{2+} levels that we observed, we should simultaneously measure these two functions in more animals. While we have only imaged neural activity with Ca^{2+} indicators and CBF with injected dextran in one animal, the results were promising. The prolonged elevation of intracellular Ca^{2+} in a cell in close proximity and closely following a capillary stall is strongly correlative and highly suggestive. For future experiments we could look for capillary stalls after mild TBI and see if neighboring neurons become suppressed, hyperactive, or lose ionic balance. Tracking the same cells over time with chronic imaging would show how the activity evolves for neurons near

capillaries continuously stalled or repeatedly stalled for long durations. After mild TBI stalling was very heterogeneous throughout different capillaries so within a single cortical region of an animal we could compare activity in neurons adjacent to capillary stalls to activity in other neurons near normally-flowing capillaries. Alternatively, we could induce capillary stalls in an animal without injury by injecting 4 μm diameter microspheres (Reeson et al., 2018) to determine if capillary stalling alone (without vasoconstriction, hemorrhaging, or other obvious vascular damage) disrupts neural activity and ion homeostasis, which would provide greater evidence that reduced blood flow in capillaries is responsible for abnormal neuronal physiology.

5.3.5 Tissue pO_2 measurements

To better determine if there is a causal relationship between decreased CBF and altered neural activity, we could measure the oxygenation levels of brain tissue and see if the levels are reduced when CBF drops. As mentioned earlier in chapter 4 and above in the *Neural activity & CBF* subsection, neurons need oxygen and glucose for both activity and to maintain general health (Verweij et al., 2007). Given how dramatic the decrease in CBF was and the percentage of capillaries that were stalled, it is almost certain that the reduced CBF would change neural activity. Furthermore, previous studies have found a spike in glucose utilization within the first 2 hours of injury when CBF is down (Ginsberg et al., 1997; Richards et al., 2001), indicating greater metabolic demand. However, the oxygenation of tissue is affected not only by CBF but also by the oxygen extraction fraction (OEF). OEF is simply the percentage of how much oxygen is extracted from the blood and is measured by the oxygenation saturation levels in arteries

versus veins. A study in severe TBI in human patients found that although CBF dropped to critically low levels at 8-14 hours after injury, OEF rose to meet neural metabolic demand and thus prevent energy failure (Diringer et al., 2002). While we could measure the OEF in our animals before and after mild TBI, a more direct measurement to see if neurons are receiving enough oxygen is to measure the oxygenation of the actual neural tissue. Additionally, OEF is a general measurement for the whole neural tissue and would not detect local changes in tissue oxygenation, which could arise from differences in capillary flow and cytotoxic edema. For example, with OCT we observed stalls in many capillaries following mild TBI but not all so there is very likely heterogeneity in oxygenation levels of the tissue we imaged. Other studies have also found a decrease in the apparent diffusion coefficient through the tissue caused by cytotoxic edema (Albensi et al., 2000; Putten et al., 2005) so there may be an even greater difference than usual in the oxygenation of tissue closer to vessels than tissue farther away if oxygen cannot diffuse normally.

2P imaging of nicotinamide adenine dinucleotide (NADH), an intrinsically fluorescent coenzyme involved in energy metabolism in mitochondria, has been used to measure intracellular oxygen levels *in vivo* (Kasischke et al., 2011; Mayevsky and Barbiro-Michaely, 2009). NADH imaging allows for measuring cortical tissue oxygenation down to ~200 μm (Kasischke et al., 2011), but it is an indirect measurement of oxygenation and levels of the coenzyme can be also be influenced by enzyme synthesis and other processes in the mitochondria, not just available oxygen (Takahashi et al., 2006). NADH imaging also gives only relative values of oxygenation (Mayevsky

and Barbiro-Michaely, 2009). Alternatively, development of a 2P-enhanced phosphorescent nanoprobe now allows for *in vivo* measurement of absolute oxygen partial pressure (pO2) in neural tissue (Sakadžić et al., 2010). The phosphorescent nanoprobe may be limited to a depth of ~100 μm for extravascular measurements in neural tissue, but it has excellent spatial and temporal resolution allowing us detect differences in oxygenation of tissue in a small region, such as near a stalled capillary.

5.4 FUTURE DIRECTIONS: TESTING TREATMENTS

Based on our own results and those of the other researchers showing the harmful effects of reduced CBF after TBI or stroke (Jullienne et al., 2016; Lo et al., 2003; Verweij et al., 2007), improving CBF is a prime candidate for treating TBI. If CBF is low enough to induce an energy crisis, many processes including ion homeostasis, mitochondria function, and neural activity are disrupted. In other words, CBF reduction may be one of the first steps in the harmful cascade that occurs after TBI. There are a few important factors to consider when developing TBI treatments though.

First, because there are many different pathologies and disrupted processes occurring after TBI, there are multiple potential pathways to target, even for narrowing the focus to CBF. However, this also means that a combination of treatments may work best and that treatments should ideally act directly on the reaction in the pathway that is disturbed rather than relying on other upstream or downstream reactions in the pathway to still be functional. For example, L-dopa is a common treatment for Parkinson's disease to replace the lost dopamine from neurodegeneration of the parts of the basal ganglia, especially the substantia nigra. While dopamine cannot cross the BBB, the dopamine pre-

cursor L-dopa can so it is effectively taken as an oral medication. The problem of the lack of dopamine is solved by adjusting a reaction upstream in the pathway. However, if the enzyme responsible for converting L-dopa to dopamine (DOPA-decarboxylase) is dysfunctional or extremely scarce, the reaction creating more dopamine will not occur. Fortunately, DOPA-decarboxylase usually functions well enough in individuals with Parkinson's (Lloyd and Hornykiewicz, 1970), but assuming different upstream or downstream reactions are working normally can be problematic in TBI.

Hypertension and vasospasm can occur after head injury, especially if there is subarachnoid hemorrhage. One treatment strategy might be to provide patients with a drug that locally releases nitric oxide, a known vasodilator. Nitric oxide works by activating guanylate cyclase that synthesizes cyclic GMP to hyperpolarize and relax smooth muscle cells, allowing the arteries the muscle cells surround to also relax (Sobey, 2001). However, nitric oxide donating drugs have only been moderately effective to treat subarachnoid hemorrhage (Onoue et al., 1995; Sobey et al., 1996), potentially because of increased activity by phosphodiesterases that break down cyclic GMP and AMP (Kenney et al., 2018; Sobey and Quan, 1999; Wilson et al., 2017). In contrast, more directly targeting the disturbed reaction of cyclic GMP breakdown with phosphodiesterase inhibitors or cyclic GMP analogues resistant to phosphodiesterase have shown promise in treating TBI (Kenney et al., 2018; Sobey et al., 1996; Wilson et al., 2017).

Second, remember that TBI is very heterogeneous, and what works well to treat TBI in one individual may do more harm in another person. In the example above, we pointed out that some TBI patients have hypertension after injury, but other individuals

present with hypotension (Stocchetti et al., 1996), which could require vasoconstriction rather than vasodilation medication. Thus, there is likely no panacea for all TBIs, and it is important to identify some details about the condition and pathology of the patient before treating him or her just as physicians perform CT scans to determine whether an individual suffering from stroke has ischemic or hemorrhagic stroke. The treatment strategies listed below are based on a mild injury induced by acceleration forces and may not be ideal for more severe TBI with massive hemorrhaging.

Third, our findings on reduced CBF indicate that the time window for treating mild TBI is narrow, potentially within only 2 hours of injury. While a small therapeutic window is challenging, other conditions, such as myocardial infarction (heart attack), stroke, and anaphylaxis, also have short time windows for treatment delivery that are often met. Effective strategies for early treatment of myocardial infarction include populating public spaces with automated external defibrillators requiring little to no training (Investigators, 2004) and phone calls between doctors in hospitals and paramedics administering thrombolytic agents in rural areas where transport time to the hospital is long (Pedley et al., 2003). Individuals suspected of having ischemic stroke greatly benefit from promptly taking aspirin (Chen et al., 2000), which is readily available in most schools, homes, and work places, and obviously does not require training to ingest. Similar to myocardial infarction and stroke, the minutes matter during anaphylaxis so those at high risk often carry epinephrine auto-injectors or EpiPens. Some states now mandate that schools have EpiPens on hand and a minimum number of teachers trained to inject EpiPens (Hogue et al., 2016) so the potentially life-saving

remedy is available to all students whether or not they are believed to have an allergy. Treatment for TBI can use some of these same strategies because it can be extremely hard to predict who will receive a TBI and when a person will receive it. Progress in treating myocardial infarction, stroke, and anaphylaxis shows that therapeutic interventions on short time scales are possible, but treatments work best when they are readily available to first responders or the public and involve simple delivery or telecommunication for delivery is set-up.

If improving CBF is our therapeutic goal, we must decide what aspect or mechanism of CBF to target. In our CBF experiments detailed in chapter 4, there was clearly a drastic drop in general CBF, but it was not apparent whether the decrease was the result of vasoconstriction of arterioles and venules, capillary stalls, or potentially some other process.

5.4.1 Blocking Ca^{2+} influx

Although we observed both vasoconstriction and vasodilation, the overall effect was a reduction in vessel diameter, which would reduce CBF. Under healthy conditions, most vasoconstriction occurs in the arteries and arterioles from the contraction of smooth muscle cells surrounding the vessels. The contraction in smooth muscle cells is driven by increased levels of intracellular Ca^{2+} so blocking influx of the ion may be a good pathway to target. Nimodipine is an L-type Ca^{2+} channel blocker that primarily acts on vascular smooth muscle (Langley and Sorkin, 1989). It has shown improved outcomes after aneurysmal subarachnoid hemorrhage in humans (Allen et al., 1983; Mees et al., 2007; Philippon et al., 1986), which frequently leads to cerebral vasospasm (Izzy and

Muehlschlegel, 2013). Interestingly, at least two studies have found beneficial clinical effects of nimodipine despite the fact that the drug did not significantly prevent or reverse cerebral vasospasm as detected by x-ray angiography (Langley and Sorkin, 1989; Philippon et al., 1986). This suggests that either nimodipine has a large effect in smaller vessels than could not be readily detected using low resolution angiographies or that it improves neurological outcomes by a different mechanism than alleviating vasoconstriction. Besides smooth muscle cells, L-type Ca^{2+} channels are highly expressed in the somata of neurons (Christie et al., 1995; Leitch et al., 2009), where they are also sensitive to nimodipine (Christie et al., 1995). Nimodipine may have an additional benefit after TBI by potentially limiting extracellular Ca^{2+} influx into neurons, mitigating the loss of ion homeostasis that we found when examining neural activity. It is important to note that nimodipine has been tested and failed in two clinical trials for TBI (Injury, 1994; Teasdale et al., 1990), but the lack of success could be due to using TBI groups with very heterogeneous injuries since a separate study using TBI patients specifically with hemorrhaging did show a benefit (Harders et al., 1996).

As an aside on reducing intracellular Ca^{2+} levels specifically in neurons, *in vitro* studies have shown that the mechanical force of injury and elevated extracellular glutamate after TBI result in greater NMDA receptor activation that is also responsible for Ca^{2+} influx (Weber, 2012). In the 1990s and early 2000s several NMDA receptor antagonists were tested in clinical trials for treating TBI and stroke, but all failed from lack of efficacy or negative side effects (Ikonomidou and Turski, 2002). However, more recently a different NMDA receptor antagonist, memantine, has shown promise. It

reduced gliosis, tau pathology, and deficits in synaptic plasticity after repeated TBI (Mei et al., 2018), and it decreased neuronal death and improved performance on a sensory task in rodents after penetrating vessel occlusion (Shih et al., 2013). In humans memantine lowered the levels of a biomarker for neuronal damage and improved clinical outcome as measured by the Glasgow Coma Scale (Mokhtari et al., 2018). While memantine inhibits NMDA receptors, its binding is both low affinity and voltage-dependent so that it remains bound to the receptor during moderate extended depolarization that could lead to excitotoxicity, but the antagonist leaves upon large depolarization normally associated with postsynaptic input (Kalia et al., 2008). The difference in NMDA receptor binding between memantine and other more selective, higher affinity binding antagonists may make memantine a better choice for treating TBI. NMDA receptor activation is important for some basic neuronal processes and transcriptional activation of pro-survival genes so completely abolishing activation or inhibiting activation for a prolonged period into when neurons are engaging in recovery processes could be detrimental (Ikonomidou and Turski, 2002).

Inhibiting Ca^{2+} influx into both neurons and smooth muscle cells may be beneficial, but there are some caveats to pursuing these pathways in our TBI experiments. While we observed extremely elevated intracellular Ca^{2+} in some of our pyramidal cells, they made up a small minority of the neural population, implying that a treatment blocking Ca^{2+} influx into neurons may have limited benefit. As for Ca^{2+} levels in smooth muscle cells, studies show that nimodipine was most effective when there was extensive hemorrhaging, which was not readily apparent after our model of mild TBI. More

generally, addressing vasoconstriction could be challenging since we saw changes in vessel diameter in both directions and would not want to aggravate pathological vasodilation. It was not clear whether the simultaneous occurrence of constriction and dilation in different vessels was due to a loss of autoregulation or if the dilation in some vessels was a compensatory response to constriction in other parts of the vasculature or occlusion in the capillaries. Additionally, since we observed both vasoconstriction and vasodilation, the decrease in vessel diameter may not be the main cause of reduced CBF, suggesting that other pathways for increasing CBF should be considered such as capillary stalling.

5.4.2 Improving flow through capillaries

We saw extensive capillary stalling in all of our animals, and while vasoconstriction indicates reduced CBF, stalling in capillaries means practically zero flow (Erdener et al., 2017). Since the capillary bed is a key site of oxygen and glucose delivery (Gould et al., 2017; Sakadžić et al., 2014), it is highly likely that the interruption of CBF in this region leads to an energy crisis and is linked to the neural dysfunction (elevated intracellular Ca^{2+} and decreased neural activity) that we reported in chapter 3. While we do not know for certain what was leading to the capillary stalls, two likely causes are: 1) constriction upstream of the vessel from pericytes pinching or 2) obstruction from leukocytes or platelets adhering to vessel walls and forming microthrombi.

5.4.3 Pericyte contraction & migration

Pericytes are cells that surround the endothelium of microvasculature helping regulate CBF and forming part of the BBB (Dalkara and Alarcon-Martinez, 2015). Pericytes control blood flow by contracting or relaxing which is regulated by levels of intracellular Ca^{2+} (Kamouchi et al., 2004). Under conditions of oxidative stress from hydrogen peroxide or peroxynitrite (Kamouchi et al., 2007; Nakamura et al., 2009; Yemisci et al., 2009) or ischemia (Hall et al., 2014; Yemisci et al., 2009), pericyte intracellular Ca^{2+} rises and the cells abnormally contract, constricting microvessels and significantly reducing CBF (Hall et al., 2014; Yemisci et al., 2009). Providing a superoxide scavenger and a nitric oxide synthase inhibitor in animals allows pericytes to relaxation and improve CBF (Yemisci et al., 2009). Superoxide scavengers are an appealing treatment for increasing CBF since reducing oxidative stress would help not only pericytes but also potentially neurons and glia after TBI. However, while some studies saw pericyte contraction in pathological conditions, others have observed pericyte migration away from microvessels after ischemia and a Marmarou weight drop model of TBI (Dore-Duffy et al., 2000; Gonul et al., 2002). The microvessels without pericytes were still distorted and compressed after TBI though (Dore-Duffy et al., 2000), indicating that some other factor could be responsible for vessel constriction if pericytes leave vessels. Since there is not a consensus on how most pericytes respond after TBI, we propose investigating their role before testing a treatment. A transgenic mouse line with fluorescently-labeled pericytes is commercially available (Jax #008241) and could be used for *in vivo* imaging of pericytes after TBI. Similar to our 2P *in vivo* imaging

described in chapter 3, we could image a large number of the same pericytes before and after mild TBI, tracking to see whether they change morphology or migrate away from microvessels.

5.4.4 Reducing microthrombi

Microthrombi composed of leukocytes or platelet aggregates have been observed within vessels after TBI in animal models (Dietrich et al., 1996; Härtl et al., 1997; Lu et al., 2004; Schwarzmaier et al., 2013) and humans (LaFuente and Cervós-Navarro, 1999; Stein et al., 2004). Evaluation of the time course of microthrombi after FPI or CCI shows that the presence of microthrombi and adhesion of leukocytes or platelets rises over hours to days after injury, beginning as early as 30 minutes post-TBI (Dietrich et al., 1996; Härtl et al., 1997). While we saw capillary stalling 10 minutes following injury, only one other study has looked for microthrombi this early after TBI so microthrombi should still be considered as a possible mechanism for occluding vessels. Both antibodies for adhesion molecules of leukocytes and a platelet activating factor antagonist have effectively reduced adhesion of leukocytes or microthrombi within vessels after TBI (Härtl et al., 1997; Maeda et al., 1997; Schwarzmaier et al., 2013), and the platelet activating factor antagonist also alleviated a drop in CBF (Maeda et al., 1997). Similarly, a recent study found that neutrophils were responsible for the capillary stalls observed in a mouse model of Alzheimer's disease and that an antibody specific for neutrophils (α-Ly6G) significantly decreased the capillary stalling, improved cortical CBF, and recovered performance on memory tasks (Cruz Hernandez et al., 2017). An antibody for neutrophils, antibodies for adhesion, and an antagonist of platelet activating factor are all

potentially good options for treating TBI since they appear to act directly on the cause of occluded vessels. Given the success of the α-Ly6G antibody for reducing occlusions specifically in capillaries and also improving more general blood flow though, this antibody is a great choice for testing treatment in our TBI experiments. Additionally, since the α-Ly6G antibody was effective in a transgenic mouse model of Alzheimer's disease already expressing the disease pathology, it is likely that the antibody will work if it is administered after TBI. Drugs or therapies that only work prophylactically have limited benefit in the clinical setting since people cannot predict when they will suffer a TBI. We propose inducing a mild TBI with a modified weight drop model as we previously did then administering the α-Ly6G antibody once within a few minutes after injury when capillary stalls were at their highest and repeating our different CBF measurements to see if there is an improvement in capillary stalls, vessel diameter, and general CBF. If we find that the α-Ly6G antibody is successful at treating some of the CBF changes after TBI, we would also test the effects of antibody treatment on neural activity with Ca^{2+} imaging.

5.5 CONCLUSION

In conclusion, we took a multidisciplinary approach to ask how cortical neural function and CBF are altered after mild TBI. The cortex is responsible for many of the cognitive tasks and sensory processing that are disturbed following injury so understanding cortical changes may be key to developing therapies to treat TBI rather than simply addressing the symptoms. Using a variety of techniques to look at two aspects of neural function (synaptic input, activity) and multiple systems (neural,

vascular, and a little glial) allowed us to have a more complete picture of what changes are occurring after injury. Because there is a significant amount of interplay between functions and systems, a more complete picture is especially valuable.

We focused on the acute phase of injury that is understudied but is when harmful TBI-induced cascades begin and thus a therapy could potentially be the most effective. For two measurements we used the more advanced techniques of *in vivo* Ca^{2+} imaging and OCT that have not previously been employed for examining the cortex after TBI in order to see more biologically relevant alterations in the intact brain and changes at a higher spatial resolution. The improved spatial resolution allowed for detection of heterogeneity in neural activity and blood flow through individual capillaries. We found increased excitation in synaptic inputs onto pyramidal cells in slices made 1 hour after injury that recovered by 48 hours, further emphasizing the importance of early time points. With *in vivo* Ca^{2+} imaging, we observed substantial suppression of overall neural activity and loss of ion homeostasis around 1 hour after mild TBI confirming physiological disruptions in the acute phase of injury. Using laser speckle contrast imaging and OCT, we detected a dramatic loss of general CBF and blood flow through the microvasculature beginning within 5-10 minutes and lasting over 1 hour following mild TBI. Given neurons' high metabolic demand when firing and even at rest, the large drop in CBF likely accounts for the altered activity and ion imbalance.

Our results provide new insight into what changes are occurring after mild TBI, including that the changes begin taking place within the first hour of injury and that a reduction in blood flow through the microvasculature may be the driver. It is critical for

future research to build on these foundational studies by continuing to examine the details of these alterations in order to identify a mechanism for treating TBI. Improving blood flow through the microvasculature by countering vasoconstriction or reducing microthrombi are promising therapeutic avenues that could benefit the rest of the vascular system and the neural system that depends on steady CBF. With an identified time window, future work should focus on early time points when examining mechanisms and testing potential treatments that 69 million people throughout the world so desperately need.

BIBLIOGRAPHY

Albensi, B.C., Knoblach, S.M., Chew, B.G.M., O'Reilly, M.P., Faden, A.I., and Pekar, J.J. (2000). Diffusion and High Resolution MRI of Traumatic Brain Injury in Rats: Time Course and Correlation with Histology. Experimental Neurology *162*, 61-72.

Allen, G.S., Ahn, H.S., Preziosi, T.J., Battye, R., Boone, S.C., Chou, S.N., Kelly, D.L., Weir, B.K., Crabbe, R.A., Lavik, P.J*., et al.* (1983). Cerebral Arterial Spasm – A Controlled Trial of Nimodipine in Patients with Subarachnoid Hemorrhage. New England Journal of Medicine *308*, 619-624.

Alves, O.L., Bullock, R., Clausen, T., Reinert, M., and Reeves, T.M. (2005). Concurrent Monitoring of Cerebral Electrophysiology and Metabolism after Traumatic Brain Injury: An Experimental and Clinical Study. Journal of Neurotrauma *22*, 733-749.

Alwis, D.S., Yan, E.B., Morganti-Kossmann, M.C., and Rajan, R. (2012). Sensory cortex underpinnings of traumatic brain injury deficits. PLoS One *7*, e52169.

Annegers, J.F., Hauser, W.A., Coan, S.P., and Rocca, W.A. (1998). A Population-based Study of Seizures after Traumatic Brain Injuries. The New England Journal of Medicine *338*, 20-24.

Armonda, R.A., Bell, R.S., Vo, A.H., Ling, G., DeGraba, T.J., Crandall, B., Ecklund, J., and Campbell, W.W. (2006). Wartime Traumatic Cerebral Vasospasm: Recent Review of Combat Casualties. Neurosurgery *59*(6), 1215–1225; discussion 1225.

Arthur, D.C., MacDermid, S., and Kiley, K.C. (2007). An Achievable Vision: Report of the Department of Defense Task Force on Mental Health, D.H. Board, ed. (Falls Church, VA).

Balestreri, M., Czosnyka, M., Hutchinson, P., Steiner, L.A., Hiler, M., Smielewski, P., and Pickard, J.D. (2006). Impact of intracranial pressure and cerebral perfusion pressure on severe disability and mortality after head injury. Neurocritical Care *4*, 8-13.

Bankhead, P., Scholfield, C.N., McGeown, J.G., and Curtis, T.M. (2012). Fast retinal vessel detection and measurement using wavelets and edge location refinement. PLoS One *7*, e32435.

Bartnik-Olson, B.L., Holshouser, B., Wang, H., Grube, M., Tong, K., Wong, V., and Ashwal, S. (2014). Impaired Neurovascular Unit Function Contributes to Persistent Symptoms after Concussion: A Pilot Study. Journal of Neurotrauma *31*, 1497-1506.

Bathellier, B., Margrie, T.W., and Larkum, M.E. (2009). Properties of Piriform Cortex Pyramidal Cell Dendrites: Implications for Olfactory Circuit Design. The Journal of Neuroscience *29*, 12641-12652.

Bergsneider, M., Hovda, D.A., Shalmon, E., Kelly, D.F., Vespa, P.M., Martin, N.A., Phelps, M.E., McArthur, D.L., Caron, M.J., Kraus, J.F.*, et al.* (1997). Cerebral hyperglycolysis following severe traumatic brain injury in humans: a positron emission tomography study. Journal of Neurosurgery *86*(2), 241–251.

Bir, C., VandeVord, P., Shen, Y., Raza, W., and Haacke, E.M. (2012). Effects of variable blast pressures on blood flow and oxygen saturation in rat brain as evidenced using MRI. Magnetic Resonance Imaging *30*, 527-534.

Blennow, K., Hardy, J., and Zetterberg, H. (2012). The neuropathology and neurobiology of traumatic brain injury. Neuron *76*, 886-899.

Blinder, P., Shih, A.Y., Rafie, C., and Kleinfeld, D. (2010). Topological basis for the robust distribution of blood to rodent neocortex. Proceedings of the National Academy of Sciences of the United States of America *107*, 12670-12675.

Blinder, P., Tsai, P.S., Kaufhold, J.P., Knutsen, P.M., Suhl, H., and Kleinfeld, D. (2013). The cortical angiome: an interconnected vascular network with noncolumnar patterns of blood flow. Nature Neuroscience *16*, 889-897.

Boas, D.A., and Dunn, A.K. (2010). Laser speckle contrast imaging in biomedical optics. Journal of Biomedical Optics (SPIE) *15,* 011109-1-011109-12.

Bolay, H., Gürsoy-Özdemir, Y., Sara, Y., Onur, R., Can, A., and Dalkara, T. (2002). Persistent Defect in Transmitter Release and Synapsin Phosphorylation in Cerebral Cortex After Transient Moderate Ischemic Injury. Stroke *33*, 1369-1375.

Bolding, K.A., and Franks, K.M. (2018). Recurrent cortical circuits implement concentration-invariant odor coding. Science *361*.

Bouma, G.J., and Muizelaar, J.P. (1990). Relationship between cardiac output and cerebral blood flow in patients with intact and with impaired autoregulation. Journal of Neurosurgery *73*, 368-374.

Bouma, G.J., Muizelaar, J.P., Stringer, W.A., Choi, S.C., Fatouros, P., and Young, H.F. (1992). Ultra-early evaluation of regional cerebral blood flow in severely head-injured patients using xenon-enhanced computerized tomography. Journal of Neurosurgery *77*, 360.

Bragin, D.E., Bush, R.C., and Nemoto, E.M. (2013). Effect of Cerebral Perfusion Pressure on Cerebral Cortical Microvascular Shunting at High Intracranial Pressure in Rats. Stroke *44*, 177-181.

Brini, M., Calì, T., Ottolini, D., and Carafoli, E. (2014). Neuronal calcium signaling: function and dysfunction. Cellular and Molecular Life Sciences *71*, 2787-2814.

Brown, C.E., Wong, C., and Murphy, T.H. (2008). Rapid morphologic plasticity of peri-infarct dendritic spines after focal ischemic stroke. Stroke *39*, 1286-1291.

Bryan, R.M., Cherian, L., and Robertson, C. (1995). Regional Cerebral Blood Flow After Controlled Cortical Impact Injury in Rats. Anesthesia & Analgesia *80*, 687-695.

Buckley, E.M., Miller, B.F., Golinski, J.M., Sadeghian, H., McAllister, L.M., Vangel, M., Ayata, C., Meehan, W.P., 3rd, Franceschini, M.A., and Whalen, M.J. (2015). Decreased microvascular cerebral blood flow assessed by diffuse correlation spectroscopy after repetitive concussions in mice. Jouranl of Cerebral Blood Flow & Metabolism *35*, 1995-2000.

Caeyenberghs, K., Leemans, A., Leunissen, I., Gooijers, J., Michiels, K., Sunaert, S., and Swinnen, S.P. (2014). Altered structural networks and executive deficits in traumatic brain injury patients. Brain Structure and Function *219*, 193-209.

Camandola, S., and Mattson, M.P. (2011). Aberrant subcellular neuronal calcium regulation in aging and Alzheimer's disease. Biochimica et Biophysica Acta (BBA) - Molecular Cell Research *1813*, 965-973.

Candelario-Jalil, E., Al-Dalain, S.M., Castillo, R., Martinez, G., and Fernandez, O.S. (2001). Selective vulnerability to kainate-induced oxidative damage in different rat brain regions. Journal of Applied Toxicology *21*, 403-407.

Cantu, D., Walker, K., Andresen, L., Taylor-Weiner, A., Hampton, D., Tesco, G., and Dulla, C.G. (2015). Traumatic Brain Injury Increases Cortical Glutamate Network Activity by Compromising GABAergic Control. Cerebral Cortex *25*(8), 2306–2320.

Carroll, L., Cassidy, J.D., Peloso, P., Borg, J., von Holst, H., Holm, L., Paniak, C., and Pépin, M. (2004). Prognosis for mild traumatic brain injury: results of the who collaborating centre task force on mild traumatic brain injury. Journal of Rehabilitation Medicine *36*, 84-105.

Cassidy, J.D., Carroll, L., Peloso, P., Borg, J., x000F, rgen, von Holst, H., Holm, L., Kraus, J., and Coronado, V. (2004). Incidence, risk factors and prevention of mild traumatic brain injury: results of the who collaborating centre task force on mild traumatic brain injury. Journal of Rehabilitation Medicine *36*, 28-60.

CDC (2017). TBI: Get the Facts (Centers for Disease Control and Prevention: USA.gov).

Cernak, I., Merkle, A.C., Koliatsos, V.E., Bilik, J.M., Luong, Q.T., Mahota, T.M., Xu, L., Slack, N., Windle, D., and Ahmed, F.A. (2011). The pathobiology of blast injuries and blast-induced neurotrauma as identified using a new experimental model of injury in mice. Neurobiology of Disease *41*, 538-551.

Chadwick, D. (2000). Seizures and epilepsy after traumatic brain injury. The Lancet *355*, 334-336.

Chang, B.S., and Lowenstein, D.H. (2003). Epilepsy. New England Journal of Medicine *349*, 1257-1266.

Chen, S., and Buckmaster, P.S. (2005). Stereological analysis of forebrain regions in kainate-treated epileptic rats. Brain Research *1057*, 141-152.

Chen, Y., and Huang, W. (2011). Non-impact, blast-induced mild TBI and PTSD: Concepts and caveats. Brain Injury *25*, 641-650.

Chen, Z., Sandercock, P., Pan, H., Counsell, C., Collins, R., Liu, L., Xie, J., Warlow, C., and Peto, R. (2000). Indications for Early Aspirin Use in Acute Ischemic Stroke. Stroke *31*, 1240-1249.

Christie, B.R., Eliot, L.S., Ito, K., Miyakawa, H., and Johnston, D. (1995). Different Ca2+ channels in soma and dendrites of hippocampal pyramidal neurons mediate spike-induced Ca2+ influx. Journal of Neurophysiology *73*, 2553-2557.

Clark, R.S.B., Schiding, J.K., Kaczorowski, S.L., Marion, D.W., and Kochanek, P.M. (1994). Neutrophil Accumulation After Traumatic Brain Injury in Rats: Comparison of Weight Drop and Controlled Cortical Impact Models. Journal of Neurotrauma *11*, 499-506.

Courville, C.B. (1942). Coup-contrecoup mechanism of craniocerebral injuries: Some observations. Archives of Surgery *45*, 19-43.

Cruz Hernandez, J.C., Bracko, O., Kersbergen, C.J., Muse, V., Haft-Javaherian, M., Berg, M., Park, L., Vinarcsik, L.K., Ivasyk, I., Kang, Y.*, et al.* (2017). Neutrophil adhesion in brain capillaries contributes to cortical blood flow decreases and impaired memory function in a mouse model of Alzheimer's disease. bioRxiv, 226886.

Dalkara, T., and Alarcon-Martinez, L. (2015). Cerebral microvascular pericytes and neurogliovascular signaling in health and disease. Brain Research *1623*, 3-17.

Daneyemez, M. (1999). Microangiographic changes following cerebral contusion in rats. Neuroscience *92*, 783-790.

Davalos, D., Grutzendler, J., Yang, G., Kim, J.V., Zuo, Y., Jung, S., Littman, D.R., Dustin, M.L., and Gan, W.B. (2005). ATP mediates rapid microglial response to local brain injury *in vivo*. Nature Neuroscience *8*, 752-758.

De Guise, E., Leblanc, J., Dagher, J., Lamoureux, J., Jishi, A.A., Maleki, M., Marcoux, J., and Feyz, M. (2009). Early outcome in patients with traumatic brain injury, pre-injury alcohol abuse and intoxication at time of injury. Brain Injury *23*, 853-865.

DeFord, S.M., Wilson, M.S., Rice, A.C., Clausen, T., Rice, L.K., Barabnova, A., Bullock, R., and Hamm, R.J. (2002). Repeated Mild Brain Injuries Result in Cognitive Impairment in B6C3F1 Mice. Journal of Neurotrauma *19*, 427-438.

Denny-Brown, D.E., and Russell, W.R. (1941). Experimental Concussion: (Section of Neurology). Proceedings of the Royal Society of Medicine *34*, 691-692.

Deshpande, L.S., Sun, D.A., Sombati, S., Baranova, A., Wilson, M.S., Attkisson, E., Hamm, R.J., and DeLorenzo, R.J. (2008). Alterations in neuronal calcium levels are associated with cognitive deficits after traumatic brain injury. Neuroscience Letters *441*, 115-119.

Devor, A., Sakadžić, S., Saisan, P.A., Yaseen, M.A., Roussakis, E., Srinivasan, V.J., Vinogradov, S.A., Rosen, B.R., Buxton, R.B., Dale, A.M*., et al.* (2011). “Overshoot” of O₂ Is Required to Maintain Baseline Tissue Oxygenation at Locations Distal to Blood Vessels. The Journal of Neuroscience *31*, 13676-13681.

Devor, A., Tian, P., Nishimura, N., Teng, I.C., Hillman, E.M.C., Narayanan, S.N., Ulbert, I., Boas, D.A., Kleinfeld, D., and Dale, A.M. (2007). Suppressed Neuronal Activity and Concurrent Arteriolar Vasoconstriction May Explain Negative Blood Oxygenation Level-Dependent Signal. The Journal of Neuroscience *27*, 4452-4459.

Dewan, M.C., Rattani, A., Gupta, S., Baticulon, R.E., Hung, Y.-C., Punchak, M., Agrawal, A., Adeleye, A.O., Shrime, M.G., Rubiano, A.M*., et al.* (2018). Estimating the global incidence of traumatic brain injury. Journal of Neurosurgery 1-18.

DeWitt, D.S., Jenkins, L.W., Wei, E.P., Lutz, H., Becker, D.P., and Kontos, H.A. (1986). Effects of fluid-percussion brain injury on regional cerebral blood flow and pial arteriolar diameter. Journal of Neurosurgery *64*, 787-794.

DeWitt, D.S., and Prough, D.S. (2003). Traumatic Cerebral Vascular Injury: The Effects of Concussive Brain Injury on the Cerebral Vasculature. Journal of Neurotrauma *20*, 795-825.

DeWitt, D.S., Smith, T.G., Deyo, D.J., Miller, K.R., Uchida, T., and Prough, D.S. (1997). L-Arginine and Superoxide Dismutase Prevent or Reverse Cerebral Hypoperfusion after Fluid-Percussion Traumatic Brain Injury. Journal of Neurotrauma *14*, 223-233.

Dietrich, W.D., Alonso, O., Busto, R., Prado, R., Dewanjee, S., Dewanjee, M.K., and Ginsberg, M.D. (1996). Widespread Hemodynamic Depression and Focal Platelet Accumulation after Fluid Percussion Brain Injury: A Double-Label Autoradiographic Study in Rats. Journal of Cerebral Blood Flow & Metabolism *16*, 481-489.

Dietrich, W.D., Alonso, O., and Halley, M. (1994). Early Microvascular and Neuronal Consequences of Traumatic Brain Injury: A Light and Electron Microscopic Study in Rats. Journal of Neurotrauma *11*, 289-301.

Ding, M.C., Wang, Q., Lo, E.H., and Stanley, G.B. (2011). Cortical excitation and inhibition following focal traumatic brain injury. The Journal of Neuroscience *31*, 14085-14094.

Diringer, M.N., Videen, T.O., Yundt, K., Zazulia, A.R., Aiyagari, V., Dacey, R.G., Grubb, R.L., and Powers, W.J. (2002). Regional cerebrovascular and metabolic effects of hyperventilation after severe traumatic brain injury. Journal of Neurosurgery *96*, 103-108.

Dixon, C.E., Clifton, G.L., Lighthall, J.W., Yaghmai, A.A., and Hayes, R.L. (1991). A controlled cortical impact model of traumatic brain injury in the rat. Journal of Neuroscience Methods *39*, 253-262.

Dixon, C.E., Lyeth, B.G., Povlishock, J.T., Findling, R.L., Hamm, R.J., Marmarou, A., Young, H.F., and Hayes, R.L. (1987). A fluid percussion model of experimental brain injury in the rat. Journal of Neurosurgery *67*, 110-119.

Dore-Duffy, P., Owen, C., Balabanov, R., Murphy, S., Beaumont, T., and Rafols, J.A. (2000). Pericyte Migration from the Vascular Wall in Response to Traumatic Brain Injury. Microvascular Research *60*, 55-69.

Dreier, J.P. (2011). The role of spreading depression, spreading depolarization and spreading ischemia in neurological disease. Nature Medicine *17*, 439.

Ehlers, M.D. (2003). Activity level controls postsynaptic composition and signaling via the ubiquitin-proteasome system. Nature Neuroscience *6*, 231.

Ekelund, L., Nilsson, B., and Pontén, U. (1974). Carotid angiography after experimental head injury in the rat. Neuroradiology *7*, 209-214.

Enevoldsen, E.M., and Jensen, F.T. (1978). Autoregulation and CO2 responses of cerebral blood flow in patients with acute severe head injury. Journal of Neurosurgery *48*, 689-703.

Erdener, S.E., Tang, J., Sajjadi, A., Kilic, K., Kura, S., Schaffer, C.B., and Boas, D.A. (2017). Spatio-temporal dynamics of cerebral capillary segments with stalling red blood cells. Journal of Cerebral Blood Flow & Metabolism, 271678X17743877.

Erecińska, M., and Silver, I.A. (1994). Ions and energy in mammalian brain. Progress in Neurobiology *43*, 37-71.

Fabricius, M., Fuhr, S., Bhatia, R., Boutelle, M., Hashemi, P., Strong, A.J., and Lauritzen, M. (2006). Cortical spreading depression and peri-infarct depolarization in acutely injured human cerebral cortex. Brain *129*, 778-790.

Faul, M., Xu, L., Wald, M.M., and Coronado, V.G. (2010). Traumatic Brain Injury in the United States: Emergency Visits, Hospitalizations and Deaths 2002-2006, Centers for Disease Control and Prevention, ed. (Atlanta, GA).

Feeney, D.M., Boyeson, M.G., Linn, R.T., Murray, H.M., and Dail, W.G. (1981). Responses to cortical injury: I. Methodology and local effects of contusions in the rat. Brain Research *211*, 67-77.

Fernández-Klett, F., Offenhauser, N., Dirnagl, U., Priller, J., and Lindauer, U. (2010). Pericytes in capillaries are contractile in vivo, but arterioles mediate functional hyperemia in the mouse brain. Proceedings of the National Academy of Sciences *107*, 22290-22295.

Fernandez-Klett, F., and Priller, J. (2015). Diverse Functions of Pericytes in Cerebral Blood Flow Regulation and Ischemia. Journal of Cerebral Blood Flow & Metabolism *35*, 883-887.

Fleidervish, I.A., Gebhardt, C., Astman, N., Gutnick, M.J., and Heinemann, U. (2001). Enhanced Spontaneous Transmitter Release Is the Earliest Consequence of Neocortical Hypoxia That Can Explain the Disruption of Normal Circuit Function. The Journal of Neuroscience *21*, 4600-4608.

Foda, M.A.A.-E., and Marmarou, A. (1994). A new model of diffuse brain injury in rats: Part II: Morphological characterization. Journal of Neurosurgery *80*, 13.

Franks, K.M., and Isaacson, J.S. (2005). Synapse-specific downregulation of NMDA receptors by early experience: a critical period for plasticity of sensory input to olfactory cortex. Neuron *47*, 101-114.

Franks, K.M., and Isaacson, J.S. (2006). Strong Single-Fiber Sensory Inputs to Olfactory Cortex: Implications for Olfactory Coding. Neuron *49*, 357-363.

Franks, K.M., Russo, M.J., Sosulski, D.L., Mulligan, A.A., Siegelbaum, S.A., and Axel, R. (2011). Recurrent circuitry dynamically shapes the activation of piriform cortex. Neuron *72*, 49-56.

Gale, K. (1988). Progression and Generalization of Seizure Discharge: Anatomical and Neurochemical Substrates. Epilepsia *29*, S15-S34.

Gerberding, J.L., and Binder, S. (2003). Report to Congress on Mild Traumatic Brain Injury in the United States: Steps to Prevent a Serious Public Health Problem, N.C.f.I.P.a. Control, ed. (Atlanta, GA).

Ginsberg, M.D., Zhao, W., Alonso, O.F., Loor-Estades, J.Y., Dietrich, W.D., and Busto, R. (1997). Uncoupling of local cerebral glucose metabolism and blood flow after acute fluid-percussion injury in rats. American Journal of Physiology-Heart and Circulatory Physiology *272*, H2859-H2868.

Girouard, H., and Iadecola, C. (2006). Neurovascular coupling in the normal brain and in hypertension, stroke, and Alzheimer disease. Journal of Applied Physiology *100*, 328-335.

Giza, C.C., and Hovda, D.A. (2014). The new neurometabolic cascade of concussion. Neurosurgery *75 Suppl 4*, S24-33.

Golarai, G., Greenwood, A.C., Feeney, D.M., and Connor, J.A. (2001). Physiological and Structural Evidence for Hippocampal Involvement in Persistent Seizure Susceptibility after Traumatic Brain Injury. The Journal of Neuroscience *21*, 8523-8537.

Golding, E.M. (2002). Sequelae following traumatic brain injury: The cerebrovascular perspective. Brain Research Reviews *38*, 377-388.

Goldstein, L.E., Fisher, A.M., Tagge, C.A., Zhang, X.L., Velisek, L., Sullivan, J.A., Upreti, C., Kracht, J.M., Ericsson, M., Wojnarowicz, M.W.*, et al.* (2012). Chronic traumatic encephalopathy in blast-exposed military veterans and a blast neurotrauma mouse model. Science Translational Medicine *4*, 134ra160.

Gonul, E., Duz, B., Kahraman, S., Kayali, H., Kubar, A., and Timurkaynak, E. (2002). Early Pericyte Response to Brain Hypoxia in Cats: An Ultrastructural Study. Microvascular Research *64*, 116-119.

Gould, I.G., Tsai, P., Kleinfeld, D., and Linninger, A. (2017). The capillary bed offers the largest hemodynamic resistance to the cortical blood supply. Journal of Cerebral Blood Flow & Metabolism *37*, 52-68.

Greer, J.E., Povlishock, J.T., and Jacobs, K.M. (2012). Electrophysiological abnormalities in both axotomized and nonaxotomized pyramidal neurons following mild traumatic brain injury. The Journal of Neuroscience *32*, 6682-6687.

Grienberger, C., Rochefort, N.L., Adelsberger, H., Henning, H.A., Hill, D.N., Reichwald, J., Staufenbiel, M., and Konnerth, A. (2012). Staged decline of neuronal function in vivo in an animal model of Alzheimer's disease. Nature Communications *3*, 774.

Griesemer, D., and Mautes, A.M. (2007). Closed head injury causes hyperexcitability in rat hippocampal CA1 but not in CA3 pyramidal cells. Journal of Neurotrauma *24*, 1823-1832.

Grutzendler, J., Kasthuri, N., and Gan, W.B. (2002). Long-term dendritic spine stability in the adult cortex. Nature *420*, 812-816.

Gullotti, D.M., Beamer, M., Panzer, M.B., Chia Chen, Y., Patel, T.P., Yu, A., Jaumard, N., Winkelstein, B., Bass, C.R., Morrison, B.*, et al.* (2014). Significant Head Accelerations Can Influence Immediate Neurological Impairments in a Murine Model of Blast-Induced Traumatic Brain Injury. Journal of Biomechanical Engineering *136*, 091004-091004-091011.

Haider, B., Häusser, M., and Carandini, M. (2012). Inhibition dominates sensory responses in the awake cortex. Nature *493*, 97.

Hájos, N., Ellender, T.J., Zemankovics, R., Mann, E.O., Exley, R., Cragg, S.J., Freund, T.F., and Paulsen, O. (2009). Maintaining network activity in submerged hippocampal slices: importance of oxygen supply. The European journal of neuroscience *29*, 319-327.

Hall, C.N., Reynell, C., Gesslein, B., Hamilton, N.B., Mishra, A., Sutherland, B.A., O'Farrell, F.M., Buchan, A.M., Lauritzen, M., and Attwell, D. (2014). Capillary pericytes regulate cerebral blood flow in health and disease. Nature *508*, 55-60.

Halonen, T., Tortorella, A., Zrebeet, H., and Gale, K. (1994). Posterior piriform and perirhinal cortex relay seizures evoked from the area tempestas: role of excitatory and inhibitory amino acid receptors. Brain Research *652*, 145-148.

Hansen, M.K.R., DeWalt, M.G.J., Mohammed, D.A.I., Tseng, D.H.-a., Abdulkerim, M.M.E., Bensussen, M.S., Saligrama, D.V., Nazer, D.B., Eldred, D.W.D., and Han, D.X. (2018). Mild Blast Injury Produces Acute Changes in Basal Intracellular Calcium Levels and Activity Patterns in Mouse Hippocampal Neurons. Journal of Neurotrauma.

Harders, A., Kakarieka, A., and Braakman, R. (1996). Traumatic subarachnoid hemorrhage and its treatment with nimodipine. Journal of Neurosurgery *85*, 82-89.

Harper, S.L., Bohlen, H.G., and Rubin, M.J. (1984). Arterial and microvascular contributions to cerebral cortical autoregulation in rats. American Journal of Physiology-Heart and Circulatory Physiology *246*, H17-H24.

Hartings, J.A., Shuttleworth, C.W., Kirov, S.A., Ayata, C., Hinzman, J.M., Foreman, B., Andrew, R.D., Boutelle, M.G., Brennan, K., Carlson, A.P.*, et al.* (2017). The continuum of spreading depolarizations in acute cortical lesion development: Examining Leão's legacy. Journal of Cerebral Blood Flow & Metabolism *37*, 1571-1594.

Härtl, R., Medary, M.B., Ruge, M., Arfors, K.E., and Ghajar, J. (1997). Early White Blood Cell Dynamics after Traumatic Brain Injury: Effects on the Cerebral Microcirculation. Journal of Cerebral Blood Flow & Metabolism *17*, 1210-1220.

Hayward, N.M.E.A., Tuunanen, P.I., Immonen, R., Ndode-Ekane, X.E., Pitkänen, A., and Gröhn, O. (2011). Magnetic resonance imaging of regional hemodynamic and cerebrovascular recovery after lateral fluid-percussion brain injury in rats. Journal of cerebral blood flow and metabolism : official journal of the International Society of Cerebral Blood Flow and Metabolism *31*, 166-177.

Hekmatpanah, J., and Hekmatpanah, C.R. (1985). Micro vascular alterations following cerebral contusion in rats. Journal of Neurosurgery *62*, 888.

Hill, R.A., Tong, L., Yuan, P., Murikinati, S., Gupta, S., and Grutzendler, J. (2015). Regional Blood Flow in the Normal and Ischemic Brain Is Controlled by Arteriolar Smooth Muscle Cell Contractility and Not by Capillary Pericytes. Neuron *87*, 95-110.

Hirsch, S., Reichold, J., Schneider, M., Székely, G., and Weber, B. (2012). Topology and Hemodynamics of the Cortical Cerebrovascular System. Journal of Cerebral Blood Flow & Metabolism *32*, 952-967.

Hofmeijer, J., and Putten, M.J.A.M.v. (2012). Ischemic Cerebral Damage. Stroke *43*, 607-615.

Hoge, C.W., McGurk, D., Thomas, J.L., Cox, A.L., Engel, C.C., and Castro, C.A. (2008). Mild Traumatic Brain Injury in U.S. Soldiers Returning from Iraq. New England Journal of Medicine *358*, 453-463.

Hogue, S.L., Goss, D., Hollis, K., Silvia, S., and White, M.V. (2016). Training and administration of epinephrine auto-injectors for anaphylaxis treatment in US schools: results from the EpiPen4Schools(®) pilot survey. Journal of Asthma and Allergy *9*, 109-115.

Holtmaat, A., Bonhoeffer, T., Chow, D.K., Chuckowree, J., De Paola, V., Hofer, S.B., Hubener, M., Keck, T., Knott, G., Lee, W.C.*, et al.* (2009). Long-term, high-resolution imaging in the mouse neocortex through a chronic cranial window. Nature Protocols *4*, 1128-1144.

Huang, D., Swanson, E., Lin, C., Schuman, J., Stinson, W., Chang, W., Hee, M., Flotte, T., Gregory, K., Puliafito, C.*, et al.* (1991). Optical coherence tomography. Science *254*, 1178-1181.

Hulkower, M.B., Poliak, D.B., Rosenbaum, S.B., Zimmerman, M.E., and Lipton, M.L. (2013). A Decade of DTI in Traumatic Brain Injury: 10 Years and 100 Articles Later. American Journal of Neuroradiology *34*, 2064-2074.

Iadecola, C. (2004). Neurovascular regulation in the normal brain and in Alzheimer's disease. Nature Reviews. Neuroscience *5*, 347.

Ibata, K., Sun, Q., and Turrigiano, G.G. (2008). Rapid Synaptic Scaling Induced by Changes in Postsynaptic Firing. Neuron *57*, 819-826.

Ikonomidou, C., and Turski, L. (2002). Why did NMDA receptor antagonists fail clinical trials for stroke and traumatic brain injury? The Lancet Neurology *1*, 383-386.

Iliff, J.J., Chen, M.J., Plog, B.A., Zeppenfeld, D.M., Soltero, M., Yang, L., Singh, I., Deane, R., and Nedergaard, M. (2014). Impairment of glymphatic pathway function promotes tau pathology after traumatic brain injury. The Journal of Neuroscience *34*, 16180-16193.

Imai, Y., Ibata, I., Ito, D., Ohsawa, K., and Kohsaka, S. (1996). A Novel Geneiba1in the Major Histocompatibility Complex Class III Region Encoding an EF Hand Protein Expressed in a Monocytic Lineage. Biochemical and Biophysical Research Communications *224*, 855-862.

Injury, T.E.S.G.o.N.i.S.H. (1994). A multicenter trial of the efficacy of nimodipine on outcome after severe head injury. The European Study Group on Nimodipine in Severe Head Injury. Journal of Neurosurgery *80*, 797-804.

Investigators, T.P.A.D.T. (2004). Public-Access Defibrillation and Survival after Out-of-Hospital Cardiac Arrest. New England Journal of Medicine *351*, 637-646.

Isaacson, Jeffry S., and Scanziani, M. (2011). How Inhibition Shapes Cortical Activity. Neuron *72*, 231-243.

Ito, D., Imai, Y., Ohsawa, K., Nakajima, K., Fukuuchi, Y., and Kohsaka, S. (1998). Microglia-specific localisation of a novel calcium binding protein, Iba1. Molecular Brain Research *57*, 1-9.

Izzy, S., and Muehlschlegel, S. (2013). Cerebral Vasospasm After Aneurysmal Subarachnoid Hemorrhage and Traumatic Brain Injury. Current Treatment Options in Neurology *16*, 278.

Jackson, G.L., Hamilton, N.S., and Tupler, L.A. (2008). Detecting Traumatic Brain Injury Among Veterans of Operations Enduring and Iraqi Freedom. North Carolina Medical Journal *69*, 5.

Johnson, D.M.G., Illig, K.R., Behan, M., and Haberly, L.B. (2000). New Features of Connectivity in Piriform Cortex Visualized by Intracellular Injection of Pyramidal Cells Suggest that "Primary" Olfactory Cortex Functions Like "Association" Cortex in Other Sensory Systems. The Journal of Neuroscience *20*, 6974-6982.

Johnstone, V.P., Shultz, S.R., Yan, E.B., O'Brien, T.J., and Rajan, R. (2014). The acute phase of mild traumatic brain injury is characterized by a distance-dependent neuronal hypoactivity. Journal of Neurotrauma *31*, 1881-1895.

Johnstone, V.P., Yan, E.B., Alwis, D.S., and Rajan, R. (2013). Cortical hypoexcitation defines neuronal responses in the immediate aftermath of traumatic brain injury. PLoS One *8*, e63454.

Jones, T.H., Morawetz, R.B., Crowell, R.M., Marcoux, F.W., FitzGibbon, S.J., DeGirolami, U., and Ojemann, R.G. (1981). Thresholds of focal cerebral ischemia in awake monkeys. Journal of Neurosurgery *54*, 773-782.

Jullienne, A., Obenaus, A., Ichkova, A., Savona-Baron, C., Pearce, W.J., and Badaut, J. (2016). Chronic cerebrovascular dysfunction after traumatic brain injury. Journal of Neuroscience Research *94*, 609-622.

Jünger, E.C., Newell, D.W., Grant, G.A., Avellino, A.M., Ghatan, S., Douville, C.M., Lam, A.M., Aaslid, R., and Winn, H.R. (1997). Cerebral autoregulation following minor head injury. Journal of Neurosurgery *86*, 425-432.

Kalia, L.V., Kalia, S.K., and Salter, M.W. (2008). NMDA receptors in clinical neurology: excitatory times ahead. The Lancet Neurology *7*, 742-755.

Kallakuri, S., Bandaru, S., Zakaria, N., Shen, Y., Kou, Z., Zhang, L., Haacke, E.M., and Cavanaugh, J.M. (2015). Traumatic Brain Injury by a Closed Head Injury Device Induces Cerebral Blood Flow Changes and Microhemorrhages. Journal of Clinical Imaging Science *5*, 52-52.

Kamouchi, M., Kitazono, T., Ago, T., Wakisaka, M., Kuroda, J., Nakamura, K., Hagiwara, N., Ooboshi, H., Ibayashi, S., and Iida, M. (2007). Hydrogen peroxide-induced Ca2+ responses in CNS pericytes. Neuroscience Letters *416*, 12-16.

Kamouchi, M., Kitazono, T., Ago, T., Wakisaka, M., Ooboshi, H., Ibayashi, S., and Iida, M. (2004). Calcium influx pathways in rat CNS pericytes. Molecular Brain Research *126*, 114-120.

Kane, M.J., Angoa-Perez, M., Briggs, D.I., Viano, D.C., Kreipke, C.W., and Kuhn, D.M. (2012). A mouse model of human repetitive mild traumatic brain injury. Journal of Neuroscience Methods *203*, 41-49.

Karve, I.P., Taylor, J.M., and Crack, P.J. (2016). The contribution of astrocytes and microglia to traumatic brain injury. British Journal of Pharmacology *173*, 692-702.

Kasischke, K.A., Lambert, E.M., Panepento, B., Sun, A., Gelbard, H.A., Burgess, R.W., Foster, T.H., and Nedergaard, M. (2011). Two-photon NADH imaging exposes boundaries of oxygen diffusion in cortical vascular supply regions. Journal of cerebral blood flow and metabolism : official journal of the International Society of Cerebral Blood Flow and Metabolism *31*, 68-81.

Kassell, N.F., Helm, G., Simmons, N., Phillips, C.D., and Cail, W.S. (1992). Treatment of cerebral vasospasm with intra-arterial papaverine. Journal of Neurosurgery *77*, 848-852.

Kaur, C., Singh, J., Lim, M.K., Ng, B.L., Yap, E.P.H., and Ling, E.A. (1995). The response of neurons and microglia to blast injury in the rat brain. Neuropathology and Applied Neurobiology *21*, 369-377.

Keck, T., Keller, Georg B., Jacobsen, R.I., Eysel, Ulf T., Bonhoeffer, T., and Hübener, M. (2013). Synaptic Scaling and Homeostatic Plasticity in the Mouse Visual Cortex In Vivo. Neuron *80*, 327-334.

Keck, T., Scheuss, V., Jacobsen, R.I., Wierenga, Corette J., Eysel, Ulf T., Bonhoeffer, T., and Hübener, M. (2011). Loss of Sensory Input Causes Rapid Structural Changes of Inhibitory Neurons in Adult Mouse Visual Cortex. Neuron *71*, 869-882.

Kelly, D.F., Martin, N.A., Kordestani, R., Counelis, G., Hovda, D.A., Bergsneider, M., McBride, D.Q., Shalmon, E., Herman, D., and Becker, D.P. (1997). Cerebral blood flow as a predictor of outcome following traumatic brain injury. Journal of Neurosurgery *86*, 633-641.

Kenney, K., Amyot, F., Haber, M., Pronger, A., Bogoslovsky, T., Moore, C., and Diaz-Arrastia, R. (2016). Cerebral Vascular Injury in Traumatic Brain Injury. Experimental Neurology *275 Pt 3*, 353-366.

Kenney, K., Amyot, F., Moore, C., Haber, M., Turtzo, L.C., Shenouda, C., Silverman, E., Gong, Y., Qu, B.-X., Harburg, L.*, et al.* (2018). Phosphodiesterase-5 inhibition potentiates cerebrovascular reactivity in chronic traumatic brain injury. Annals of Clinical and Translational Neurology *5*, 418-428.

Kharatishvili, I., Nissinen, J.P., McIntosh, T.K., and Pitkanen, A. (2006). A model of posttraumatic epilepsy induced by lateral fluid-percussion brain injury in rats. Neuroscience *140*, 685-697.

Kılıç, T., and Akakın, A. (2008). Anatomy of Cerebral Veins and Sinuses. In Frontiers of Neurology and Neuroscience, J. Bougousslavsky, ed. (Basel, Switzerland: Karger).

Kislin, M., Sword, J., Fomitcheva, I.V., Croom, D., Pryazhnikov, E., Lihavainen, E., Toptunov, D., Rauvala, H., Ribeiro, A.S., Khiroug, L.*, et al.* (2017). Reversible Disruption of Neuronal Mitochondria by Ischemic and Traumatic Injury Revealed by Quantitative Two-Photon Imaging in the Neocortex of Anesthetized Mice. The Journal of Neuroscience *37*, 333-348.

Kodandaramaiah, S.B., Franzesi, G.T., Chow, B.Y., Boyden, E.S., and Forest, C.R. (2012). Automated whole-cell patch-clamp electrophysiology of neurons in vivo. Nature Methods *9*, 585.

Koliatsos, V.E., Cernak, I., Xu, L., Song, Y., Savonenko, A., Crain, B.J., Eberhart, C.G., Frangakis, C.E., Melnikova, T., Kim, H.*, et al.* (2011). A Mouse Model of Blast Injury to Brain: Initial Pathological, Neuropathological, and Behavioral Characterization. Journal of Neuropathology & Experimental Neurology *70*, 399-416.

Kreutzberg, G.W. (1996). Microglia: a sensor for pathological events in the CNS. Trends in Neurosciences *19*, 312-318.

Kuehn, R., Simard, P.F., Driscoll, I., Keledjian, K., Ivanova, S., Tosun, C., Williams, A., Bochicchio, G., Gerzanich, V., and Simard, J.M. (2011). Rodent model of direct cranial blast injury. Journal of Neurotrauma *28*, 2155-2169.

LaFuente, J.V., and Cervós-Navarro, J. (1999). Craniocerebral Trauma Induces Hemorheological Disturbances. Journal of Neurotrauma *16*, 425-430.

Langfitt, T.W., Obrist, W.D., Gennarelli, T.A., O'Connor, M.J., and Weeme, C.A. (1977). Correlation of cerebral blood flow with outcome in head injured patients. Annals of surgery *186*, 411-414.

Langley, M.S., and Sorkin, E.M. (1989). Nimodipine. Drugs *37*, 669-699.

Large, A.M., Vogler, N.W., Canto-Bustos, M., Friason, F.K., Schick, P., and Oswald, A.-M.M. (2018). Differential inhibition of pyramidal cells and inhibitory interneurons along the rostrocaudal axis of anterior piriform cortex. Proceedings of the National Academy of Sciences of the United States of America *115*, E8067-E8076.

Large, A.M., Vogler, N.W., Mielo, S., and Oswald, A.-M.M. (2016). Balanced feedforward inhibition and dominant recurrent inhibition in olfactory cortex. Proceedings of the National Academy of Sciences *113*, 2276-2281.

Laurer, H.L., Bareyre, F.M., Lee, V.M.Y.C., Trojanowski, J.Q., Longhi, L., Hoover, R., Saatman, K.E., Raghupathi, R., Hoshino, S., Grady, M.S.*, et al.* (2001). Mild head injury increasing the brain's vulnerability to a second concussive impact. Journal of Neurosurgery *95*, 859-870.

Lauritzen, M., Dreier, J.P., Fabricius, M., Hartings, J.A., Graf, R., and Strong, A.J. (2011). Clinical Relevance of Cortical Spreading Depression in Neurological Disorders: Migraine, Malignant Stroke, Subarachnoid and Intracranial Hemorrhage, and Traumatic Brain Injury. Journal of Cerebral Blood Flow & Metabolism *31*, 17-35.

Lee, A.K., Manns, I.D., Sakmann, B., and Brecht, M. (2006). Whole-Cell Recordings in Freely Moving Rats. Neuron *51*, 399-407.

Lee, J., Wu, W., Jiang, J.Y., Zhu, B., and Boas, D.A. (2012). Dynamic light scattering optical coherence tomography. Optics Express *20*, 22262-22277.

Lee, S.-T., and Lui, T.-N. (1992). Early Seizures after Mild Closed Head Injury. Journal of Neurosurgery *76*, 435-439.

Lees, K.R., Bluhmki, E., von Kummer, R., Brott, T.G., Toni, D., Grotta, J.C., Albers, G.W., Kaste, M., Marler, J.R., Hamilton, S.A.*, et al.* (2010). Time to treatment with intravenous alteplase and outcome in stroke: an updated pooled analysis of ECASS, ATLANTIS, NINDS, and EPITHET trials. The Lancet *375*, 1695-1703.

Leitch, B., Szostek, A., Lin, R., and Shevtsova, O. (2009). Subcellular distribution of L-type calcium channel subtypes in rat hippocampal neurons. Neuroscience *164*, 641-657.

Levin, H., Cooper, P., Levin, H., and Cooper, P. (1987). Neurobehavioral sequelae of head injury (Williams & Wilkins).

Levin, H.S., Gary, H.E., Eisenberg, H.M., Ruff, R.M., Barth, J.T., Kreutzer, J., High, W.M., Portman, S., Foulkes, M.A., Jane, J.A.*, et al.* (1990). Neurobehavioral outcome 1 year after severe head injury. Journal of Neurosurgery *73*, 699-709.

Lew, H.L., Poole, J.H., Vanderploeg, R.D., Goodrich, G.L., Dekelboum, S., Guillory, S.B., Sigford, B., and Cifu, D.X. (2007). Program development and defining characteristics of returning military in a VA Polytrauma Network Site. The Journal of Rehabilitation Research and Development *44*, 1027-1034.

Lewelt, W., Jenkins, L.W., and Miller, J.D. (1980). Autoregulation of cerebral blood flow after experimental fluid percussion injury of the brain. Journal of Neurosurgery *53*, 500-511.

Lighthall, J.W. (1988). Controlled Cortical Impact: A New Experimental Brain Injury Model. Journal of Neurotrauma *5*, 1-15.

Lingsma, H.F., Roozenbeek, B., Steyerberg, E.W., Murray, G.D., and Maas, A.I.R. (2010). Early prognosis in traumatic brain injury: from prophecies to predictions. The Lancet Neurology *9*, 543-554.

Lipton, P., and Whittingham, T. (1984). Energy metabolism and brain slice function. In Brain slices, R. Dingledine, ed. (New York: Plenum Press).

Lloyd, K., and Hornykiewicz, O. (1970). Parkinson's Disease: Activity of L-Dopa Decarboxylase in Discrete Brain Regions. Science *170*, 1212-1213.

Lo, E.H., Dalkara, T., and Moskowitz, M.A. (2003). Mechanisms, challenges and opportunities in stroke. Nature Reviews Neuroscience *4*, 399.

Loane, D.J., and Byrnes, K.R. (2010). Role of microglia in neurotrauma. Neurotherapeutics *7*, 366-377.

Long, J.B., Bentley, T.L., Wessner, K.A., Cerone, C., Sweeney, S., and Bauman, R.A. (2009). Blast Overpressure in Rats: Recreating a Battlefield Injury in the Laboratory. Journal of Neurotrauma *26*, 827-840.

Lu, D., Mahmood, A., Goussev, A., Qu, C., Zhang, Z.G., and Chopp, M. (2004). Delayed Thrombosis after Traumatic Brain Injury in Rats. Journal of Neurotrauma *21*, 1756-1766.

Luna, V.M., and Schoppa, N.E. (2008). GABAergic Circuits Control Input–Spike Coupling in the Piriform Cortex. The Journal of Neuroscience *28*, 8851-8859.

Lusardi, T.A., Wolf, J.A., Putt, M.E., Smith, D.H., and Meaney, D.F. (2004). Effect of Acute Calcium Influx after Mechanical Stretch Injury In Vitro on the Viability of Hippocampal Neurons. Journal of Neurotrauma *21*, 61-72.

Lyeth, B.G. (2016). Historical Review of the Fluid-Percussion TBI Model. Frontiers in Neurology *7*.

Maeda, T., Katayama, Y., Kawamata, T., Aoyama, N., and Mori, T. (1997). Hemodynamic Depression and Microthrombosis in the Peripheral Areas of Cortical Contusion in the Rat: Role of Platelet Activating Factor (Vienna: Springer Vienna).

Majewska, A.K., Newton, J.R., and Sur, M. (2006). Remodeling of synaptic structure in sensory cortical areas *in vivo*. The Journal of Neuroscience *26*, 3021-3029.

Margrie, T.W., Brecht, M., and Sakmann, B. (2002). In vivo, low-resistance, whole-cell recordings from neurons in the anaesthetized and awake mammalian brain. Pflügers Archiv: European Journal of Physiology *444*, 491-498.

Marlin, B.J., Mitre, M., D'amour, J.A., Chao, M.V., and Froemke, R.C. (2015). Oxytocin enables maternal behaviour by balancing cortical inhibition. Nature *520*, 499.

Marmarou, A., Foda, M.A.A.-E., Brink, W.v.d., Campbell, J., Kita, H., and Demetriadou, K. (1994). A new model of diffuse brain injury in rats. Journal of Neurosurgery *80*, 291-300.

Martin, N.A., Doberstein, C., Alexander, M., Khanna, R., Benalcazar, H., Alsina, G., Zane, C., McBride, D., Kelly, D., Hovda, D.*, et al.* (1995). Posttraumatic Cerebral Arterial Spasm. Journal of Neurotrauma *12*, 897-901.

Martin, N.A., Doberstein, C., Zane, C., Caron, M.J., Thomas, K., and Becker, D.P. (1992). Posttraumatic cerebral arterial spasm: transcranial Doppler ultrasound, cerebral blood flow, and angiographic findings. Journal of Neurosurgery *77*, 575-583.

Martin, N.A., Patwardhan, R.V., Alexander, M.J., Africk, C.Z., Lee, J.H., Shalmon, E., Hovda, D.A., and Becker, D.P. (1997). Characterization of cerebral hemodynamic phases following severe head trauma: hypoperfusion, hyperemia, and vasospasm. *87*, 9.

Mattson, A.J., and Levin, H.S. (1990). Frontal Lobe Dysfunction following Closed Head Injury. A Review of the Literature. The Journal of Nervous and Mental Disease *178*, 282-291.

Max, W., MacKenzie, E.J., and Rice, D.P. (1991). Head injuries: Costs and consequences. The Journal of Head Trauma Rehabilitation *6*, 76-91.

Maxwell, W.L., Povlishock, J.T., and Graham, D.L. (1997). A Mechanistic Analysis of Nondisruptive Axonal Injury: A Review. Journal of Neurotrauma *14*, 419-440.

Mayevsky, A., and Barbiro-Michaely, E. (2009). Use of NADH fluorescence to determine mitochondrial function in vivo. The International Journal of Biochemistry & Cell Biology *41*, 1977-1988.

McIlwain, J.T., and Creutzfeldt, O.D. (1967). Microelectrode Study of Synaptic Excitation and Inhibition in the Lateral Geniculate Nucleus of the Cat. Journal of Neurophysiology *30*, 1-21.

McIntosh, T.K., Vink, R., Noble, L., Yamakami, I., Fernyak, S., Soares, H., and Faden, A.L. (1989). Traumatic brain injury in the rat: Characterization of a lateral fluid-percussion model. Neuroscience *28*, 233-244.

McKee, A.C., Cantu, R.C., Nowinski, C.J., Hedley-Whyte, E.T., Gavett, B.E., Budson, A.E., Santini, V.E., Lee, H.-S., Kubilus, C.A., and Stern, R.A. (2009). Chronic Traumatic Encephalopathy in Athletes: Progressive Tauopathy After Repetitive Head Injury. Journal of Neuropathology & Experimental Neurology *68*, 709-735.

Meaney, D.F., and Smith, D.H. (2011). Biomechanics of concussion. Clinics in sports medicine *30*, 19-vii.

Mees, S.D., Rinkel, G.J.E., Feigin, V.L., Algra, A., Bergh, W.M.v.d., Vermeulen, M., and Gijn, J.v. (2007). Calcium antagonists for aneurysmal subarachnoid haemorrhage. Cochrane Database of Systematic Reviews.

Mei, Z., Qiu, J., Alcon, S., Hashim, J., Rotenberg, A., Sun, Y., Meehan, W.P., 3rd, and Mannix, R. (2018). Memantine improves outcomes after repetitive traumatic brain injury. Behavioral Brain Research *340*, 195-204.

Melov, S., Adlard, P.A., Morten, K., Johnson, F., Golden, T.R., Hinerfeld, D., Schilling, B., Mavros, C., Masters, C.L., Volitakis, I.*, et al.* (2007). Mitochondrial oxidative stress causes hyperphosphorylation of tau. PLoS One *2*, e536-e536.

Mez, J., Daneshvar, D.H., Kiernan, P.T., and et al. (2017). Clinicopathological evaluation of chronic traumatic encephalopathy in players of american football. JAMA: The Journal of the American Medical Association *318*, 360-370.

Miyazaki, S., Katayama, Y., Lyeth, B.G., Jenkins, L.W., DeWitt, D.S., Goldberg, S.J., Newlon, P.G., and Hayes, R.L. (1992). Enduring suppression of hippocampal long-term potentiation following traumatic brain injury in rat. Brain Research *585*, 335-339.

Moeini, M., Lu, X., Avti, P.K., Damseh, R., Bélanger, S., Picard, F., Boas, D., Kakkar, A., and Lesage, F. (2018). Compromised microvascular oxygen delivery increases brain tissue vulnerability with age. Scientific Reports *8*, 8219.

Mokhtari, M., Nayeb-Aghaei, H., Kouchek, M., Miri, M.M., Goharani, R., Amoozandeh, A., Akhavan Salamat, S., and Sistanizad, M. (2018). Effect of Memantine on Serum Levels of Neuron-Specific Enolase and on the Glasgow Coma Scale in Patients With Moderate Traumatic Brain Injury. The Journal of Clinical Pharmacology *58*, 42-47.

Morales, D.M., Marklund, N., Lebold, D., Thompson, H.J., Pitkanen, A., Maxwell, W.L., Longhi, L., Laurer, H., Maegele, M., Neugebauer, E.*, et al.* (2005). Experimental models of traumatic brain injury: do we really need to build a better mousetrap? Neuroscience *136*, 971-989.

Mouzon, B., Chaytow, H., Crynen, G., Bachmeier, C., Stewart, J., Mullan, M., Stewart, W., and Crawford, F. (2012). Repetitive Mild Traumatic Brain Injury in a Mouse Model

Produces Learning and Memory Deficits Accompanied by Histological Changes. Journal of Neurotrauma *29*, 2761-2773.

Moyer, J., and Brown, T. (2002). Patch-clamp techniques applied to brain slices. In Patch-clamp analysis; advanced techniques, W.Walz et al., eds. (Totowa, New Jersey: Humana Press).

Muir, J.K., Boerschel, M., and Ellis, E.F. (1992). Continuous Monitoring of Posttraumatic Cerebral Blood Flow Using Laser-Doppler Flowmetry. Journal of Neurotrauma *9*, 355-362.

Murphy, T.H., Li, P., Betts, K., and Liu, R. (2008). Two-photon imaging of stroke onset in vivo reveals that NMDA-receptor independent ischemic depolarization is the major cause of rapid reversible damage to dendrites and spines. The Journal of Neuroscience *28*, 1756-1772.

Nakamura, H., Strong, A.J., Dohmen, C., Sakowitz, O.W., Vollmar, S., Sué, M., Kracht, L., Hashemi, P., Bhatia, R., Yoshimine, T.*, et al.* (2010). Spreading depolarizations cycle around and enlarge focal ischaemic brain lesions. Brain : a journal of neurology *133*, 1994-2006.

Nakamura, K., Kamouchi, M., Kitazono, T., Kuroda, J., Shono, Y., Hagiwara, N., Ago, T., Ooboshi, H., Ibayashi, S., and Iida, M. (2009). Amiloride inhibits hydrogen peroxide-induced Ca2+ responses in human CNS pericytes. Microvascular Research *77*, 327-334.

Naylor, D.E., Liu, H., Niquet, J., and Wasterlain, C.G. (2013). Rapid surface accumulation of NMDA receptors increases glutamatergic excitation during status epilepticus. Neurobiology of Disease *54*, 225-238.

Nilsson, P., Gazelius, B., Carlson, H., and Hillered, L. (1996). Continuous Measurement of Changes in Regional Cerebral Blood Flow following Cortical Compression Contusion Trauma in the Rat. Journal of Neurotrauma *13*, 201-207.

Nilsson, P., Hillered, L., Olsson, Y., Sheardown, M.J., and Hansen, A.J. (1993). Regional Changes in Interstitial K+ and Ca2+ Levels following Cortical Compression Contusion Trauma in Rats. Journal of Cerebral Blood Flow & Metabolism *13*, 183-192.

Nilsson, P., Ronne-Engström, E., Flink, R., Ungerstedt, U., Carlson, H., and Hillered, L. (1994). Epileptic seizure activity in the acute phase following cortical impact trauma in rat. Brain Research *637*, 227-232.

Nimmerjahn, A., Kirchhoff, F., and Helmchen, F. (2005). Resting Microglial Cells Are Highly Dynamic Surveillants of Brain Parenchyma *In Vivo*. Science *308*, 1314-1318.

Onoue, H., Kaito, N., Akiyama, M., Tomii, M., Tokudome, S., and Abe, T. (1995). Altered reactivity of human cerebral arteries after subarachnoid hemorrhage. Journal of Neurosurgery *83*, 510-515.

Oppenheimer, D.R. (1968). Microscopic lesions in the brain following head injury. Journal of Neurology, Neurosurgery, and Psychiatry *31*, 299-306.

Ostergaard, L., Engedal, T.S., Aamand, R., Mikkelsen, R., Iversen, N.K., Anzabi, M., Naess-Schmidt, E.T., Drasbek, K.R., Bay, V., Blicher, J.U.*, et al.* (2014). Capillary transit time heterogeneity and flow-metabolism coupling after traumatic brain injury. Journal of Cerebral Blood Flow & Metabolism *34*, 1585-1598.

Overgaard, J., and Tweed, W.A. (1974). Cerebral circulation after head injury. Journal of Neurosurgery *41*, 531-541.

Pandit, A.S., Expert, P., Lambiotte, R., Bonnelle, V., Leech, R., Turkheimer, F.E., and Sharp, D.J. (2013). Traumatic brain injury impairs small-world topology. Neurology *80*, 1826-1833.

Pasco, A., Lemaire, L., Franconi, F., Lefur, Y., Noury, F., Saint-André, J.-P., Benoit, J.-P., Cozzone, P.J., and Jeune, J.-J.L. (2007). Perfusional Deficit and the Dynamics of Cerebral Edemas in Experimental Traumatic Brain Injury Using Perfusion and Diffusion-Weighted Magnetic Resonance Imaging. Journal of Neurotrauma *24*, 1321-1330.

Pedley, D.K., Bissett, K., Connolly, E.M., Goodman, C.G., Golding, I., Pringle, T.H., McNeill, G.P., Pringle, S.D., and Jones, M.C. (2003). Prospective observational cohort study of time saved by prehospital thrombolysis for ST elevation myocardial infarction delivered by paramedics. BMJ: British Medical Journal *327*, 22-26.

Peppiatt, C.M., Howarth, C., Mobbs, P., and Attwell, D. (2006). Bidirectional control of CNS capillary diameter by pericytes. Nature *443*, 700.

Pereira, P.M.G., Insausti, R., Artacho-Pérula, E., Salmenperä, T., Kälviäinen, R., and Pitkänen, A. (2005). MR Volumetric Analysis of The Piriform Cortex and Cortical Amygdala in Drug-Refractory Temporal Lobe Epilepsy. American Journal of Neuroradiology *26*, 319-332.

Philippon, J., Grob, R., Dagreou, F., Guggiari, M., Rivierez, M., and Viars, P. (1986). Prevention of vasospasm in subarachnoid haemorrhage. A controlled study with nimodipine. Acta Neurochirurgica *82*, 110-114.

Piredda, S., and Gale, K. (1985). A crucial epileptogenic site in the deep prepiriform cortex. Nature *317*, 623.

Pitkanen, A., Immonen, R.J., Grohn, O.H., and Kharatishvili, I. (2009). From traumatic brain injury to posttraumatic epilepsy: what animal models tell us about the process and treatment options. Epilepsia *50 Suppl 2*, 21-29.

Pittman, R.N. (2011). Matching Oxygen Supply to Oxygen Demand. In Regulation of Tissue Oxygenation (San Rafael, CA: Morgan & Claypool Life Sciences), pp. 4.

Povlishock, J.T., and Katz, D.I. (2005). Update of Neuropathology and Neurological Recovery After Traumatic Brain Injury. The Journal of Head Trauma Rehabilitation *20*, 76-94.

Prins, M.L., Lee, S.M., Cheng, C.L.Y., Becker, D.P., and Hovda, D.A. (1996). Fluid percussion brain injury in the developing and adult rat: a comparative study of mortality, morphology, intracranial pressure and mean arterial blood pressure. Developmental Brain Research *95*, 272-282.

Proskynitopoulos, P.J., Stippler, M., and Kasper, E.M. (2016). Post-traumatic anosmia in patients with mild traumatic brain injury (mTBI): A systematic and illustrated review. Surgical Neurology International *7*, S263-275.

Putten, H.P.V., Bouwhuis, M.G., Muizelaar, J.P., Lyeth, B.G., and Berman, R.F. (2005). Diffusion-Weighted Imaging of Edema following Traumatic Brain Injury in Rats: Effects of Secondary Hypoxia. Journal of Neurotrauma *22*, 857-872.

Reeson, P., Choi, K., and Brown, C.E. (2018). VEGF signaling regulates the fate of obstructed capillaries in mouse cortex. Elife *7*.

Reeves, T.M., Kao, C.-Q., Phillips, L.L., Bullock, M.R., and Povlishock, J.T. (2000). Presynaptic excitability changes following traumatic brain injury in the rat. Journal of Neuroscience Research *60*, 370-379.

Reeves, T.M., Lyeth, B.G., Phillips, L.L., Hamm, R.J., and Povlishock, J.T. (1997). The effects of traumatic brain injury on inhibition in the hippocampus and dentate gyrus. Brain Research *757*, 119-132.

Reeves, T.M., Lyeth, B.G., and Povlishock, J.T. (1995). Long-term potentiation deficits and excitability changes following traumatic brain injury. Experimental Brain Research *106*, 248-256.

Richards, H.K., Simac, S., Piechnik, S., and Pickard, J.D. (2001). Uncoupling of Cerebral Blood Flow and Metabolism after Cerebral Contusion in the Rat. Journal of Cerebral Blood Flow & Metabolism *21*, 779-781.

Rimel, R.W., Giordani, B., Barth, J.T., Boll, T.J., and Jane, J.A. (1981). Disability Caused by Minor Head Injury. Neurosurgery *9*, 221-228.

Risher, W.C., Andrew, R.D., and Kirov, S.A. (2009). Real-time passive volume responses of astrocytes to acute osmotic and ischemic stress in cortical slices and in vivo revealed by two-photon microscopy. Glia *57*, 207-221.

Rodríguez-Baeza, A., Reina-de la Torre, F., Poca, A., Martí, M., and Garnacho, A. (2003). Morphological features in human cortical brain microvessels after head injury: A three-dimensional and immunocytochemical study. The Anatomical Record Part A: Discoveries in Molecular, Cellular, and Evolutionary Biology *273A*, 583-593.

Rodriguez, U.A., Zeng, Y., Deyo, D., Parsley, M.A., Hawkins, B.E., Prough, D.S., and DeWitt, D.S. (2018). Effects of Mild Blast Traumatic Brain Injury on Cerebral Vascular, Histopathological, and Behavioral Outcomes in Rats. Journal of Neurotrauma *35*, 375-392.

Rogatsky, G.G., Sonn, J., Kamenir, Y., Zarchin, N., and Mayevsky, A. (2003). Relationship between Intracranial Pressure and Cortical Spreading Depression following Fluid Percussion Brain Injury in Rats. Journal of Neurotrauma *20*, 1315-1325.

Sakadžić, S., Mandeville, E.T., Gagnon, L., Musacchia, J.J., Yaseen, M.A., Yucel, M.A., Lefebvre, J., Lesage, F., Dale, A.M., Eikermann-Haerter, K.*, et al.* (2014). Large arteriolar component of oxygen delivery implies a safe margin of oxygen supply to cerebral tissue. Nature Communications *5*, 5734.

Sakadžić, S., Roussakis, E., Yaseen, M.A., Mandeville, E.T., Srinivasan, V.J., Arai, K., Ruvinskaya, S., Devor, A., Lo, E.H., Vinogradov, S.A.*, et al.* (2010). Two-photon high-resolution measurement of partial pressure of oxygen in cerebral vasculature and tissue. Nature Methods *7*, 755.

Salehi, A., Zhang, J.H., and Obenaus, A. (2017). Response of the cerebral vasculature following traumatic brain injury. Journal of Cerebral Blood Flow & Metabolism *37*, 2320-2339.

Santhakumar, V., Bender, R., Frotscher, M., Ross, S.T., Hollrigel, G.S., Toth, Z., and Soltesz, I. (2000). Granule cell hyperexcitability in the early post‐traumatic rat dentate gyrus: the ‘irritable mossy cell’ hypothesis. The Journal of Physiology *524*, 117-134.

Santhakumar, V., Ratzliff, A.D.H., Jeng, J., Toth, Z., and Soltesz, I. (2001). Long-term hyperexcitability in the hippocampus after experimental head trauma. Annals of Neurology *50*, 708-717.

Sato, S., Kawauchi, S., Okuda, W., Nishidate, I., Nawashiro, H., and Tsumatori, G. (2014). Real-time optical diagnosis of the rat brain exposed to a laser-induced shock wave: observation of spreading depolarization, vasoconstriction and hypoxemia-oligemia. PLoS One *9*, e82891-e82891.

Schaffer, C.B., Friedman, B., Nishimura, N., Schroeder, L.F., Tsai, P.S., Ebner, F.F., Lyden, P.D., and Kleinfeld, D. (2006). Two-Photon Imaging of Cortical Surface Microvessels Reveals a Robust Redistribution in Blood Flow after Vascular Occlusion. PLoS Biology *4*, e22.

Schmitt, J.M. (1999). Optical coherence tomography (OCT): a review. IEEE Journal of Selected Topics in Quantum Electronics *5*, 1205-1215.

Schneider, D.M., Nelson, A., and Mooney, R. (2014). A synaptic and circuit basis for corollary discharge in the auditory cortex. Nature *513*, 189.

Schwarzmaier, S.M., Kim, S.-W., Trabold, R., and Plesnila, N. (2010). Temporal Profile of Thrombogenesis in the Cerebral Microcirculation after Traumatic Brain Injury in Mice. Journal of Neurotrauma *27*, 121-130.

Schwarzmaier, S.M., Zimmermann, R., McGarry, N.B., Trabold, R., Kim, S.-W., and Plesnila, N. (2013). In vivo temporal and spatial profile of leukocyte adhesion and migration after experimental traumatic brain injury in mice. Journal of Neuroinflammation *10*, 808.

Shapira, Y., Shohami, E., Sidi, A., Soffer, D., Freeman, S., and Cotev, S. (1988). Experimental closed head injury in rats: mechanical, pathophysiologic, and neurologic properties. Critical Care Medicine *16*, 258-265.

Shen, Y., Kou, Z., Kreipke, C.W., Petrov, T., Hu, J., and Haacke, E.M. (2007). In vivo measurement of tissue damage, oxygen saturation changes and blood flow changes after experimental traumatic brain injury in rats using susceptibility weighted imaging. Magnetic Resonance Imaging *25*, 219-227.

Sheridan, D.C., Hughes, A.R., Erdelyi, F., Szabo, G., Hentges, S.T., and Schoppa, N.E. (2014). Matching of feedback inhibition with excitation ensures fidelity of information flow in the anterior piriform cortex. Neuroscience *275*, 519-530.

Shibata, M., Ohtani, R., Ihara, M., and Tomimoto, H. (2004). White matter lesions and glial activation in a novel mouse model of chronic cerebral hypoperfusion. Stroke *35*, 2598-2603.

Shih, A.Y., Blinder, P., Tsai, P.S., Friedman, B., Stanley, G., Lyden, P.D., and Kleinfeld, D. (2013). The smallest stroke: occlusion of one penetrating vessel leads to infarction and a cognitive deficit. Nature Neuroscience *16*, 55-63.

Shitaka, Y., Tran, H.T., Bennett, R.E., Sanchez, L., Levy, M.A., Dikranian, K., and Brody, D.L. (2011). Repetitive Closed-Skull Traumatic Brain Injury in Mice Causes Persistent Multifocal Axonal Injury and Microglial Reactivity. Journal of Neuropathology & Experimental Neurology *70*, 551-567.

Smith, C.J., Xiong, G., Elkind, J.A., Putnam, B., and Cohen, A.S. (2015). Brain Injury Impairs Working Memory and Prefrontal Circuit Function. Frontiers in Neurology *6*, 240.

Smith, D.H., and Meaney, D.F. (2000). Axonal Damage in Traumatic Brain Injury. The Neuroscientist *6*, 13.

Sobey, C.G. (2001). Cerebrovascular Dysfunction After Subarachnoid Haemorrhage: Novel Mechanisms And Directions For Therapy. Clinical and Experimental Pharmacology and Physiology *28*, 926-929.

Sobey, C.G., Heistad, D.D., and Faraci, F.M. (1996). Effect of subarachnoid hemorrhage on dilatation of rat basilar artery in vivo. American Journal of Physiology-Heart and Circulatory Physiology *271*, H126-H132.

Sobey, C.G., and Quan, L. (1999). Impaired cerebral vasodilator responses to NO and PDE V inhibition after subarachnoid hemorrhage. American Journal of Physiology-Heart and Circulatory Physiology *277*, H1718-H1724.

Soustiel, J.F., Glenn, T.C., Shik, V., Boscardin, J., Mahamid, E., and Zaaroor, M. (2005). Monitoring of Cerebral Blood Flow and Metabolism in Traumatic Brain Injury. Journal of Neurotrauma *22*, 955-965.

Srinivasan, V.J., Sakadžić, S., Gorczynska, I., Ruvinskaya, S., Wu, W., Fujimoto, J.G., and Boas, D.A. (2010). Quantitative cerebral blood flow with Optical Coherence Tomography. Optics Express *18*, 2477-2494.

Staal, J.A., Dickson, T.C., Gasperini, R., Liu, Y., Foa, L., and Vickers, J.C. (2010). Initial calcium release from intracellular stores followed by calcium dysregulation is linked to secondary axotomy following transient axonal stretch injury. Journal of Neurochemistry *112*, 1147-1155.

Stablum, F., Mogentale, C., and Umiltà, C. (1996). Executive Functioning Following Mild Closed Head Injury. Cortex *32*, 261-278.

Stein, S.C., Graham, D.I., Chen, X.-H., and Smith, D.H. (2004). Association between Intravascular Microthrombosis and Cerebral Ischemia in Traumatic Brain Injury. Neurosurgery *54*, 687-691.

Stocchetti, N., Furlan, A., and Volta, F. (1996). Hypoxemia and Arterial Hypotension at the Accident Scene in Head Injury. Journal of Trauma: Injury, Infection, and Critical Care *40*, 4.

Streit, W.J. (2000). Microglial Response to Brain Injury: A Brief Synopsis. Toxicologic Pathology *28*, 28-30.

Struchen, M.A., Hannay, H.J., Contant, C.F., and Robertson, C.S. (2001). The Relation Between Acute Physiological Variables and Outcome on the Glasgow Outcome Scale and Disability Rating Scale Following Severe Traumatic Brain Injury. Journal of Neurotrauma *18*, 115-125.

Sultana, R., and Butterfield, D.A. (2010). Role of oxidative stress in the progression of Alzheimer's disease. Journal of Alzheimers Disease *19*, 341-353.

Sun, D.A., Deshpande, L.S., Sombati, S., Baranova, A., Wilson, M.S., Hamm, R.J., and DeLorenzo, R.J. (2008). Traumatic brain injury causes a long-lasting calcium (Ca2+)-plateau of elevated intracellular Ca levels and altered Ca2+ homeostatic mechanisms in hippocampal neurons surviving brain injury. European Journal of Neuroscience *27*, 1659-1672.

Suzuki, N., and Bekkers, J.M. (2007). Inhibitory interneurons in the piriform cortex. Clinical and Experimental Pharmacology and Physiology *34*, 1064-1069.

Suzuki, N., and Bekkers, J.M. (2011). Two Layers of Synaptic Processing by Principal Neurons in Piriform Cortex. The Journal of Neuroscience *31*, 2156-2166.

Svoboda, K., Helmchen, F., Denk, W., and Tank, D.W. (1999). Spread of dendritic excitation in layer 2/3 pyramidal neurons in rat barrel cortex in vivo. Nature Neuroscience *2*, 65.

Tagge, C.A., Fisher, A.M., Minaeva, O.V., Gaudreau-Balderrama, A., Moncaster, J.A., Zhang, X.-L., Wojnarowicz, M.W., Casey, N., Lu, H., Kokiko-Cochran, O.N.*, et al.* (2018). Concussion, microvascular injury, and early tauopathy in young athletes after impact head injury and an impact concussion mouse model. Brain *141*, 422-458.

Takahashi, E., Takano, T., Nomura, Y., Okano, S., Nakajima, O., and Sato, M. (2006). In vivo oxygen imaging using green fluorescent protein. American Journal of Physiology-Cell Physiology *291*, C781-C787.

Tang, A.C., and Hasselmo, M.E. (1994). Selective suppression of intrinsic but not afferent fiber synaptic transmission by baclofen in the piriform (olfactory) cortex. Brain Research *659*, 75-81.

Taylor, C.A., Bell, J.M., Breiding, M.J., and Xu, L. (2017). Traumatic Brain Injury–Related Emergency Department Visits, Hospitalizations, and Deaths — United States, 2007 and 2013. In MMWR Surveillance Summaries (CDC), pp. 1-16.

Teasdale, G., Bailey, I., Bell, A., Gray, J., Gullan, R., Heiskanan, U., Marks, P.V., Marsh, H., Mendelow, A.D., Murray, G.*, et al.* (1990). The Effect of Nimodipine on Outcome After Head Injury: A Prospective Randomised Control Trial (Vienna: Springer Vienna).

Thiagarajan, P., Ciuffreda, K.J., and Ludlam, D.P. (2011). Vergence dysfunction in mild traumatic brain injury (mTBI): a review. Ophthalmic and Physiological Optics *31*, 456-468.

Thomale, U.-W., Kroppenstedt, S.-N., Beyer, T.F., Schaser, K.-D., Unterberg, A.W., and Stover, J.F. (2002). Temporal Profile of Cortical Perfusion and Microcirculation after Controlled Cortical Impact Injury in Rats. Journal of Neurotrauma *19*, 403-413.

Tortorella, A., Halonen, T., Sahibzada, N., and Gale, K. (1997). A Crucial Role of the α-Amino-3-Hydroxy-5-Methylisoxazole-4-Propionic Acid Subtype of Glutamate Receptors in Piriform and Perirhinal Cortex for the Initiation and Propagation of Limbic Motor Seizures. Journal of Pharmacology and Experimental Therapeutics *280*, 1401-1405.

Tsai, P.S., Kaufhold, J.P., Blinder, P., Friedman, B., Drew, P.J., Karten, H.J., Lyden, P.D., and Kleinfeld, D. (2009). Correlations of Neuronal and Microvascular Densities in Murine Cortex Revealed by Direct Counting and Colocalization of Nuclei and Vessels. The Journal of Neuroscience *29*, 14553-14570.

Turrigiano, G.G., Leslie, K.R., Desai, N.S., Rutherford, L.C., and Nelson, S.B. (1998). Activity-dependent scaling of quantal amplitude in neocortical neurons. Nature *391*, 892.

Turrigiano, G.G., and Nelson, S.B. (2004). Homeostatic plasticity in the developing nervous system. Nature Reviews. Neuroscience *5*, 97.

Verweij, B.H., Amelink, G.J., and Muizelaar, J.P. (2007). Current concepts of cerebral oxygen transport and energy metabolism after severe traumatic brain injury. In Progress in Brain Research, J.T. Weber, and A.I.R. Maas, eds. (Elsevier), pp. 111-124.

von Baumgarten, L., Trabold, R., Thal, S., Back, T., and Plesnila, N. (2008). Role of Cortical Spreading Depressions for Secondary Brain Damage after Traumatic Brain Injury in Mice. Journal of Cerebral Blood Flow & Metabolism *28*, 1353-1360.

von Bornstädt, D., Houben, T., Seidel, J.L., Zheng, Y., Dilekoz, E., Qin, T., Sandow, N., Kura, S., Eikermann-Haerter, K., Endres, M*., et al.* (2015). Supply-Demand Mismatch Transients in Susceptible Peri-infarct Hot Zones Explain the Origins of Spreading Injury Depolarizations. Neuron *85*, 1117-1131.

Weber, J.T. (2012). Altered calcium signaling following traumatic brain injury. Frontiers in Pharmacology *3*, 60.

Weber, J.T., Rzigalinski, B.A., and Ellis, E.F. (2001). Traumatic injury of cortical neurons causes changes in intracellular calcium stores and capacitative calcium influx. Journal of Biological Chemistry *276*, 1800-1807.

Werner, C., and Engelhard, K. (2007). Pathophysiology of traumatic brain injury. British Journal of Anaesthesia *99*, 4-9.

Wilson, N.M., Gurney, M.E., Dietrich, W.D., and Atkins, C.M. (2017). Therapeutic benefits of phosphodiesterase 4B inhibition after traumatic brain injury. PLoS ONE *12*, e0178013.

Winship, I.R., and Murphy, T.H. (2008). *In Vivo* Calcium Imaging Reveals Functional Rewiring of Single Somatosensory Neurons after Stroke. The Journal of Neuroscience *28*, 6592-6606.

Witgen, B.M., Lifshitz, J., Smith, M.L., Schwarzbach, E., Liang, S.L., Grady, M.S., and Cohen, A.S. (2005). Regional hippocampal alteration associated with cognitive deficit following experimental brain injury: a systems, network and cellular evaluation. Neuroscience *133*, 1-15.

Wolf, J.A., Stys, P.K., Lusardi, T., Meaney, D., and Smith, D.H. (2001). Traumatic Axonal Injury Induces Calcium Influx Modulated by Tetrodotoxin-Sensitive Sodium Channels. The Journal of Neuroscience *21*, 1923-1930.

Xiong, Y., Mahmood, A., and Chopp, M. (2013). Animal models of traumatic brain injury. Nature Reviews: Neuroscience *14*, 128-142.

Xu, L., Nguyen, J.V., Lehar, M., Menon, A., Rha, E., Arena, J., Ryu, J., Marsh-Armstrong, N., Marmarou, C.R., and Koliatsos, V.E. (2016). Repetitive mild traumatic brain injury with impact acceleration in the mouse: Multifocal axonopathy, neuroinflammation, and neurodegeneration in the visual system. Experimental Neurology *275 Pt 3*, 436-449.

Xue, M., Atallah, B.V., and Scanziani, M. (2014). Equalizing excitation-inhibition ratios across visual cortical neurons. Nature *511*, 596-600.

Yamakami, I., and McIntosh, T.K. (1991). Alterations in Regional Cerebral Blood Flow following Brain Injury in the Rat. Journal of Cerebral Blood Flow & Metabolism *11*, 655-660.

Yang, L., Afroz, S., Michelson, H.B., Goodman, J.H., Valsamis, H.A., and Ling, D.S. (2010). Spontaneous epileptiform activity in rat neocortex after controlled cortical impact injury. Journal of Neurotrauma *27*, 1541-1548.

Yang, S.H., Gustafson, J., Gangidine, M., Stepien, D., Schuster, R., Pritts, T.A., Goodman, M.D., Remick, D.G., and Lentsch, A.B. (2013). A murine model of mild traumatic brain injury exhibiting cognitive and motor deficits. Journal of Surgical Research *184*, 981-988.

Yemisci, M., Gursoy-Ozdemir, Y., Vural, A., Can, A., Topalkara, K., and Dalkara, T. (2009). Pericyte contraction induced by oxidative-nitrative stress impairs capillary reflow despite successful opening of an occluded cerebral artery. Nature Medicine *15*, 1031.

Yoshino, A., Hovda, D.A., Kawamata, T., Katayama, Y., and Becker, D.P. (1991). Dynamic changes in local cerebral glucose utilization following cerebral concussion in rats: evidence of a hyper- and subsequent hypometabolic state. Brain Research *561*, 106-119.

Yuan, X.-Q., Prough, D.S., Smith, T.L., and DeWitt, D.S. (1988). The Effects of Traumatic Brain Injury on Regional Cerebral Blood Flow in Rats. Journal of Neurotrauma *5*, 289-301.

Zanier, E.R., Lee, S.M., Vespa, P.M., Giza, C.C., and Hovda, D.A. (2003). Increased Hippocampal CA3 Vulnerability to Low-Level Kainic Acid following Lateral Fluid Percussion Injury. Journal of Neurotrauma *20*, 409-420.

Zhang, F., Sprague, S.M., Farrokhi, F., Henry, M.N., Son, M.G., and Vollmer, D.G. (2002). Reversal of attenuation of cerebrovascular reactivity to hypercapnia by a nitric oxide donor after controlled cortical impact in a rat model of traumatic brain injury. Journal of Neurosurgery *97*, 963-969.

CURRICULUM VITAE